AN ABSTRACT OF THE DISSERTATION OF

Mousa Diabat for the degree of Doctor of Philosophy in Water Resources Science presented on May 14, 2014.

Title: The Influence of Climate Change and Restoration on Stream Temperature.

Abstract approved:

____

Roy D. Haggerty   Steven M. Wondzell

Water temperature is an essential property of a stream. Temperature regulates physical and biochemical processes in aquatic habitats. Various factors related to climatic conditions, landscape characteristics, and channel structure directly influence stream temperature. Numerous studies indicate that increased average air temperature during the past century has led to stream warming across the world. The trend of stream warming was also present in spring-fed watersheds, where summer flow has decreased. In addition, anthropogenic practices that alter the natural landscape and channel structure, such as forest management, agriculture, and mining contributed to stream warming. For example, deforested and unshaded stream reaches or dredged channels were warmer than shaded reaches and meandering streams. Stream temperatures in North American lotic habitats are of a specific concern due to their significant economic, cultural, and ecological value. With climate projections indicating that air temperature will only continue to rise throughout the 21st century, cold- or cool-water organisms, especially fishes, will be affected. Therefore, there is a strong need to better understand the impacts of changing climate, riparian landscape, and channel structure on a stream's heat budget. This may assist in restoring the

historic thermal regime in impacted sites and mitigating the impacts of future climate change.

This study looks into the relative influences of the different factors on a stream's heat budget with three manuscripts: one on stream temperature response to diel timing of air warming, one on stream temperature response to changes in air temperature, flow, and riparian vegetation, and one on stream temperature response to air warming and channel reconstruction. I used the software Heat Source version 8.05 to simulate stream temperature for all three analyses along the Middle Fork John Day River, Oregon USA. Two of the manuscripts were applied to an upper 37 km section of the Middle Fork John Day River (presented in chapter 2 and 3), where the third manuscript was applied to a 1.5-km section.

The sensitivity analysis of stream temperature response to diel timing of air warming (Chapter 2: Diel Timing of Warmer Air under Climate Change Affects Magnitude, Timing, and Duration of Stream Temperature Change) was based on scenarios representing uniform air warming over the diel period, daytime warming, and nighttime warming. Uniform warming of air temperature is a simple representation of increases in the average daily or monthly temperatures generated by the 'delta method'. The delta method relies on adding a constant value to the air temperature time-series data. This constant value is the difference (delta) between base case average air temperatures and the projected one. Scenarios of daytime or nighttime warming represent conditions under which most of the warming of the air occurs during the daytime or the nighttime, respectively. I simulated the stream temperature response to warmer air conditions of +2 °C and +4 °C in daily average for all three cases of air warming conditions. The three cases of different diel distributions of air warming generated 7-day average daily maximum stream temperature (7DADM) increases of approximately +1.8 °C ± 0.1 °C at the downstream end of the study section relative to the base case. In most parts of the reach, the three distributions of air warming generated different ranges of stream temperatures, different 7DADM values, different durations of stream temperature changes, and different average daily temperatures. Changes of stream temperature were out of phase with imposed changes of air temperature. Therefore, nighttime warming of air temperatures would cause the greatest increase in maximum daily stream temperature, which typically occurs during the daytime.

The sensitivity analysis of the relative influences of changes in air temperature, stream flow, and riparian vegetation on stream temperature (Chapter 3: Assessing Stream Temperature Response to Cumulative Influence of Changing Air Temperature, Flow, and Riparian Vegetation). This study summarized stream temperature simulation in 36 scenarios representing possible manifestations of 21st century climate conditions and land management strategies. In addition to existing conditions (base case) of flow, air temperature, and riparian vegetation, scenarios consisted of: two air temperature increases of 2 °C and 4 °C, two stream flow variations of +30% and -30%, three spatially uniform riparian vegetation conditions that create averages of effective shade 7%, 34%, and 79%, in addition to 14% for base case conditions. Results suggest that variation in riparian vegetation was the dominant factor influencing stream temperature because it regulates incoming shortwave radiation, the largest heat input to the stream, while variation in stream flow has a negligible influence. Results indicated that increasing the effective shade along the study section, particularly in the currently unshaded sections, could mitigate the influence of increasing air temperature, and would reduce stream temperature maxima below current values even under future climate conditions of warmer air. With the small influence it had, increasing stream flow reduced the 7DADM under low shade conditions. However, increasing stream flow showed counterintuitive results as it contributed to increasing stream temperature maxima when the stream was heavily shaded.

The applied study examined the stream temperature response to restoration practices and their potential to mitigate the influence of warmer air conditions (Chapter 4: Estimating Stream Temperature Response to Restoring Channel and Riparian

Vegetation and the Potential to Mitigate Warmer Air Conditions). This study focused on a 1.5 km section along the upper part of the Middle Fork John Day River that was modified due to past anthropogenic activities of mining for gold and timber harvest. Currently, the riparian vegetation of the study site is mostly shrubs and stands of short trees. Restoration designs call for the restoration of both the channel structure and replanting the riparian vegetation. Simulation results showed that the 7DADM was higher in the restored channel than the existing channel with both conditions of low and high effective shade conditions. However, a combined restoration practice of channel reconstruction and medium effective shade conditions reduced stream temperature maxima more than restoring riparian vegetation alone. In addition, results showed that restoring riparian vegetation was sufficient to mitigate the influence of warmer air on stream temperature, while restoring the channel alone is not. Heat budget analysis showed that heat accumulation during the daytime increased in the restored channel, which was longer, narrower, and deeper than the existing channel. It is important to emphasize that stream temperature is one of many goals that restoration activities aim to improve. Furthermore, differences in 7DADM among the different scenarios of restoration are negligible. Such small differences could hardly be measure. While this study examined a short section of 1.5 km, longer stream sections may increase the differences in 7DADM.

Primary conclusions of this study are: 1) daily maxima of stream temperature will increase in response to increased air temperature regardless of the distribution of air warming during the diel cycle; 2) nighttime air warming caused a greater increase in stream temperature maximum than daytime warming; 3) riparian vegetation was the dominant factor on stream’s heat budget, more than air temperature or stream flow; 4) restoring riparian vegetation mitigated the influence of warmer air; 5) restoring channel structure alone was not sufficient to lower temperature maxima; and 6) restoration project was most successful in improving degraded stream temperature when combined with channel reconstruction and improved riparian shade.

The Influence of Climate Change and Restoration on Stream Temperature

by

Mousa Diabat

A DISSERTATION

submitted to

Oregon State University

in partial fulfillment of

the requirements for the

degree of

Doctor of Philosophy

Presented May 14, 2014

Commencement June 2014

Doctor of Philosophy dissertation of Mousa Diabat presented on May 14, 2014

APPROVED:

Major Professor, representing Water Resources Science

Director of the Water Resources Graduate Program

Dean of the Graduate School

I understand that my thesis will become part of the permanent collection of Oregon State University libraries. My signature below authorizes release of my dissertation to any reader upon request.

Mousa Diabat, Author

ACKNOWLEDGEMENTS

The journey of my doctoral degree has been supported by many people and institutions. First, I am deeply thankful to my wife Jehan for her endless support and trust, and to the two kids, Aseel and Bashir for keeping me alert along this journey. It is difficult to overstate my gratitude to my advisors, Dr. Roy Haggerty and Dr. Steven Wondzell. With their support, enthusiasm, patience, and inspiration, they helped me make this dissertation valuable and an exciting learning experience. With their editorial expertise, Roy and Steven helped me develop my communication skills to present my ideas in a simple and clear fashion.

I acknowledge my committee members, Dr. Stanley Gregory for introducing me to the scientific and cultural aspects of stream temperature, while drifting along the Willamette River for all 250 km, and also Dr. Stephen Lancaster who helped me solve the mathematical riddles on any occasion that I entered his office during my study.

I would like to thank Dr. Aaron Wolf, Dr. Mary Santelmann, and Dr. John Selker for enduring support starting with my initial application to the program and throughout my Ph.D. I am very thankful to my collaborators in the Oregon Department of Environmental Quality, Oregon Watershed Enhancement Board, the Confederated Tribes of the Warm Springs, and the Watershed Council of the North Fork John Day River.

My Ph.D. would not have been completed without the funding provided from the Fulbright Foundation, the U.S. Forest Service through the Pacific Northwest Research Station though the joint venture with Oregon State University 10-JV-11261991-055, the Water Resources Graduate Program, the International Student Office, and the Graduate School at Oregon State University.

TABLE OF CONTENTS

Page

TABLE OF CONTENTS

Page

LIST OF FIGURES

LIST OF FIGURES

LIST OF FIGURES

Figure | Page

LIST OF FIGURES

LIST OF TABLES

1. General Introduction

Stream temperature is an important property that influences the physical and biochemical processes in lotic habitats. It regulates oxygen solubility and nutrient cycling in streams in addition to the metabolism, growth rate, and mortality of aquatic organisms (Feldhaus *et al.*, 2010; McCullough, 1999; Myrick and Cech, 2005; Richter and Kolmes, 2005). Small changes to a stream's thermal regime can lead to changes in physiological and behavioral characteristics of various aquatic organisms (Reeves *et al.*, 2009; Tinus and Reeves, 2001) and more extreme changes may lead to mortalities (Feldhaus *et al.*, 2010; Lawrence *et al.*, 2012). The Middle Fork John Day River has experienced substantial warming and loss of cold-water habitats caused by anthropogenic activities. Between the late 19th century and throughout the first half of the 20th century, gold mining affected channel structure and timber harvest reduced riparian vegetation across the floodplain. In the future, stream temperature may increase in response to atmospheric warming (Mantua *et al.*, 2010), thus better understanding of quantifying the effects of changes in air temperature, riparian vegetation, and channel structure on stream temperature is an essential step in developing effective restoration projects. There are two major approaches to simulate stream temperature: regression and deterministic models.

Regression models establish statistically linear or nonlinear regressions between stream temperature and one or more independent factors. Such models of air-water temperatures are based on correlations on yearly, monthly, or weekly time scales (Crisp and Howson, 1982; Stefan and Preud'homme, 1993). Stefan and Preud'homme (1993) generated a general, linear equation that estimated water temperature (T_w) from air temperature (T_a) on a daily timescale $T_w = 5.0 + 0.75T_a$ and on a weekly timescale $T_w = 2.9 + 0.86T_a$. However, recent studies reported that correlations between air and water temperature are weak and highly variable in a number of watersheds in the Pacific Northwest of North America (Arismendi *et al.*, 2012).

Regression models with multiple parameters improve the prediction of stream temperature to daily time scales, but still cannot account for fine scale difference in subsurface exchange. Water temperature was also correlated with streamflow Sinokrot and Gulliver (2000), and reduced streamflow can cause increased stream temperature. Multiple regression models have focused on correlating stream temperature with air temperature and either flow or channel structure (Caissie *et al.*, 2001; Neumann *et al.*, 2003; Webb *et al.*, 2003). Cassie et al. (2001) indicated that incorporating flow in the air-water regression model did not improve the modeling significantly, but Webb et al. (2003) indicated that air-water relationships are stronger for flow that are lower-than the median. Incorporating streamflow in regression models provides more accurate predictions, but the degree of model improvement varies greatly (van Vliet *et al.*, 2011).

Deterministic models calculate the rate change in stream temperature (ΔT_w) as a function of heat advection and dispersion (AD) in the flowing water and heat transfer (H_T) between the stream and its environment (Brown, 1969; Davidson and Bradshaw, 1967).

$$\Delta T_w \propto AD + H_T \qquad \text{EQ. 1-1}$$

Heat advection and dispersion is solved in:

$$AD = -U \cdot \frac{\partial T_w}{\partial x} + D_L \cdot \frac{\partial^2 T_w}{\partial x^2} \qquad \text{EQ. 1-2}$$

and heat transfer is solved in:

$$H_T = \frac{H_{net}}{C_{H_2O} \cdot \rho_{H_2O} \cdot V} \qquad \text{EQ. 1-3}$$

So, the governing equation for the rate change in temperature is:

$$\frac{\partial T_w}{\partial t} = -U \cdot \frac{\partial T_w}{\partial x} + D_L \cdot \frac{\partial^2 T_w}{\partial x^2} + \frac{H_{net}}{C_{H_2O} \cdot \rho_{H_2O} \cdot V} \qquad \text{EQ. 1-4}$$

Where.

T_w = water temperature (°C)

∂t = modeling time step (sec)

∂x = modeling distance step (along the channel) (m)

U = water velocity ($m \cdot sec^{-1}$)

D_L = longitudinal dispersion coefficient ($m^2 \cdot sec^{-1}$)

H_{net} = net heat flux ($W \cdot m^{-2}$)

ρ_{H_2O} = density of water ($kg \cdot m^{-3}$)

C_{H_2O} = specific heat capacity of water (4.18 kJ· (kg· °C)$^{-1}$)

V = water volume (m^3)

Five major heat fluxes control the stream's heat exchange process (Fig. 1-1): shortwave radiation (H_{sw}), longwave radiation (H_{lw}), evaporation (H_{evap}), convection with air at the water surface (H_{conv}), and conduction at the streambed (H_{cond}) where the net heat flux is the sum of each component (Brown, 1969).

$$H_{net} = H_{sw} + H_{lw} + H_{evap} + H_{conv} + H_{cond} \qquad \text{EQ. 1-5}$$

Deterministic models calculate stream temperature in space and time to incorporate spatio-temporal heterogeneity of climate conditions, channel structure, and riparian characteristics where regression models cannot. Deterministic models are more suitable for predicting stream temperatures under specific conditions and are able deliver more diverse outputs than regression models.

Deterministic models provide a method for isolating and estimating the relative influence of different factors on stream temperature (Brazier and Brown, 1973; Brown and Krygier, 1970; Gu *et al.*, 1998; Sinokrot and Stefan, 1993). Shortwave radiation is the main input heat flux to streams that is directly influenced by the presence of riparian vegetation. Air temperature influences streams heat budgets through to longwave radiation, evaporation, and convection. Streams dissipate most of the heat in both longwave radiation and evaporation. Therefore, changing air temperatures may influence the potential to dissipate heat in streams. Temperature is a function of heat concentration (the net heat load in a volume of water), thus the magnitude of discharge influences the energy required to elevate water temperature. Gu et al. (1998) quantified a stream temperature-buffering coefficient, which relates increased stream discharge with a reduced warming rate. Drawbacks of deterministic models are the requirements for extensive input data and high computational demands.

Studies of stream's heat budget suggested various restoration strategies such as riparian re-vegetation, augmenting streamflow, and channel reconstruction. Brown (1969) suggested the replanting of riparian vegetation as a strategy to control stream temperatures. Brown and Krygier (1970) also identified that streams warmed up significantly following a clear-cut timber harvest. Overall, increasing the effective shade decreases maximum temperatures along shaded reaches (Johnson, 2004; Rutherford *et al.*, 1997; Wilkerson *et al.*, 2006; Zwieniecki and Newton, 1999). In addition, reducing diversions and establishing minimum streamflows can reduce warming associated with loss of riparian vegetation but it cannot eliminate increases in stream temperature (Sinokrot and Gulliver, 2000).

This study quantifies stream temperature response to projected changes in climate, forest management, hydrology, and channel structure. To accomplish this goal, we 1) developed new software to strengthen an existing model, 2) conducted sensitivity analyses of stream temperature response to the interactive influence of multiple factors: air temperature, riparian vegetation, stream flow, and channel structure, and 3)measured physical properties of a stream to model stream temperature response to ongoing restoration practices.

The study objectives are to:

- Estimate stream temperature response to temporally uniform and non-uniform air temperature over the diurnal cycle.
- Quantify stream temperature response to potential conditions of climate, riparian vegetation, and flow.
- Identify and quantify the relative influence of projected conditions of air temperature, riparian vegetation, and flow on stream temperature.
- Predict stream temperature response to the restoration practices of channel reconstruction and riparian vegetation.

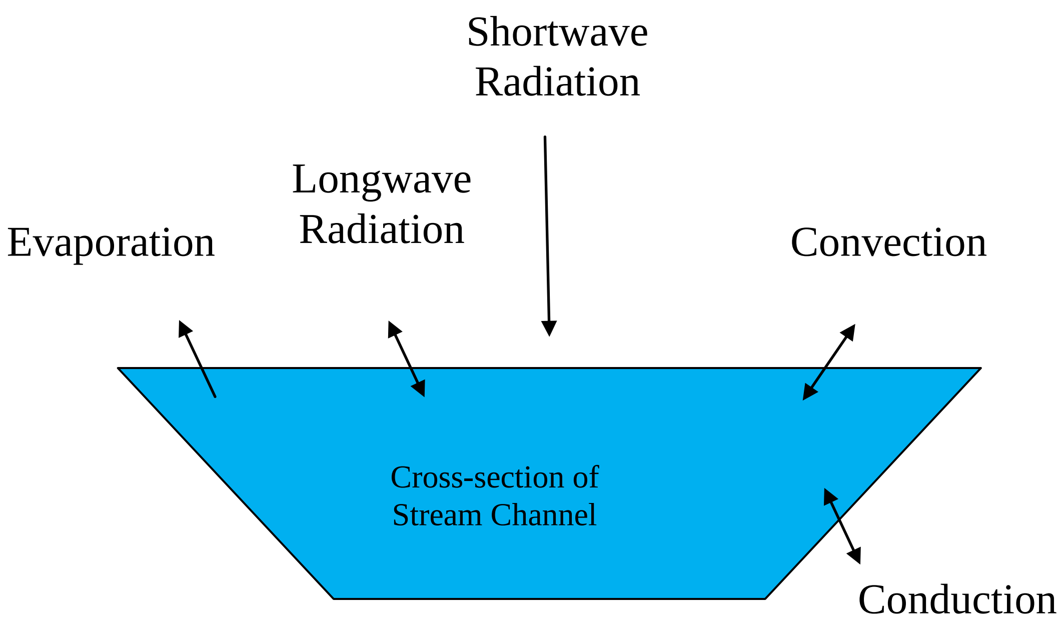

Figure 1-1: Heat transfer process showing all five major heat fluxes.

2. Diurnal Timing of Warmer Air Under Climate Change Affects Magnitude, Timing and Duration of Stream Temperature Change

Mousa Diabat
Roy Haggerty
Steven M. Wondzell

Journal of Hydrological Processes
D.O.I. 10.1002/hyp.9533

Abstract

Stream temperature will be subject to changes due to atmospheric warming in the future. I investigated the effects of the diurnal timing of air temperature changes – daytime warming vs. nighttime warming – on stream temperature. Using the physically-based model, Heat Source, I performed a sensitivity analysis of summer stream temperatures to 3 diurnal air temperature distributions of +4 °C mean air temperature: 1) uniform increase over the whole day; 2) warmer daytime; and 3) warmer nighttime. The stream temperature model was applied to a 37-km section of the Middle Fork John Day River in northeastern Oregon, USA. The 3 diurnal air temperature distributions generated 7-day average daily maximum (7DADM) stream temperatures increases of approximately +1.8 ±0.1 °C at the downstream end of the study section. The 3 air temperature distributions, with the same daily mean, generated different ranges of stream temperatures, different 7DADM temperatures, different durations of stream temperature changes, and different average daily temperatures in most parts of the reach. The stream temperature changes were out of phase with air temperature changes and, therefore in many places, the greatest daytime increase in stream temperature was caused by nighttime warming of air temperatures. Stream temperature changes tended to be more extreme and of longer duration when driven by air temperatures concentrated in either daytime or nighttime instead of uniformly distributed across the diurnal cycle.

Introduction

Stream temperature has been recognized as an important environmental factor in freshwater ecosystems since the 1960's (Caissie, 2006; Webb et al., 2008). Naturally, stream temperature fluctuates on seasonal as well as daily cycles (Sinokrot and Stefan, 1993), and these fluctuations are important to ecosystems. For example, the River Continuum Concept points to the variability in stream temperature (annual, daily and seasonal cycles) as important influences on aquatic species and habitats (Vannote et al., 1980). Recent studies show that North American watersheds have witnessed noticeable increases in water temperature for the past few decades (Bartholow, 2005; Beschta and Taylor, 1988; Mohseni et al., 1999; Webb, 1996). Efforts have been made to predict the influence of future climate change on stream temperature and aquatic ecosystems to help restoration efforts and planning. However, the future magnitude of increases is poorly constrained, and the diurnal timing and durations of the increases have received little study.

Cold-water fish (such as salmonid species) are affected by increasing stream temperatures. Feldhaus et al. (2010) found that levels of heat shock protein 70 in redband rainbow trout (*Oncorhynchus mykiss gairdneri*) were positively correlated with stream temperature. Thermal stress in the short term leads to behavioral changes over the fish life cycle. Among fish populations in the Pacific Northwest of the USA, metabolism, food consumption, growth, and reproduction ability, have been found to be affected by stream temperatures (McCullough, 1999; Myrick and Cech, 2005; Myrick and Cech, 2003; Myrick and Cech, 2000; Myrick and Cech, 2004; Selong et al., 2001).

Stream temperature is the product of heat exchange between water in the stream and its environment. Therefore, environmental changes may lead to changes in stream temperature. The stream exchanges heat with its environment via five major sources and sinks: shortwave (solar) radiation, longwave (thermal) radiation, streambed heat transfer (conduction), evaporation, and convection (Khangaonkar and Yang, 2008;

Stefan and Sinokrot, 1993). Further, stream temperature is influenced by boundary conditions (the temperature and discharge of upstream flow and incoming tributaries). The governing equation for heat budget and exchange in an open channel is the advection dispersion equation with aforementioned sources and sinks (Brown, 1969; Wright and Horrall, 1967).

Diurnal fluctuations of air temperature vary in range, maxima, and minima due to atmospheric conditions, elevation, topography and land cover. Maxima typically occur during the late afternoon to early evening, while minima occur during the late night to early morning. These diurnal fluctuations have a great impact on the stream's heat budget because air temperature affects the heat exchange between the air and water. However, models of warming climate typically project an increase in the annual and monthly average air temperatures (IPCC, 2007), rather than the hourly changes important to stream temperature. Nevertheless, prediction of future stream temperature requires the use of results from these climate models (Caissie et al., 2007; Gooseff et al., 2005; Mantua et al., 2009; Stefan and Sinokrot, 1993).

Modeling stream temperature can be divided into two approaches: statistical and deterministic. Statistical models correlate stream temperature with one or more variables such as air temperature and streamflow. Linear regression models are easier to use and require less input data compared to complex statistical models that involve correlating stream temperatures with more variables that can become mathematically complicated (Webb and Nobilis, 2007). Numerous studies have established statistical (linear and non-linear) correlations between air and water temperatures. These correlations have been used to predict future stream temperatures under projected changes in climate. Stefan and Preud'homme (1993) and Pilgrim et al. found a linear correlation between air and water temperatures in the central USA. They detected that water temperature responses to air temperature changes were different according to the size of the river. Mohseni et al. (1998) developed a non-linear regression function correlating the average weekly stream temperature with air temperature for different streams around USA. Studying a southwest English stream, Webb et al. (2003) found better correlation of air and water temperatures in rivers with below-average flow. Benyahya et al. (2007) used autoregression and periodic autoregression models to predict temperature in the Deschutes River, Oregon, USA. Statistical methods are commonly used to model past and future stream temperatures at annual, monthly, and weekly time scales rather than at daily or diurnal time scales (Mohseni, et al., 1998; Webb et al., 2003; Cassie, 2006).

Deterministic models explicitly incorporate the heat budget, physics of flow, and changes to these processes in streams. These models require detailed input data to calculate heat fluxes (Caissie *et al.*, 2007; Stefan and Sinokrot, 1993), including meteorology, topography, stream geomorphology, and hydrology. Stefan and Sinokrot (1993) studied five streams in the USA using a deterministic model and predicted that increasing air temperature could lead to a 2.4 to 4.7 °C increase in stream temperatures, while removing riparian vegetation could lead to a 6 °C increase. Cristea and Burges (2010) predicted that a 4 °C increase in air temperature in the Wenatchee River, Washington, USA would increase stream's maximum temperatures by 2.5 − 3.6 °C in the 2040s. Modelers who use deterministic models modify existing data of atmospheric and initial conditions to generate future scenarios to modify the impact on stream temperature.

There are a number of methods to modify an existing air temperature data to model future scenarios of global warming. Chief among these is the uniform case where a single increase in air temperature is added uniformly to the whole data. This is sometimes called the 'delta case' or 'delta method'. The uniform case generates a uniform increase in air temperature over the diurnal cycle. It generates projected daily average, maxima, and daily minima temperatures that are higher than the originals by the same value. However, I do not know if temperatures will change uniformly.

Alexander *et al.* (2006) and Morak *et al.* (2011) reported that during the second half of the 20th century, minima increased faster than maxima over most of the planet. In addition, the diurnal temperature range (DTR) has been decreasing over the same period (Vose *et al.*, 2005). Consequently, a diurnal uniform increase in air temperature is not the only method to modify air temperature data in the deterministic models that aim to simulate future scenarios. The expected increases in the monthly average air temperature might result more from an increased nighttime air temperatures than the increased daytime temperatures. Conversely, the expected increases in the monthly average air temperature might result from increased daytime air temperatures.

These findings increase the uncertainty in modeling future impact of air temperature warming on stream temperatures. While numerous studies examined past diurnal air-water temperature correlation, the majority of future projection deals with weekly and daily correlations. I use sensitivity analysis to compare and contrast the two most extreme cases with the uniform case, examining the changes in stream temperature resulting from daytime versus nighttime warming.

The only study that investigated non-uniform changes in air temperature over the diurnal cycle was Gooseff *et al.* (2005). Using a deterministic model of the Lower Madison River, Montana, USA, and output from the general circulation models (GCMs), Gooseff *et al.* found that daytime warming (of air) warmed streams beyond the upper zero net growth temperature for rainbow trout *(Oncorhynchus mykiss*) by more time than nighttime warming. In addition, Gooseff *et al.* found that combining nighttime warming and changing shortwave radiation warmed stream beyond the maximum temperature for growth for rainbow trout by more time than daytime warming of air and changed shortwave radiation. Gooseff *et al.* did not isolate the effects of changed air temperatures from those of changed solar radiation.

The objective of this study is to understand the response in stream temperatures to the timing of diurnal changes in air temperature under climate change and to isolate those effects from changes in shortwave radiation. To meet this objective, a calibrated physics-based stream temperature model for the Middle Fork John Day River, Oregon, USA, was changed to reflect possible timing scenarios for future air temperature warming.

Methods

I based the study on an upper section of the Middle Fork John Day River (MFJD) in northeastern Oregon, USA (Fig. 2-1). The study section extends for 37.0 km beginning immediately upstream of the confluence with Clear Creek (44°35’48”N, 118°29’36”W) and ending immediately downstream of Camp Creek. The drainage area of the study section is 827 km^2 (663 km^2 excluding the area of Camp Creek sub-basin) and elevations range from 1,000 to 1,250 m with a total of 19 tributaries. The upper elevations of the study section’s drainage basin receive an annual average of 1270 mm of precipitation, with less than 10% falling during the hottest months of July and August. Flow in the MFJD at Clear Creek drops from 2.5 m^{3}s^{-1} at the beginning of May to 0.2 m^{3}s^{-1} at the end of September with slowly declining discharge through July and August. The study section is made up of unconstrained sub-reaches running through wide riparian meadows connected by confined sub-reaches with narrow valley floors (Crown and Butcher, 2010). Bedrock geology in the reach is predominantly Columbia River Basalt Group and felsic volcanic and volcaniclastics of the John Day Group (Hunt and Stepleton, 2004). Gold mining, dredging, and railway constructions during the second half of the 19th century to early 20th century lead to tree clear-cutting along the riparian zone and geomorphologic changes in the valley. Sinuosity was reduced, and banks were hardened. Furthermore, trees were removed for cattle grazing and firewood, and could not be replanted due to the coarse texture of the mining spoils, leading to large scale reduction in tree cover in some sub-reaches (Beschta and Ripple, 2005).

I used the model Heat Sources in the simulations. Heat Source (Boyd and Kasper, 2003; Boyd, 1996) is a physically-based finite-difference model that simulates stream thermodynamics and hydrodynamics. It is distributed and maintained by the Oregon Department of Environmental Quality (http://www.deq.state.or.us/wq/tmdls/tools.htm) and has been used in a number of stream temperature studies and reports. Heat Source simulates advection and dispersion of heat, and heat exchange processes including fluxes of shortwave and longwave radiation, air/water interface convection, evaporation rate, and bed conduction. The current version (8.0) contains packages that calculate local channel hydraulics and the hourly solar radiation flux on the water surface based on sun angle, vegetation, topography and the water surface and the wetted channel dimensions.

Crown and Butcher (2010) parameterized and calibrated Heat Source to simulate MFJD stream temperature based on records and measurements from the years 2002 and 2004 as part of a total maximum daily load (TMDL) assessment for the John Day River. Original data for discharge and temperature were generated by a combination of in-stream measurements, thermal infrared surveys, and a generic temperature profile (Crown and Butcher, 2010). I extracted the relevant model input elements for the study section in the MFJD from Crown and Butcher’s model. The stream section uses stream temperature records from seven data loggers located along the mainstem MFJD (records from 2002 at river km (rkm) 3.2, 13.2, 13.75, 17.45, 19.15, 20.55, and 28.3- numbering according to the study section) and five data loggers on major tributaries installed between May and October 2004. At each data logger location, values for cloudiness, humidity, wind speed, and air temperature were adjusted from the Agrimet site in Prairie City, Oregon (22.0 km away from upstream end of reach at 44°27’42”N, 118°42’50”W, and elevation 1079 m). The accuracy/error of the model was confirmed for key days (hottest days) at locations where data loggers were installed (See Crown and Butcher (2010) for further information).

Records showed that at the upper end of the study section, stream temperature ranged from 11.6 to 27.7 °C in July 2002, while at the lower part of the study section (data logger at rkm 3.2), river temperature ranged from 12.4 to 28.7 °C in July 2002. The air temperature ranged between 4.8 and 39.9 °C in the same month.

The sensitivity analysis did not include any changes in the boundary conditions. The flow regime and stream water temperature at the upstream boundary of the study section were kept at their 2002 values (See Table 1). In addition, the discharge and temperature of tributaries entering the mainstem MFJD were not changed in the study section. Crown and Butcher (2010) reported the flow and temperature of the major tributaries entering the MFJD. Their report also lays out the method for estimating the missing information for tributaries' temperature and discharge. Thus, tributary and upstream boundary temperatures fluctuated over time, both diurnally and over longer periods, following the temperatures observed during the 2002 base year. Discharge also varied over the simulation period to include the values over the year (for example, snowmelt flow and summer flow). While I expect the temperature and discharge of the upstream boundary and the tributaries to change with climate, the focus here is not a prediction of future temperature, but an investigation of sensitivity to the diurnal timing of air warming.

Mantua *et al.* (2010) calculated spatially and temporally downscaled future air temperature from the A1B and the B1 emission scenarios based on results from the Fourth Assessment Report of the Intergovernmental Panel on Climate Change (IPCC AR4), providing average monthly air temperatures for many watersheds throughout the Pacific Northwest (Bates *et al.*, 2008). Elsner *et al.* (2010) projected future air temperature on a monthly basis on a 1/16° grid for the A1 scenario. Both the A1B and B1 assume the same growth rate in the world's population while the B1 scenario uses lower emissions and cleaner energy technologies. Results of A1B emission scenarios by Mantua *et al* (2010) for July-August have an average increase in air temperature of 3.43 °C by the 2040s, and 5.88 °C by the 2080s. Their B1 July-August results have an average increase in air temperature of 2.64 °C by the 2040s, and 4.24 °C by the

2080s. Given the range of these projections, this study uses a base case of +4 °C warming in July's monthly average air temperature relative to July 2002.

Air temperature averaged 21.0 °C for July 2002. I increased air temperature by 4 °C in the scenario, resulting in a monthly average air temperature of 25.0 °C for the sensitivity analysis. Air temperature was modified with three different algorithms by adding a specified value to the hourly 2002 air temperature, but maintaining a +4 °C average for each day (midnight to midnight). The first algorithm was the uniform case whereby all hourly values were increased by +4 °C. The second and third algorithms used the "rubber band method". In the warmer nighttime case, the maximum daily temperature was held constant and other temperatures were changed in proportion to their difference from the maximum daily temperature. The minimum daily temperature (nighttime) was increased the most so I refer to this as the "warmer nighttime case". In the warmer day case, the minimum daily temperature was held constant and other temperatures were changed in proportion to their difference from the minimum daily temperature. The maximum daily temperature (daytime) was increased the most so I refer to this as the "warmer daytime case". I reemphasize − the change in each day's average temperature was +4 °C for all three cases.

The equations for the mean values are, for all cases,

$$\overline{T_{d\Delta}} = \frac{\sum(T_i + \Delta)}{24} \qquad \text{EQ. 2-1}$$

$$\overline{T_{m\Delta}} = \frac{\sum_{j=1}^{d_e} \frac{\sum(T_i + \Delta)}{24}}{d_e} \qquad \text{EQ. 2-2}$$

where $\overline{T_{d_\Delta}}$ is the new average daily value after the addition; T_i is the air temperature at i hour of the 2002 day; Δ is the change in mean air temperature on a monthly basis; $\overline{T_{m_\Delta}}$ is the new average monthly value after the addition; and d_e is the number of days in the month.

The equation for the uniform case is simply

$$T_i^* = T_i + \Delta \qquad \text{EQ. 2-1}$$

The equation for warmer daytime temperatures is

$$T_i^* = T_i + \frac{\Delta(T_i - Min_d)}{\overline{T_d} - Min_d} \qquad \text{EQ. 2-3}$$

Where $\overline{T_d}$ is the old daily average temperature; T_i^* is the new air temperature at *i* hour; and Min_d is the daily minimum temperature. Other variables are as previously defined.

The equation for warmer nighttime temperatures is

$$T_i^* = T_i + \frac{\Delta(Max_d - T_i)}{Max_d - \overline{T_d}} \qquad \text{EQ. 2-4}$$

Where Max_d is the daily maximum temperature. A comparison of (3), (4) and (5) shows that their averages are the same. Water discharge and temperatures inputs at the upper end of the study section and from the tributaries were not modified from the original data since the objective is to study the influence of the diurnal timing of air temperature. The water balance and input stream temperatures were the same as the original 2002 validated Heat Source model (Crown and Butcher, 2010).

For a detailed analysis of the effects of diurnal timing of air temperature changes, I chose two locations along the study section and one typical day in July. I chose an upstream site, at rkm 22, and a downstream site, at rkm 4. The upstream site is located at the edge of a relatively shaded stretch of the stream, downstream of some tributaries and minor diversions, and at the location of the lowest 7DADM value (Fig. 2-1). The downstream site is located some distance from a shaded section, downstream of one major tributary (Big Boulder Creek) and major diversions (at rkm 6.3 and 5.2), and at the location of a higher 7DADM value than the upstream site. The upstream site is located at a section that is characterized with high effective shade

(>50%), while the downstream site is at a section with low effective shade (<10%). Additionally, I chose one typical day in July for the sub daily analysis. A typical day, as I characterize it, has an average temperature and diurnal temperature range that represents the month. I chose 26 July 2002 as a typical day − the- stream temperature average was 20.35 °C and the stream temperature range was 6.57 °C.

The 7-Day Average of the Daily Maximum (7DADM) is a major water quality standard used by policy makers and stakeholders in Oregon and number of states in USA (USEPA, 2003). It is determined by calculating the moving average for the daily maximum for every model segment simulated by the model run. In the simulations, this period is May 1st to August 31st.

Results

Air temperature for the month of July averaged 25.0 °C at rkm 3.2 for all simulated cases (Fig. 2-2). However, the range of air temperatures was different for each case. The uniform case maintained the diurnal temperature variation present in 2002. The warmer daytime case generated a wider range of air temperatures than the warmer nighttime case.

The 7DADM stream temperatures increased, relative to 2002, for all three cases (Fig. 2-3a and 2-3b). The 7DADM increase was greatest in the upper part of the study section for the daytime warming case and was greatest in the lower part of the study section for the nighttime warming case. The increase in 7DADM temperatures differed between cases by more than 1 °C in some locations, but was the same between cases in other locations. The largest differences among the cases occurred at rkm 7 − 10 (moderate shade) and at rkm 16 − 20 (low shade). At the upstream site (rkm 22), the 7DADM increased by 1.1 °C under the uniform case, 1.2 °C under the warmer daytime case, and 1.3 °C under the warmer nighttime case. At the downstream site (rkm 4), the 7DADM increased by 1.8 °C under the uniform case and 1.9 °C under both the warmer daytime and nighttime cases.

Diurnal changes in stream temperature in response to the three different warming cases (Fig. 2-4) show that the uniform case generated an increase in stream temperature that was nearly constant throughout the day, 1.0 to 1.1 °C warmer at the upstream site and 1.8 to 2.1 °C warmer at the downstream site. The other two cases, however, generated an increase in stream temperature that varied throughout the day. Stream temperature increases ranged from as little as 0.4 °C warmer to as much as 2.2 °C warmer at the upstream site and from 1.1 to 2.7 °C warmer at the downstream site. For warmer daytimes, the stream temperature increases tended to be out of phase with stream temperature. For warmer nighttimes, the stream temperature increases tended to be in phase with stream temperature. Consequently, for the warmer daytime case, the largest stream temperature increases occurred around midnight, and these changes commonly decreased temperature swings from day to night. For the warmer nighttime case, the largest stream temperature increases occurred around midday, and these changes commonly increased temperature swings from day to night.

The temporal distribution of warmer air along the diurnal cycle influenced the magnitude and timing of change in stream temperatures (Fig. 2-5). The uniform case resulted in smaller variability in changes in stream temperature relative to either the warmer daytime or the warmer nighttime. Both the warmer daytime and warmer nighttime cases generated many instances when stream temperatures were nearly 1.0 °C warmer or cooler than the uniform case.

The diurnal distribution of changes in air temperature influenced the duration (the number of hours per day) that stream temperatures increased (Fig. 2-6). Warmer daytimes and nighttimes generated increases of stream temperature lasting for 1 – 2 hd^{-1} across a range of temperatures at the upstream site and 2 – 3 hd^{-1} across a range of temperatures at the downstream site. The uniform warming generated increases of about 8 hd^{-1}concentrated around +1.1 °C at the upstream site and about 7 hd^{-1} concentrated around +1.8 °C at the downstream site. Table 2 provides detailed duration information for two specific temperatures (18 and 22 °C). All warming scenarios show higher exceedance durations for both comparison temperatures at both sites. Yet, warmer daytime and nighttime differ than uniform warming. In particular, stream temperature increased for longer durations exceeding 22 °C under warmer daytime and nighttime. The downstream site shows the most differences in duration and variability between the different warming scenarios.

Discussion

The Effects of Climate Change on the Heat Budget

The stream's total heat flux for the 2002 base case (Fig. 2-7) was positive (heat gain) during the daytime and negative (heat loss) during the nighttime. Solar radiation dominated the heat budget during the daytime; evaporation and longwave radiation (LW) dominated the heat budget during the nighttime. Throughout the diel cycle, air convection and bed conduction alternated between sources and sinks but were minor components of the heat budget.

The net heat gain increased in all warmer air cases during most of the diel cycle (Fig. 2-8). In contrast to the total heat flux, longwave radiation and air convection were the largest contributors to the change. Solar radiation, the largest overall component of the total heat flux (Fig. 2-7), was unchanged assuming cloud cover was unchanged.

For the uniform case (Fig. 2-8a), the changes in the four major heat fluxes were approximately constant over the diurnal cycle. Relative to the 2002 base case, energy gains in air convection and longwave radiation added ~40 Wm^{-2} to the stream's total heat flux. Energy losses in evaporation and bed conduction removed ~10 $W\ m^{-2}$ from the stream's total heat flux. For the uniform case, the difference between air temperatures and stream temperatures increased everywhere and at all times. This difference was the primary factor of the nearly constant change in increased (net positive) air convection and longwave radiation heat fluxes and in decreased (net negative) evaporation heat flux. Total heat flux changes generated by diurnally uniform air temperature changes have been qualitatively similar in other studies (Cristea and Burges, 2010; Mohseni *et al.*, 1999; Stefan and Preud'homme, 1993).

For the warmer daytime and nighttime cases (Figures 8b and 8c), some of the heat fluxes varied significantly over the diurnal cycle. Relative to the 2002 base case, energy gains in air convection and longwave radiation added ~0 to ~70 Wm^{-2} to the stream's heat budget at different times of the day. Energy losses in evaporation and bed conduction removed ~5 to ~15 Wm^{-2} from the stream's heat budget. The change in the heat fluxes peaked between noon and midnight for warmer daytime case. The opposite was true for the warmer nighttime case, where the changes in the heat fluxes peaked between midnight and noon.

In general, the heat changes were in-phase with air temperature changes but stream temperatures changes were out-of-phase with air temperature changes. Warmer daytime air temperatures generated positive daytime heat flux changes. In a simple, static system, temperature change is proportional to the integral of heat fluxes – i.e., heat fluxes have a cumulative effect on temperature. While the heat budget of a stream is not simple and the system is not static, heat fluxes still tend to have a cumulative effect on temperature. The simulation showed that the effect of changes in air temperature on stream temperature was lagged. Stream temperature changes tended to be greatest after several hours of changed heat flux, so that warmer daytime air temperatures generated the greatest changes in water temperature at night. Similarly, warmer nighttime air temperatures were also out of phase with stream temperature changes, which were largest during the daytime. All three cases vary in influencing 7DADM calculations, among other stream temperature standards.

The 7DADM is calculated from the daily maximum stream temperatures. In the John Day River, those temperatures generally occur during the daytime (afternoon to evening). Daily maximum temperatures are lower at the upstream site than the downstream site. In addition, these maximum temperatures occur during the early afternoon at the upstream site and towards the end of the day at the downstream site (Fig. 2-4 shows a typical daily temperature cycle in July). The simulations showed that the timing of air warming and its magnitude influence both the timing and the magnitude of stream warming. The results (Fig. 2-4) indicated that nighttime air warming increased the 7DADM the most during the daytime than the other warming cases. At the upstream site for July 26th, the maximum difference in 7DADM between warmer daytime and nighttime scenarios was 1.6 °C at 11:00, while the difference at the maximum daily temperature was 0.7 °C at 15:00. At the downstream site, the maximum difference in the 7DADM between warmer daytime and nighttime scenarios was 0.9 °C at 14:00, while the difference at the maximum daily temperature was 0.6 °C at 17:00. Because the difference between stream temperatures under the warming scenarios is lower at the downstream site, the 7DADM values at this site tend to be similar.

The similarities in 7DADM values at the downstream site are partly due to cold-water inflow immediately upstream of this site. Tributaries entering the stream along the study section have influence on the stream heat budget. Although the warmer nighttime scenario has the potential to cause higher 7DADM values, cold tributaries entering the stream can modify the effect of a warmer nighttime. Two cold tributaries entering the stream upstream of the site: Dunston Creek and Big Boulder Creek. Both streams have lower temperatures than the mainstem Middle Fork John Day. In addition, Big Boulder Creek's discharge is relatively high when compared to other tributaries. Under these circumstances, warmer nighttime will yield smaller increases in daytime stream temperature and so the 7DADM is not increased as much, and warmer daytime will not have as large effect on daytime stream temperatures.

The increase in stream temperature averaged over 14 July was only 1.2 °C at the upstream site where heat fluxes were higher, as opposed to a 1.9 °C at the downstream site where heat fluxes were lower. This counter-intuitive result is partly an artifact of the way I set up the model runs. I held the upstream boundary condition for discharge and water temperature constant at its 2002 values for all simulations. Stream water heated as it flowed downstream because it was exposed to much warmer air temperatures. This heating was cumulative, so that downstream locations warmed more than upstream locations, regardless the heat fluxes at a particular point. This highlights the fact that stream temperature is a function of both cumulative upstream effects and heat fluxes at a given point throughout the diel period.

Model Limitations

As is the case for any modeling study, the scope of the results is limited by the assumptions. The simulations disregarded changes in boundary conditions for discharge and temperature at both the headwaters and the incoming tributaries. The longitudinal increase in stream temperature in the model simulations is, at least in part, an artifact of the modeling approach in which I kept upstream and tributaries discharge and temperature the same as the 2002 base case. I expect that the boundary conditions have significant impact on the stream's temperatures. These impacts are possibly critical to prediction of stream temperature in a changing climate. However, the goal of this study was not the prediction influence of future condition on stream temperatures, but to understand the sensitivity of stream temperatures to the timing of changes in air temperatures.

In the study, I used the "one-at-a-time" sensitivity analyses approach to simulate the influence of changing one factor on stream temperature; i.e., air temperature (See Saltelli *et al.* 2006, for further information). I added one level of complexity when simulated the time-related change in air temperature. In real stream conditions many other factors are expected to change due to warmer climate. The influence of these changes on stream temperature was not studied in this paper. Yet, modeling the influence of all changes in the system as a whole would yield better representation of future conditions.

Implications of Different Diurnal Patterns of Air Temperature Increases

I examined what is, perhaps, the simplest alternative way to distribute an average air temperature increase over time. Data currently available to us included downscaled projections of future air temperature changes resulting from ensemble means of many GCM runs (Mantua *et al.*, 2009 and 2010). These data provided an estimate of the future change in mean monthly air temperatures. However, modeling the sensitivity of stream temperatures to air temperature timing required hourly inputs of a variety of micro-meteorological data, including solar radiation, air temperature, relative humidity, and wind speed. This disparity between the data source and the data needed to run the model makes it difficult to use GCM outputs to project future changes in stream temperature.

Most previous attempts to model changes in stream temperature resulting from climate change have used the “delta method”, or uniform case, by taking a time series of weather data and adding a constant value to the air temperature (Caissie *et al.*, 2007; Cristea and Burges, 2010). However, climate-induced changes in air temperature are unlikely to be uniform (Alexander *et al.*, 2006; Morak *et al.*, 2011). Unfortunately, there are an unlimited number of ways that increased air temperatures could be manifest. They could result from short periods (days to a week) of each month with historically unprecedented and extremely hot weather, with air temperatures over much of the intervening time running near current long term means. Alternatively, long periods could be slightly warmer than the historical mean. Clearly, an infinite number of potential time series could be produced for a sensitivity analysis using mechanistic models to examine possible effects on stream temperature. I chose to examine the potential effects of differential nighttime versus daytime warming because some studies have found that warm nights have become more frequent with time (Alexander *et al.*, 2006). Also, the daytime and nighttime scenarios could be considered end-members of possible distributions of warmer air, at least over a 24-h period.

Gooseff *et al.* (2005) found that warmer daytime air and increases in solar radiation lead to larger maximum increases in stream temperature than warmer nighttime air, but that warmer nighttime air leads to more hours of moderate increase in stream temperature than warmer daytime air. Gooseff *et al.*'s study differed from ours in that their model's solar radiation changed. This difference, in addition to a different location, makes direct comparison difficult. However, the differences in results suggest that some conditions may generate in-phase changes of air temperature and stream temperature, while other conditions may generate out-of-phase changes. The reasons for the differences should be clarified by future research. That said, the results are in agreement with Gooseff *et al.* that nighttime warming of air is likely to lead to longer times of moderately warmer stream temperatures than daytime warming of air. Climate change with predominantly warmer nights or predominantly warmer days are likely to generate more extreme stream temperatures ranges.

The results show that air temperatures of equal daily average but of different diurnal range, lead to different distributions of stream temperature changes. The warmer day/night cases generated periods of several hours duration that were warmer than would occur for the uniform case. Whether this difference is important will depend on the details of a stream's ecology and on the associated thresholds for ecological damage. Where streams are already close to temperature thresholds, the details of daytime or nighttime warming may be critical.

The 7DADM and the duration curves are similar for nighttime warming and daytime warming of the air. However, details on the timing are different – e.g., nighttime vs. daytime warming of stream temperature. The impact of these timing details is unknown. Much research for cold-water fish species has examined upper lethal temperature thresholds. Stream temperature regulates a number of environmental variables, from concentration of dissolved oxygen to rates of biogeochemical processes via Arrhenius' equation. Consequently, ecosystems may be sensitive in different ways to changes in the nighttime and daytime stream temperature regimes.

Conclusions

In the Middle Fork John Day River of Oregon, USA, simulations of a +4 °C increase in average July air temperature generated approximately +1.8 °C warmer 7DADM stream temperatures at the downstream end of a 37-km study section. Temperature changes concentrated in one part of the day (e.g., warmer daytime or warmer nighttime) lead to a wider range of stream temperatures, and more extreme temperatures, than a uniform increase in air temperature. Changes in air temperature over the diurnal cycle had different timing than the changes in stream temperature. The changes in air temperature were generally out of phase with changes in stream temperature because of the cumulative nature of changes in heat fluxes on stream temperature. Warmer days and nights generate longer durations of the warmest stream temperatures. Together, the results suggest that stream temperatures in a warming climate are sensitive not only to the average temperature increase, but also to the timing of the increase. I emphasize, however, that the upstream and tributary temperatures were not changed in the simulations. In order to make predictions of true changes to stream temperature, upstream and tributary temperatures matter, as well as any changes in shade and geomorphology.

Acknowledgements

The authors thank the following agencies and staff for funding and constructive collaboration. The US Geological Survey and the US Forest Service Pacific Northwest Research Station provided funding through joint venture agreement 10-JV-11261991-055 with Oregon State University. Julia Crown and Dan Turner from the Oregon Department of Environmental Quality and Cyrus Curry from Oregon Watershed Enhancement Board collaboration and the Intensively Monitored Watersheds project's staff provided the technical support for the Heat Source model, the TMDL reports and monitoring records. Stephane Charette from the Oxbow Conservation Area Habitat and the Confederated Tribes of the Warm Springs provided support for fieldwork and access to the study area. The authors thank two anonymous reviewers for evaluating this paper and making comprehensive comments.

Table 2-1: Summary of boundary conditions over the simulation period (stream discharge and temperature of tributaries and upper end). Values were extracted from 2002 data- modified from Crown and Butcher (2010). Model inputs were not changed in any air warming scenarios.

#	**Name**	**river km**	**River Bank**	**Discharge (m^3s^{-1})**			**Temperature (°C)**		
				Max	Min	Average	Max	Min	Average
	Upper End Flow	36.95	-	0.58	0.17	0.30	27.69	11.57	19.23
a	Clear Creek	35.5	Left	0.16	0.06	0.09	28.0	12.0	20.5
b	Bridge Creek	34.7	Left	0.11	0.04	0.06	28.4	12.2	20.8
c	1st Cert. 82405 Divers.	33.75	-	0.00	-0.06	0.00			
d	Davis Creek	33.35	Left	0.04	0.02	0.03	32.2	13.8	23.6
e	Vinegar Creek	32.65	Right	0.08	0.02	0.04	34.6	14.8	25.4
f	2nd Cert. 82405 Divers.	32.3	-	0.00	-0.06	0.00			
g	Vincent Creek	31.55	Right	0.03	0.01	0.02	29.8	12.8	21.8
h	Dead Cow Creek	31.45	Right	0.01	0.00	0.00	17.1	9.9	12.7
i	Deerhorn Creek	26.6	Left	0.08	0.03	0.05	35.2	15.2	25.7
j	Little Boulder Creek	25.85	Right	0.04	0.02	0.02	35.4	15.2	25.9
l	Little Butte Creek	23.75	Left	0.01	0.00	0.01	32.4	13.9	23.8
m	Hunt Gulch	23.3	Right	0.00	0.00	0.00	32.7	14.1	24.0
n	Butte Ck	19.25	Left	0.07	0.03	0.04	23.3	9.2	15.9
o	Granite Boulder Ck	17.55	Right	0.09	0.01	0.06	21.9	8.3	15.0
p	Ruby Creek	16.2	Left	0.02	0.01	0.01	22.0	9.0	15.7
q	Beaver Creek	16.15	Right	0.01	0.01	0.01	22.5	9.4	16.5
r	Ragged Creek	15.88	Left	0.01	0.00	0.00	25.8	11.2	18.9
s	Dry Creek	12.9	Right	0.00	0.00	0.00	38.3	16.4	28.0
t	Big Boulder Ck	11.4	Right	0.17	0.01	0.11	22.8	9.8	16.7
u	Dunston Creek	7.6	Left	0.00	0.00	0.00	27.7	11.9	20.3
v	1st Permit 28039 Divers.	6.35	-	-0.12	-0.12	-0.12			
w	2nd Permit 28039 Divers.	5.2	-	-0.03	-0.03	-0.03			
x	Camp Creek	3.25	Left	0.06	0.02	0.05	32.0	11.2	21.0

Table 2-2: Exceedance duration under 2002 conditions simulation and under 4 °C increase in air temperature for the uniform warming, warmer daytime, and warmer nighttime (summary for July). Simulation results all warming scenarios show longer durations of exceedance at both sites for both selected temperatures (18 and 22 °C). Results of warmer daytime and nighttime simulations show various durations compared to the uniform warming.

		2002	**Uniform warming**		**Warmer Day**		**Warmer Night**	
Stream Temp.	Site	(hd^{-1})	(hd^{-1})	Relative to 2002 (hd^{-1})	(hd^{-1})	Relative to uniform (hd^{-1})	(hd^{-1})	Relative to uniform (hd^{-1})
>18 °C	Upstream	16.4	19	+2.6	18.7	-0.3	18.9	-0.1
	Downstream	19.7	23.4	+3.7	23.4	0	23.4	0
>22 °C	Upstream	4.5	7.6	+2.9	8.5	+0.9	7.9	+0.3
	Downstream	7.8	13.4	+5.6	13.7	+0.3	13	-0.4

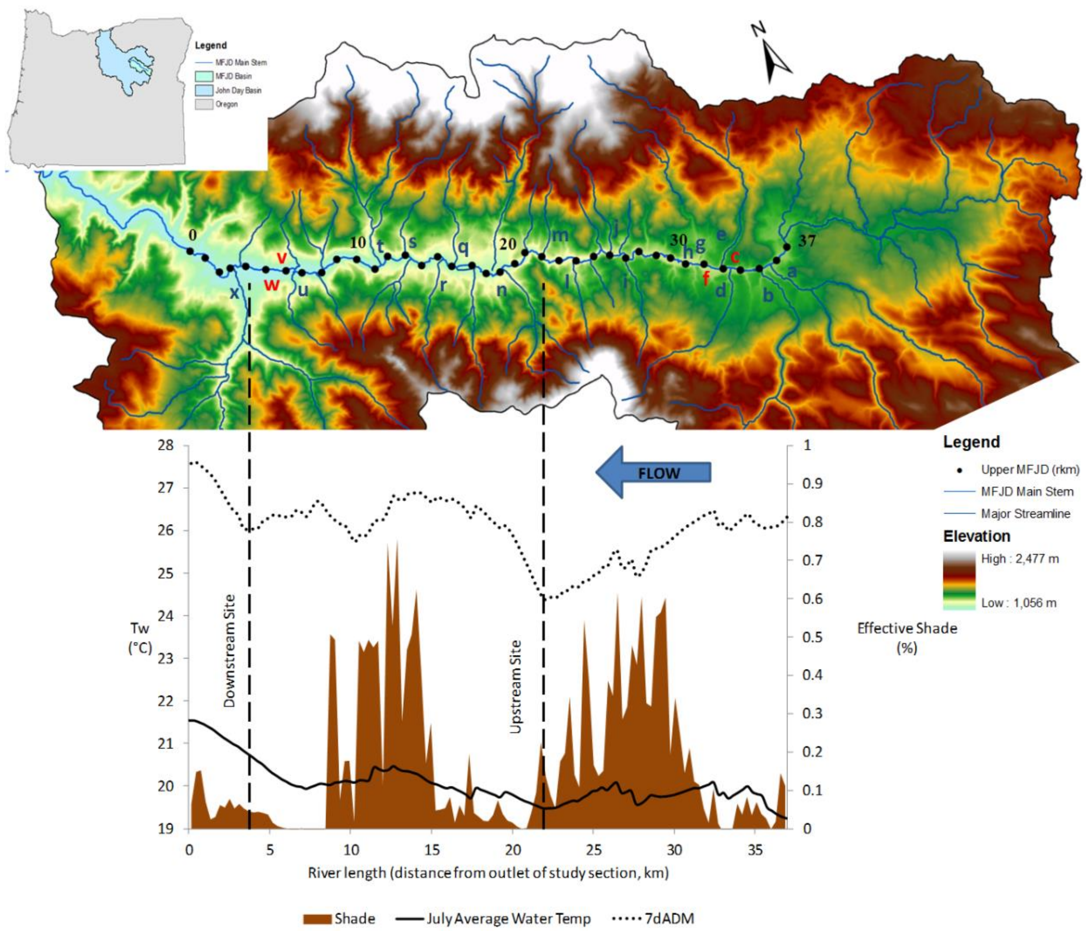

Figure 2-1: Map of the study section of the Middle Fork John Day (MFJD) and summary data of longitudinal effective shade, 7DADM stream temperature and average stream temperature during July 2002.

Figure 2-2: Air temperatures input at 3.2 rkm in July (close to the downstream site). (a) Diurnal temperature for 48 h for 2002 and for the warmer climate cases (all +4 °C): uniform, warmer daytime and warmer nighttime. (b) Air temperature ranges in July for 2002 and for warmer air cases.

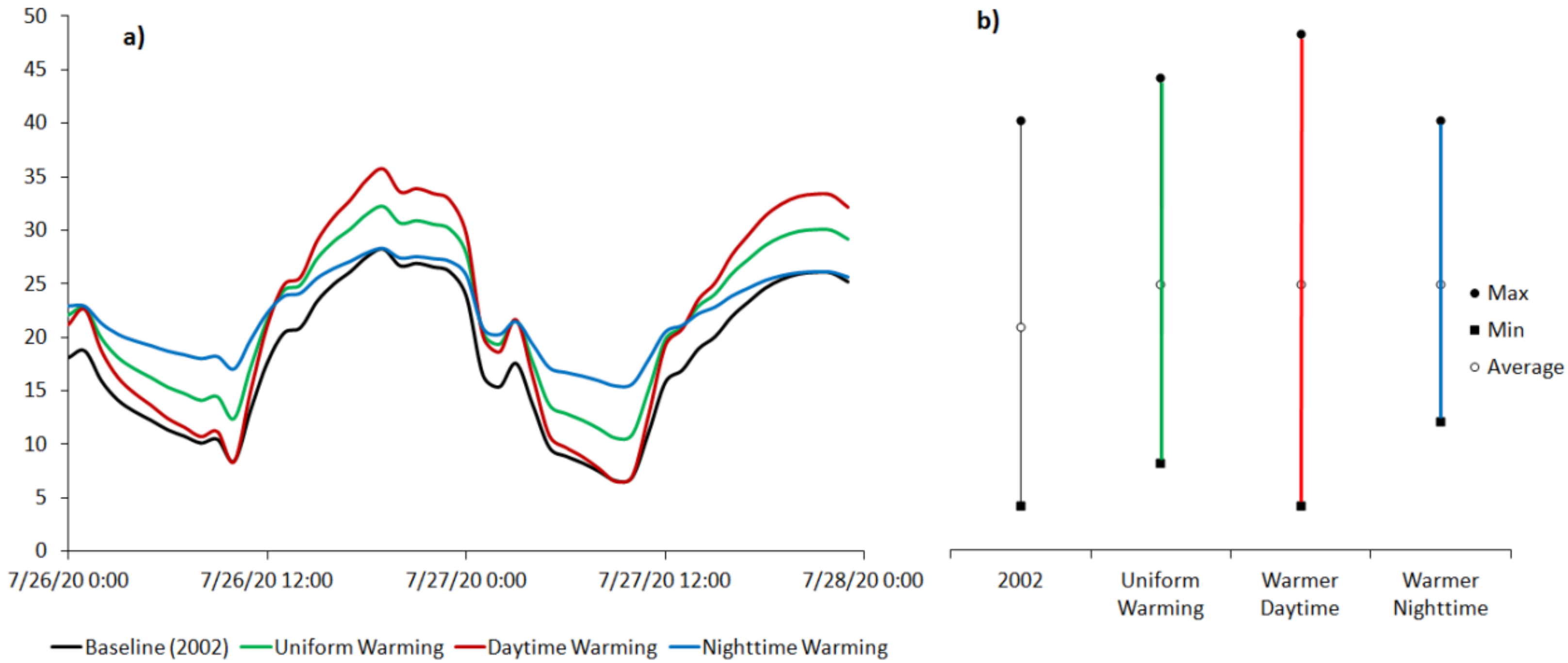

a)
b)
50
45
40
35
30
25
20
15
10
5
0
7/26/20 0:00
7/26/20 12:00
7/27/20 0:00
7/27/20 12:00
7/28/20 0:00
Baseline (2002)
Uniform Warming
Daytime Warming
Nighttime Warming
2002
Uniform Warming
Warmer Daytime
Warmer Nighttime
Max
Min
Average

Figure 2-2

Figure 2-3: (a) 7DADM of stream temperatures responding to the three cases of warmer air (4 °C increase in average monthly air temperature), June–August. (b) Change in 7DADM stream temperatures responding to 4 °C increase in average monthly air temperature. The compared sites (indicated by dashed dark line) are at points where there is small different in 7DADM.

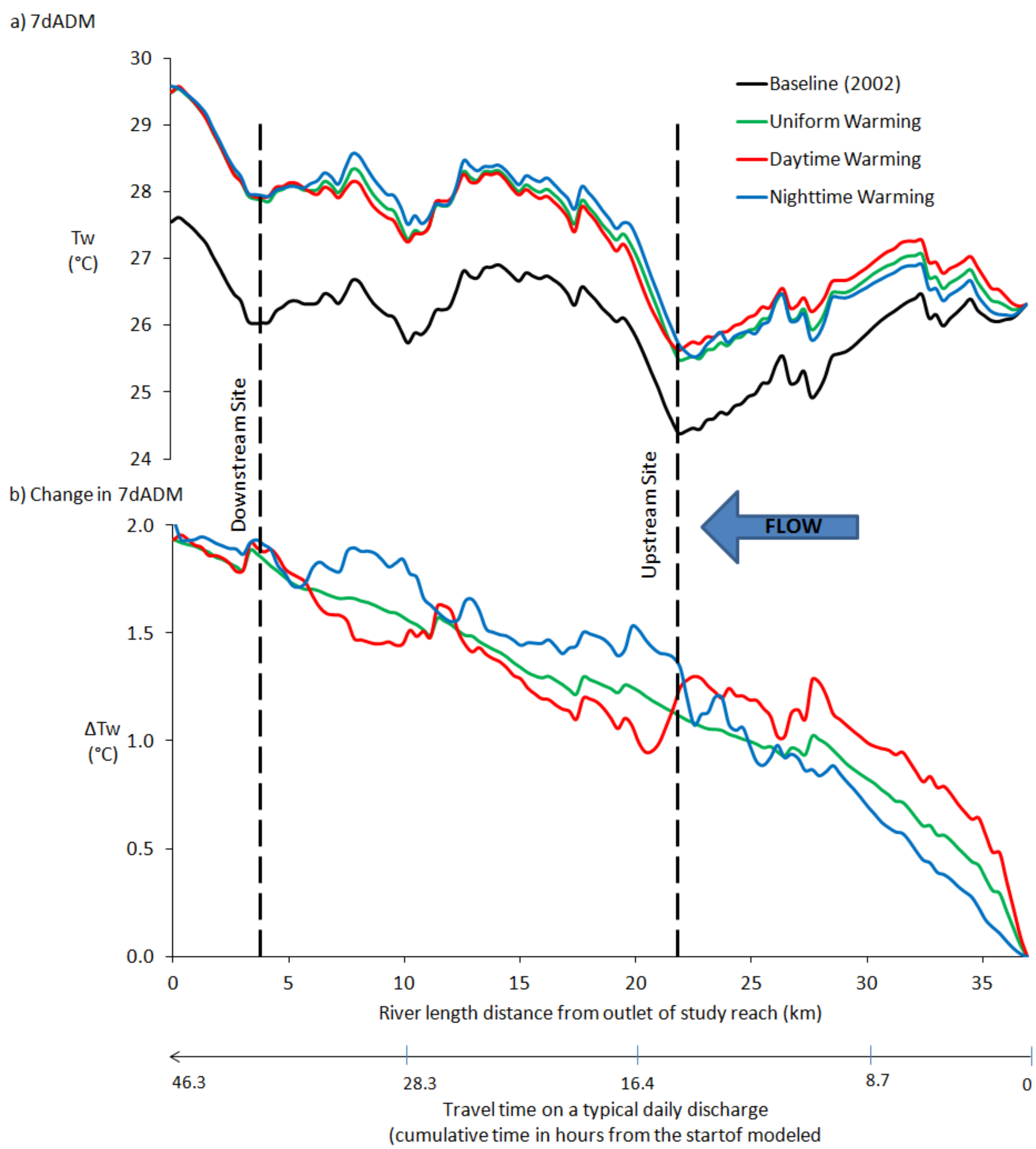
a) 7dADM
Tw
(°C)
30
29
28
27
26
25
24
Baseline (2002)
Uniform Warming
Daytime Warming
Nighttime Warming
b) Change in 7dADM
ΔTw
(°C)
2.0
1.5
1.0
0.5
0.0
Downstream Site
Upstream Site
FLOW
0
5
10
15
20
25
30
35
River length distance from outlet of study reach (km)
46.3
28.3
16.4
8.7
0
Travel time on a typical daily discharge
(cumulative time in hours from the startof modeled

Figure 2-3

Figure 2-4: Diurnal fluctuation of stream temperature in 2002 (black line) and stream temperature changes responding to the three cases of warmer air. (a) Upstream site and (b) downstream site. The figure shows the results of a single day—26 July. The peak temperature in the 2002 case occurs earlier in the day at the upstream site than the downstream site, whereas the downstream site shows lower difference between warmer daytime and warmer nighttime change than the upstream site at the time of the peak temperature.

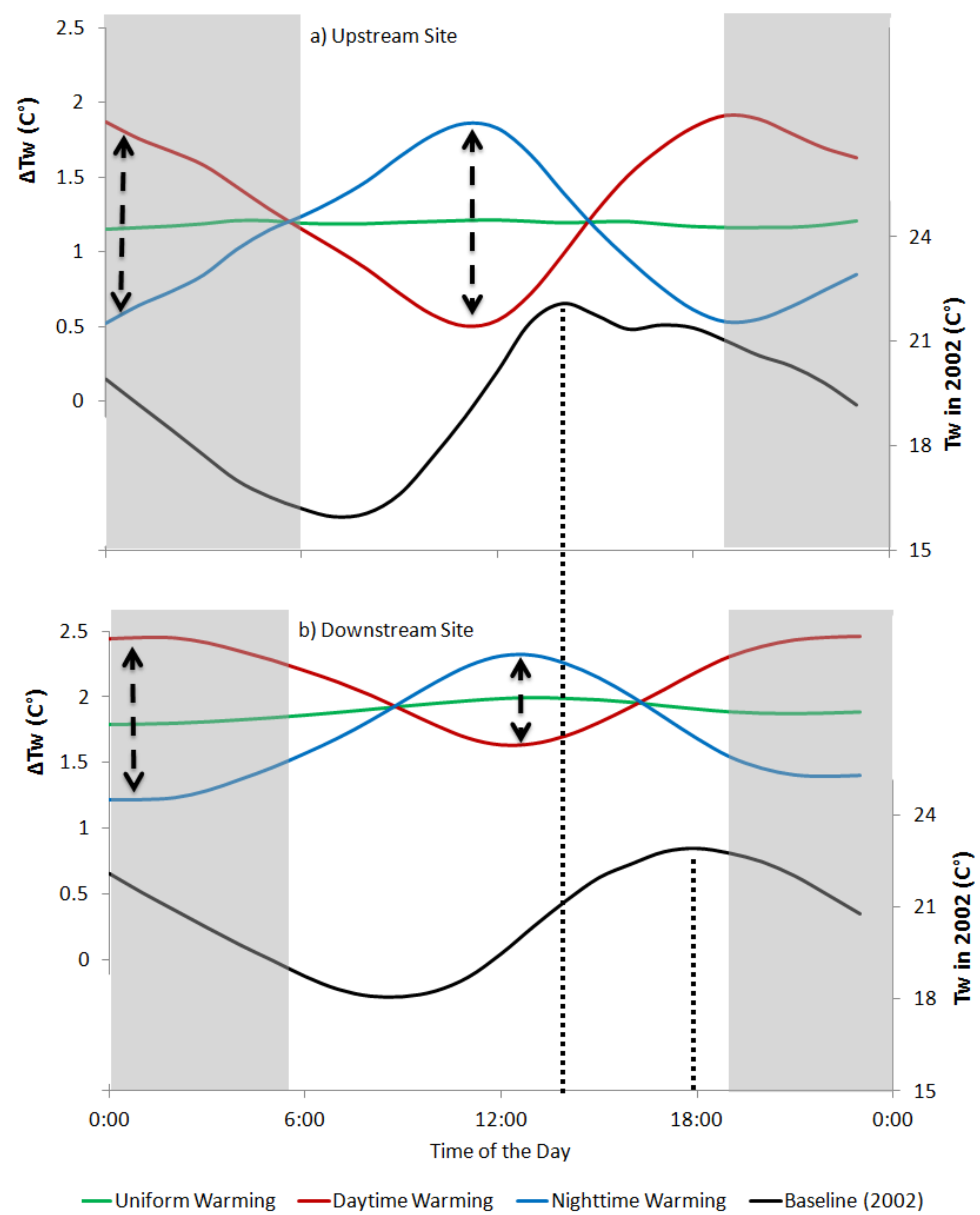

a) Upstream Site
b) Downstream Site
ΔTw (C°)
Tw in 2002 (C°)
2.5
2
1.5
1
0.5
0
24
21
18
15
0:00
6:00
12:00
18:00
0:00
Time of the Day
Uniform Warming
Daytime Warming
Nighttime Warming
Baseline (2002)

Figure 2-4

Figure 2-5: Range of changes in stream temperature relative to 2002 (simulation results) responding to the different warmer air cases at the upstream and the downstream sites. (a and b) Uniform case. (c and d) Warmer daytime case. (e and f) Warmer nighttime case.

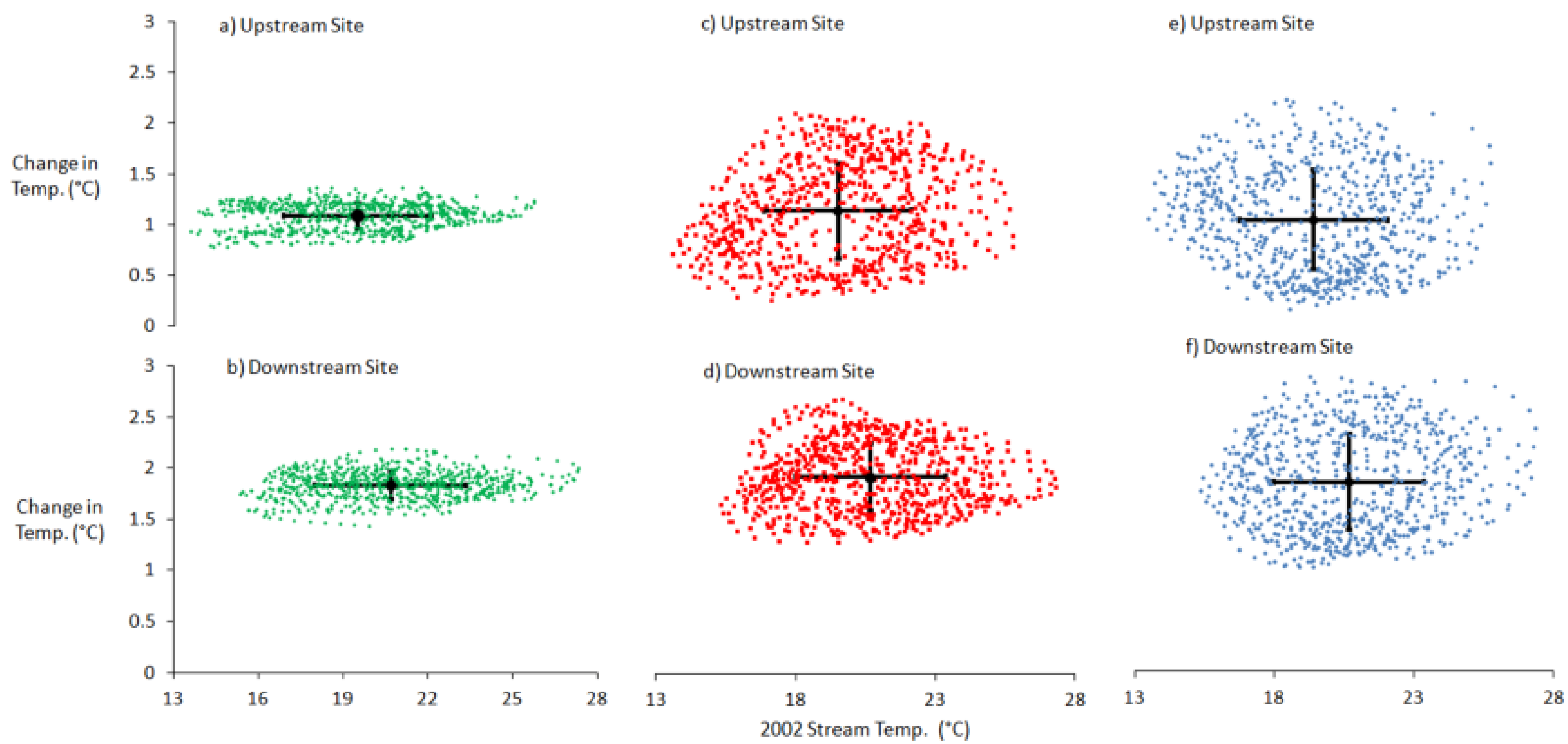
a) Upstream Site
b) Downstream Site
c) Upstream Site
d) Downstream Site
e) Upstream Site
f) Downstream Site
Change in Temp. (°C)
Change in Temp. (°C)
0
0.5
1
1.5
2
2.5
3
13
16
19
22
25
28
13
18
23
28
2002 Stream Temp. (°C)

Figure 2-5

Figure 2-6: The daily average duration (hd^{-1}) of the change in stream temperature (summary for July simulation results). (a) Upstream site and (b) downstream site. The uniform case resulted in a moderate, narrow range of stream temperature increases for a longer duration than the warmer daytime and nighttime cases, which resulted in shorter durations for a wide range of change in stream temperature. Note that at 4 rkm, the warmer nighttime resulted in lower increases in stream temperatures than the warmer daytime.

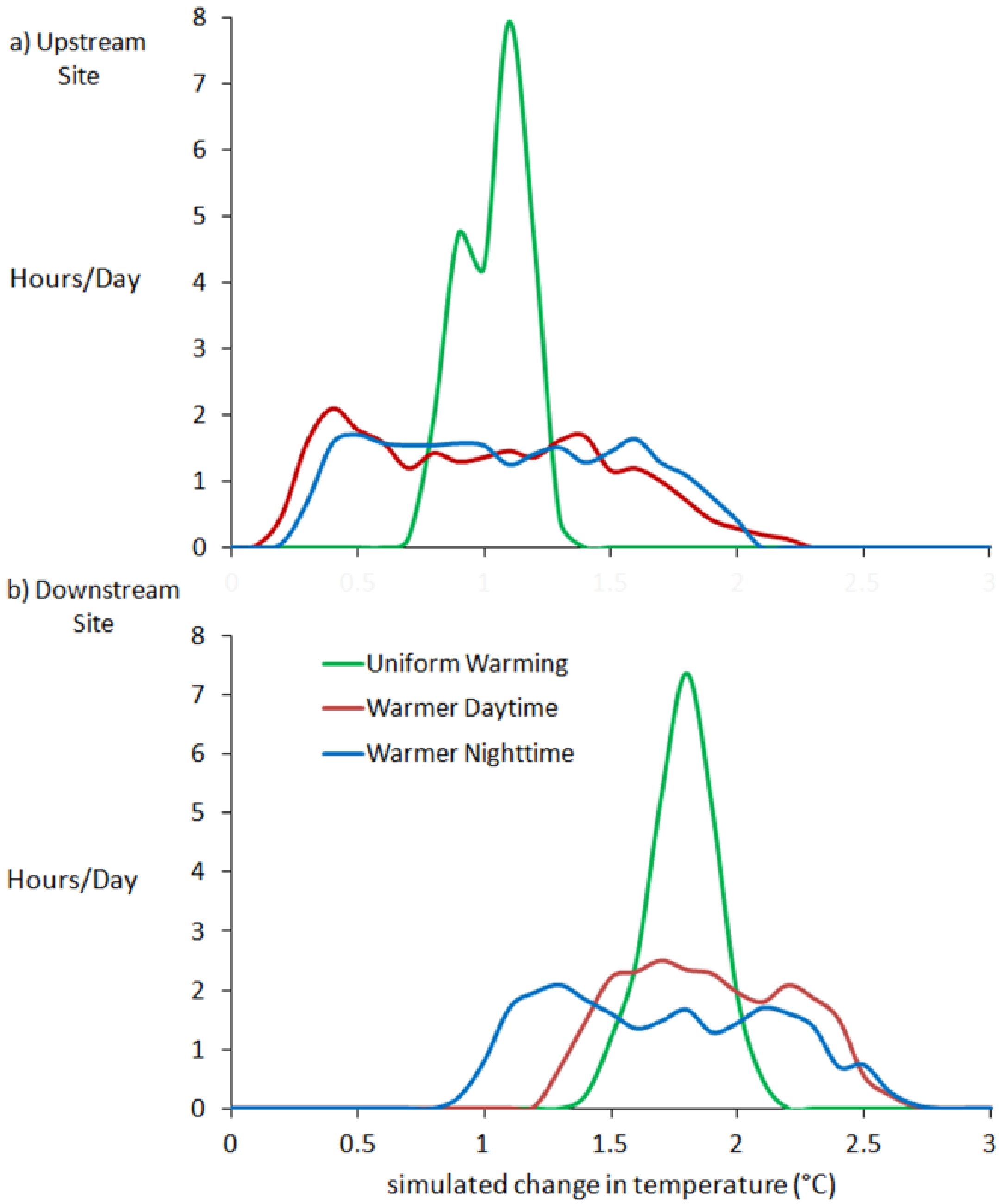
a) Upstream Site
Hours/Day
8
7
6
5
4
3
2
1
0
b) Downstream Site
Hours/Day
Uniform Warming
Warmer Daytime
Warmer Nighttime
0
0.5
1
1.5
2
2.5
3
simulated change in temperature (°C)

Figure 2-6

Figure 2-7: Components of the heat budget in 2002 at the downstream site. Solar radiation is the main factor of stream heat budget followed by longwave and evaporation. Air convection and bed conduction are the lowest.

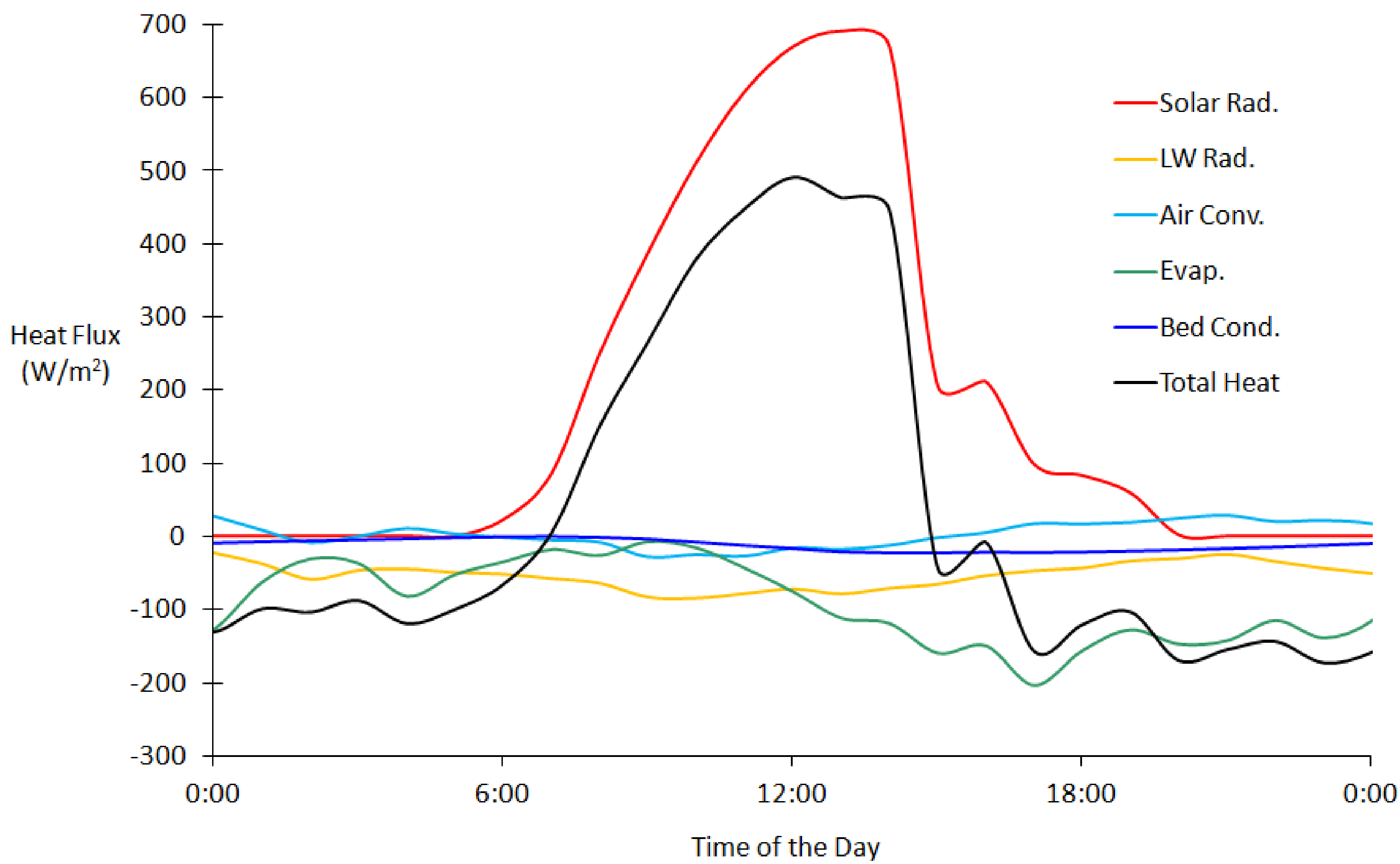
700
600
500
400
300
200
100
0
-100
-200
-300
Heat Flux
(W/m²)
0:00
6:00
12:00
18:00
0:00
Time of the Day
Solar Rad.
LW Rad.
Air Conv.
Evap.
Bed Cond.
Total Heat

Figure 2-7

Figure 2-8: Changes to the heat fluxes under a warmer climate. The uniform warming case resulted a semi-uniform changes to all heat fluxes (other than solar radiation, whereas the model assumes no change to solar radiation). Counterintuitive results were shown under warmer daytime and nighttime cases: most of the change in heat fluxes occurred during the nighttime under daytime warming and during the daytime under nighttime warming. Changes to heat fluxes at the downstream site (not shown) were almost identical to those at the upstream site.

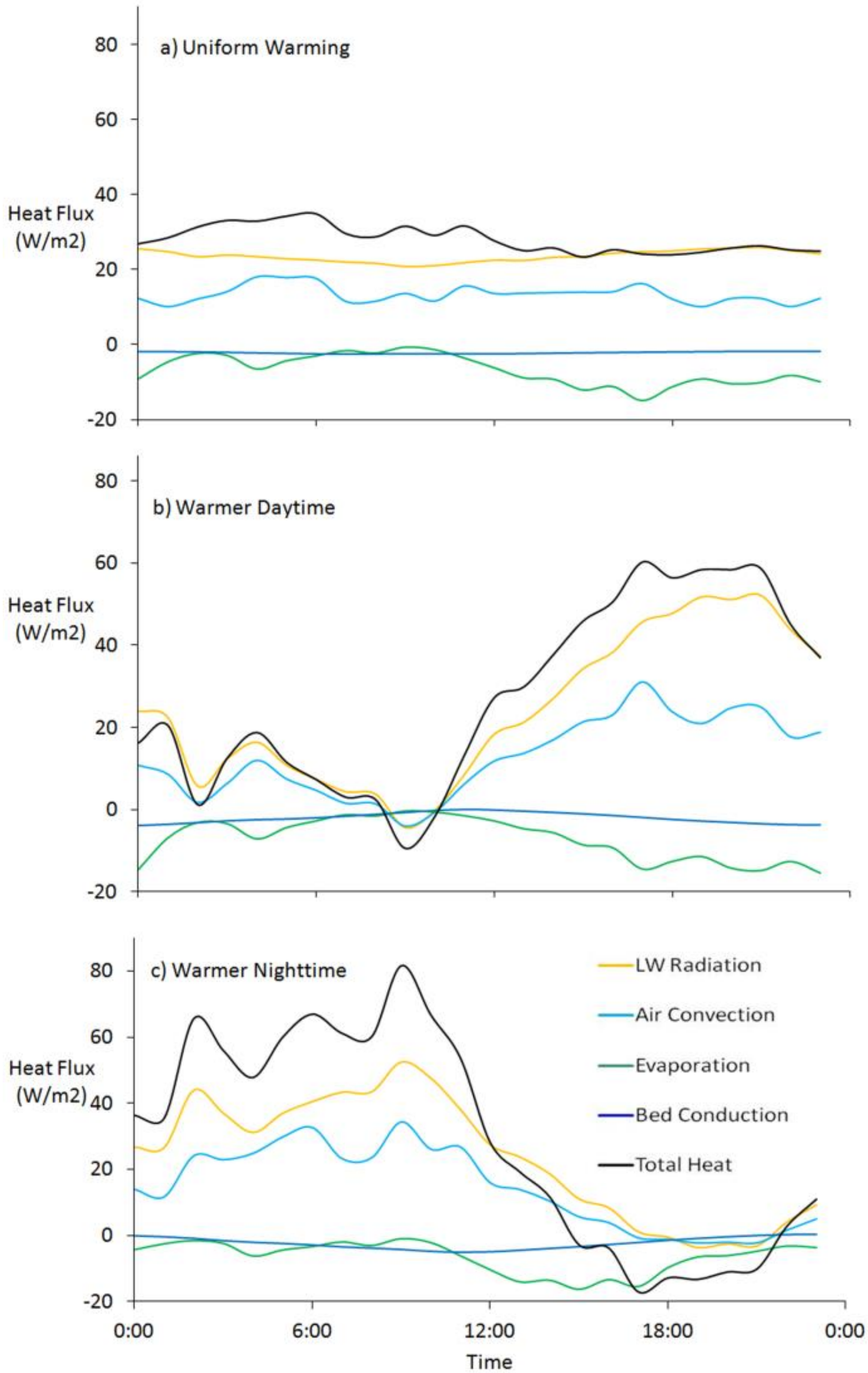

a) Uniform Warming
b) Warmer Daytime
c) Warmer Nighttime
Heat Flux (W/m2)
80
60
40
20
0
-20
0:00
6:00
12:00
18:00
0:00
Time
LW Radiation
Air Convection
Evaporation
Bed Conduction
Total Heat

Figure 2-8

3. Estimating Stream Temperature Response to Cumulative Influence of Changing Air Temperature, Flow, and Riparian Vegetation

Mousa Diabat
Steven M. Wondzell
Roy Haggerty

Abstract

Stream temperature response to changes in environmental conditions is of great concern for freshwater aquatic ecosystems. I analyzed changes in both stream temperature and heat budget along an upper 37-km section of the Middle Fork John Day River in northeastern Oregon, USA, in response to changing air temperature, stream flow, and riparian vegetation. I used the software Heat Source, a mechanistic model calibrated to the current conditions of the study section, and simulated the response of summer stream temperature to two air temperature increases of 2 °C and 4 °C, two stream flow variations of +30% and -30%, and three riparian vegetation conditions of 7%, 34%, and 79% effective shade. All these conditions represent possible scenarios of 21st century climate change and land management strategies. Results suggest that riparian vegetation had the greatest influence on stream temperature, while stream flow has a negligible influence. The 7-day average daily maximum of stream temperature (7DADM) varied over a range of about 10 °C due to changing the effective shade, while the 7DADM varied over a range of only 1 °C due to changing stream flow. Increasing the effective shade along the study section, especially the unshaded sections, can mitigate the influence of increasing air temperature. In fact, the 7DADM can be decreased below current values even under future climate conditions of warmer air if the riparian vegetation is restored to increase the effective shade. While 4 °C air warming increased the 7DADM by up to 2 °C, increasing the effective shade reduced the 7DADM by as much as 6.9 °C below the current conditions.

Introduction

Stream temperature is an essential, physical property of freshwater ecosystems that moderates metabolism and growth of aquatic organisms (McCullough, 1999; Myrick and Cech, 2005; Richter and Kolmes, 2005), impacts their reproductive ability, and may limit the distribution of different salmonid species (McCullough, 1999; Myrick and Cech, 2005; Richter and Kolmes, 2005). The main environmental parameters influencing stream temperature are climate conditions, watershed hydrology, and land-use. However, the majority of studies have investigated stream temperature response to one or two input parameters and have rarely investigated stream temperature response to the cumulative influence of multiple parameters (LeBlanc *et al.*, 1997; Roth *et al.*, 2010).

Across the globe, stream temperature increases have been correlated with or attributed to air warming, diverting stream water, or declining riparian vegetation (Constantz, 1998; Groom *et al.*, 2011; Imholt *et al.*, 2013; Mellina *et al.*, 2002; Mohseni *et al.*, 1999; Sinokrot and Gulliver, 2000; Sugimoto *et al.*, 1997; Webb *et al.*, 2003). Climate projections for the Pacific Northwest indicate that air temperature will increase and stream flow will vary with a tendency to decrease during the summer (Mantua *et al.*, 2009, 2010). Timber harvest in the Pacific Northwest significantly decreased effective shade and is considered a major cause of increasing stream temperature, especially for small streams and headwaters (Johnson and Jones, 2000; Kibler *et al.*, 2013; Mitchell, 1999; Pollock *et al.*, 2009). Replanting riparian vegetation is a common restoration practice both to improve habitat conditions of degraded stream temperatures and to mitigate the effect of future climate changes (Beschta and Ripple, 2005; Johnson, 2004; St-Hilaire *et al.*, 2000).

Assessing stream temperature in the near future depends on forecasts of climate, watershed hydrology, and vegetation. Forecasts of the 21st century's climate overwhelmingly indicate increasing air temperatures (Elsner *et al.*, 2010; Hamlet *et* *al.*, 2013; Mantua *et al.*, 2009). I conducted a sensitivity analysis of stream temperature in the Middle Fork John Day River to improve the understanding of the cumulative influence of air temperature, stream flow, and riparian vegetation on stream temperature. To explain the cumulative influence of changing multiple parameters on stream temperature, I investigated the response of a stream's heat budget to changing climate and environmental conditions. The objectives of the study are (1) to identify the individual stream temperature sensitivity to each parameter individually, (2) to identify stream temperature sensitivity to the interactive effect of simultaneous changes in all three parameters, and (3) to compare the importance of climate and land cover changes on stream temperature.

Methods

Study Section

The John Day River is among the few remaining free-flowing tributaries of the Colombia River. The study section is a 37-km reach along the upper Middle Fork John Day River (MFJD) in northeastern Oregon, USA (Fig.1) starting 1.5 km upstream of the confluence with Clear Creek (44°35'48"N, 118°29'36"W) and ending 3.25 km downstream of Camp Creek (44°42'39"N, 118°48'55"W). The study section can be characterized as a series of unconstrained subreaches running through wide riparian meadows connected by constrained subreaches with narrow valley floors (Clair and Fields, 2004; Crown and Butcher, 2010; Hunt and Stepleton, 2004). The bedrock geology of the MFJD is predominantly Columbia River Basalt Group and felsic volcanic and volcaniclastics of the John Day Group (Hunt and Stepleton, 2004). Nineteen tributaries enter the study section and drain an area of 827 km^2 (Fig. 3-1). The elevation of the streambed along the study section decreases from 1,245 m to 1,035 m. The upper elevations of the MFJD's drainage basin receive an annual average of 1,270 mm of precipitation, with less than 10% falling during the hottest months of July and August.

The natural riparian vegetation of the MFJD includes black hawthorn (*Crataegus douglasii*), wood's rose (*Rosa woodsii*), cottonwood (*Populus balsamifera*), and mountain alder (*Alnus incana*). It is also common to find sedge (*Carex spp.*) in some portions of the valley as well as ponderosa pine (*Pinus ponderosa*) on south-facing hillslopes and various conifers such as Douglas fir (*Pseudotsuga menziesii*) on north-facing hillslopes (Grant, 1994). Regional surveys report a wide range of canopy densities and tree height for current stands. Beschta and Ripple (2005) reported that some of the native tree species, especially cottonwood and aspen (*Populus tremuloides*), are mostly absent in the riparian forested areas in the MFJD and attributed the lack of native forest to historical anthropogenic activities. Later surveys by Wells (2006) and Przeszlowska and Wondzell (2009, unpublished data) reported that stands of ponderosa pine might exceed 40 m in height with 90% canopy density and cottonwood could reach 30 m in height with 80% canopy density.

A mix of anthropogenic activities between the late 1800s and early 1900s, such as gold mining, grazing, railway construction, dredging, and logging, altered riparian vegetation and channel morphology in the MFJD. In the 1860s, gold mining activities disturbed streambed gravels and reduced the riparian vegetation (Grant, 1994). Beginning in the 1880s, sheep became a major source of income for the region and consequently grazing areas expanded. Constructing a railroad along the mainstem of the MFJD and its major tributaries in the early 1900s improved timber transportation and expanded logging operations. The stream's route was also channelized and forced to the sides of the valley floor along some sections of the MFJD (Beschta and Ripple, 2005; Clair and Fields, 2004; Grant, 1994; Wissmar *et al.*, 1994). In turn, it has been estimated that the study section of the MFJD lost about 50% of the tree cover (Grant, 1994). Constructing the railroad and channel dredging activities during the first half of the 1900s limited the meandering of the active channel across the valley floor. These anthropogenic changes, particularly the loss of riparian vegetation, led to increasing stream temperatures in the MFJD and numerous watersheds across the

Pacific Northwest (Groom *et al.*, 2011; Johnson and Jones, 2000; Mellina *et al.*, 2002; Pollock *et al.*, 2009).

Rearing and spawning habitats in the John Day River are important for cold-water fish species, in particular for steelhead (*Oncorhynchus myskiss*) and spring Chinook salmon (*Oncorhynchus tshawytscha*) because they are among the last natural wild run of salmonid species in the Columbia River Basin. The John Day River enters the Columbia River upstream the Bonneville dam, which is the first downstream most dam. There have been no dams built along the John Day River and it has no fish hatcheries. The MFJD is listed as water quality limited under section 303(d) of the Federal Clean Water Act because it does not meet Oregon's water temperature standards. Restoration projects in the MFJD basin focus on improving aquatic habitat and aim to mitigate the effects of climate change on stream temperature. Current projects in the MFJD are actively replanting native trees along riparian areas and modifying the channel to its historical meanders.

Modeling Framework: Parameterized and Calibrated Models - Heat Source

I used the software Heat Source version 8.04 (Boyd and Kasper, 2003; Boyd, 1996) for the stream temperature simulations. The Oregon Department of Environmental Quality (ODEQ) maintains and distributes Heat Source (http://www.deq.state.or/wq.tmdls/tools.htm). Heat Source simulates stream temperature using a finite-difference algorithm that calculates changes to the stream's heat budget from physically-based measurements: boundary conditions, atmospheric conditions, channel structure, and spatially distributed land-cover. Boundary conditions consist of a time-series data of flow and water temperature at the upstream boundary of the simulated stream section as well as for all entry points of tributaries and groundwater sources along the stream reach. Heat Source calculates flow, average velocity, and the top width and average depth of the wetted channel for the entire length of the simulated stream section by using the data of boundary conditions and channel morphology. The atmospheric data contains air temperature, humidity, cloud cover, and wind speed.

The effective shade is calculated from land-cover data, which consists of tree height and canopy density in addition to topography's elevation along the stream's banks within a defined distance from the stream channel. The effective shade is the percentage of shortwave radiation blocked by topography and land cover and is calculated by using the algorithm in the Shade-a-lator routine embedded in Heat Source. Shade-a-lator calculates the potential solar radiation (after penetrating the atmosphere) from the position of the sun and time of the day. Then, Shade-a-lator subtracts the shortwave radiation blocked by topographic features and land-cover from the potential shortwave radiation flux.

I obtained the parameterized model of the MFJD prepared by Crown and Butcher (2010) for ODEQ's TMDL analysis and extracted the upper 37-km for the base case simulation with one modification. ODEQ ran the stream temperature simulation for the MFJD at 300 m spatial resolution. The modification was to run the simulation at 100 m spatial resolution to support detailed analysis of results. Data from the calibrated model (Crown and Butcher, 2010) show that flow at the top of the study section decreased from 0.39 m^3s^{-1} in July to 0.15 m^3s^{-1} in August 2002. During the same period, flow of the monitored tributaries varied between 0.17 m^3s^{-1} and 0.58 m^3s^{-1}. Stream temperature of the mainstem varied between 9.8 and 28.7 °C and that of tributaries varied between 4.5 and 30 °C. The study section included four diversions that removed on average 0.03 m^3s^{-1} from the stream for agricultural use during the summer months. Crown and Butcher (2010) also estimated minor groundwater inflow between rkm 34.55 and 22.

Modifying Input Data

Modifying Air Temperature

I modified air temperature data in the base case model to represent future conditions of warmer air. The modification was based on downscaled climate forecasts that were conducted by the Climate Impact Group (CIG) at the University of Washington for climate over the current century (Elsner *et al.*, 2010; Mantua *et al.*, 2010; Mote and Salathé, 2010). Researchers in CIG downscaled the results of General Circulation Models (GCMs) for two greenhouse emission scenarios (A1B and B1) from the Fourth Intergovernmental Panel on Climate Change (IPCC, 2007). Both the A1B and B1 assume the same population growth rate, but the B1 scenario represents lower emissions and cleaner energy technologies than A1B. The CIG group downscaled air temperature to a spatial resolution of 1/16° grid with a monthly time series for several watersheds in the Pacific Northwest, USA within the greater Columbia River Basin (Mantua *et al.*, 2010; Wu *et al.*, 2012).

CIG did not include air temperature projections for a station in the MFJD among those reported in the John Day River basin. To derive the projected air temperature from the above climate projections, I analyzed projections of air temperature for 10 watersheds near the MFJD (Appendix A) to calculate the change in average monthly air temperatures between the historical data to the projected. In relation to historic values, air temperature under the A1B emission scenario would increase 1.9 °C in July-August by 2020, 3.2 °C by 2040, and 5.4 °C by 2080; whereas under the B1 emission scenario, air temperature would increase 1.7 °C by 2020, 2.3 °C by 2040 and 3.6 °C by 2080. Given the range of these projections, I modified air temperature input data for the base case in Heat Source to account for +2 and +4 °C increases in average air temperature (Fig. 3-2). Hereafter, the base case air temperature is referred to as “Ta0”, +2 °C air warming is referred to as “Ta2”, and +4 °C air warming is referred to as “Ta4”.

Modifying Stream Flow

I modified stream flow data according to projected changes to streamflow in the Pacific Northwest (Hamlet *et al.*, 2010, 2013; Mote and Salathé, 2010). The CIG estimated that summer stream flow (June to September) could decrease by 30% in some Pacific Northwest watersheds by the end of the 21st century (Hamlet *et al.*, 2010, 2013; Mote and Salathé, 2010). Summer stream flow for the 10 basins adjacent to the MFJD may either increase or decrease (Hamlet *et al.*, 2010). Estimates range from a 20% increase to a 25% decrease for B1 emissions scenario and from a 27% increase to a 25% decrease for A1B emissions scenario (Appendix A). Therefore, I modified flow at the upper end of the study section to account for both 30% increase and 30% decrease in discharge. Hereafter, 30% increased flow is referred to as "HQ", 30% decreased flow is referred to as "LQ", and the base case is referred to as "BCQ". I did not modify diversions and groundwater inflow. Therefore, flow at the downstream end of the study section was 120-125% for HQ and 75-80% for LQ relative to the base case flow (Fig. 3-3).

Modifying Riparian Vegetation

I modified riparian vegetation features data to represent three potential scenarios in addition to current conditions. Riparian vegetation is an important parameter influencing the stream's heat budget. Tree height and canopy density of riparian vegetation alter the magnitude of solar radiation reaching the stream surface. Crown and Butcher (2010) generated heterogeneous riparian vegetation data of the base case scenario from field surveys conducted in 2002. Heat Source models the effective shade from riparian vegetation data that is directly adjacent to the stream's active channel. The longitudinal average of effective shade for the base case was 19% with only a few scattered reaches exceeding 50%. In addition to the base case, I modified the riparian vegetation in the model to represent three spatially homogeneous conditions of effective shade (Fig. 3-4). Low effective shade could represent loss of tree stands along the entire 37 km of the study section due to a wildfire with re-growth of herbaceous vegetation and small shrubs less than or equal to 1 m tall with 10% canopy density. Medium effective shade could represent a young re-growing forest when trees and shrubs have grown to 10 m height and 30% canopy density. Maximum effective shade could represent a fully vegetated valley floor with trees 30 m tall and 50% canopy density along the entire 37 km of the study section. Accounting for topography and stream geometry, I calculated a longitudinal average of 7%, 34%, and 79% for low, medium, and high effective shade scenarios, respectively (Fig. 3-4). Those modifications do not represent absolute lack of riparian vegetation or the tallest and densest riparian forest vegetation that could grow within the study section. In fact, all vegetation scenarios I generated currently exist along some portions of the study section where native shrub and tree species, such as alder (*Alnus incana*), willow (*Salix exigua*), ponderosa pine and cottonwood, can grow between 1 m to more than 30 m tall and provide canopy density that exceeds 50%.

I ran 36 stream temperature simulations representing all combinations of riparian vegetation, air temperature, and stream flow (Tables 1a-1c). I programmed a new graphical user interface specific to Heat Source that automatically handles modifying input parameters, runs the simulations, and imports relevant output results. I chose two sites along the study section for detailed analysis of simulation results: an upstream site at rkm 28 and a downstream site at rkm 14. The upstream site is located at the lower end of a low-shade 4-km stretch of the river (effective shade is ≤10%). There are no large tributaries and no diversions upstream of this site. The downstream site is also at the lower end of a low-shade 6-km stretch of the river.

Results of the stream's temperature and heat budget were compared across the different scenarios. I used the 7-day average daily maximum (7DADM) temperature along the full length of the study section to compare stream temperature results. The 7DADM is the maximum value of the 7-day running average of the daily maximum stream temperature for each stream segment along the simulated stream section (Zwieniecki and Newton, 1999; U.S. EPA, 2003; Pollock et al., 2009). I also analyzed the stream's heat budget on the day that the 7DADM occurred at the selected sites, which in all scenarios it was July 14th. The 7DADM occurred for most stream length occurred on this date.

I present heat exchanges as heat flow (Wm^{-1}), which is the heat flux (Wm^{-2}) multiplied by the channel's width at the water surface (m). This value enables to compare heat exchange at locations and times for which width differs. Heat flow can be interpreted as energy change in a unit of water per unit distance travelled.

Results

Single Parameter Sensitivity Analysis

Stream temperature simulations showed that riparian vegetation had a greater influence on the 7DADM (Fig. 3-5) than either air temperature or stream flow. The 7DADM varied in a range of 9.6 °C in response to changing the effective shade alone (Fig. 3-5a). With low effective shade conditions, the 7DADM increased by up to 2.3 °C and with high effective shade conditions, it decreased by up to 7.3 °C in comparison to the base case. With 4 °C warmer air, the 7DADM increased by up to 2 °C (Fig. 3-5b), while with ±30% change in stream flow, the 7DADM varied in a range less than 0.8 °C (Fig. 3-5c).

The effective shade had greater influence on the stream's heat budget than air temperature or stream flow (Fig. 3-6). Heat input from shortwave radiation decreased during the daytime by 3,600 Wm^{-1} with high effective shade conditions and by 2,000 Wm^{-1} with medium effective shade at the downstream site (Fig. 3-6a). However, heat dissipation increase at night low effective shade (Fig. 3-6b). The effect of changing effective shade was greater during the daytime than nighttime (Fig. 3-6a and Fig. 3-6b). Heat dissipation increased with low effective shade mainly due to modifying both the net longwave radiation and the convective heat leading to higher 7DADM than the base case. Conversely, heat input decreased with high effective shade mainly due to blocking shortwave radiation (Fig. 3-5c). Furthermore, the effective shade remained the greatest factor during the day compared to air temperature or stream flow (Fig. 3-5c). Over the diel cycle at the selected site, the net heat input decreased and net heat dissipation increased as effective shade was higher than the base case.

Stream flow had a minor influence on the overall heat budget relative to either air temperature or riparian vegetation (Fig. 3-6). Changing the flow influenced all components of the stream's heat budget, especially shortwave radiation and evaporation. In LQ scenario, the stream gained less heat from shortwave radiation during the day (Fig. 3-6a) and dissipated less heat in evaporation and longwave radiation during the nighttime (Fig. 3-6b) in comparison with base case scenario. In HQ scenario, the stream gained more heat from shortwave radiation during the day (Fig. 3-6a) and dissipated more heat in evaporation and longwave radiation during the nighttime (Fig. 3-6b) in comparison with base case scenario. As a result, reduced flow decreased the net heat dissipation while increased flow increased the net heat dissipation relative to the base case conditions (Fig. 3-6c). However, the daily maximum stream temperature was affected by heat budget of the day, in which LQ scenario decreased heat gain by 9% and HQ scenario decreased the heat gain by 6%.

Increasing air temperature, Ta2 or Ta4, increased heat gain by convection and reduced heat dissipation by longwave radiation relative to the base case (Ta0). Warmer air increased the daytime net heat gain mainly due to reduced heat dissipation in longwave radiation (Fig. 3-6a). However, warmer air also increased daytime evaporative heat. The effect of warmer air was also apparent in nighttime heat budget; the net nighttime heat dissipation decreased due to decreased dissipation in longwave radiation and increased heat gain in convection (Fig. 3-6b). As a result, increasing air temperature shifted the stream's daily net heat from heat dissipation to a heat gain.

The Combined Influence of Modifying Multiple Parameters

The combined influence of modifying multiple parameters stream temperature and heat budget differed from the influence of a single parameter on. The greatest increase in 7DADM occurred in a scenario that combined 4 °C warmer air (Ta4), low flow (LQ), and low effective shade. Under these conditions, the 7DADM increased by up to 2.8 °C, compared to 2.1 °C increase under low effective shade alone. Conversely, the greatest reduction in 7DADM was under conditions of high effective shade, low flow (LQ), and no change in air temperature (Ta0). Under these conditions, the 7DADM decreased by up to 7.9 °C compared to 7.3 °C reduction under high effective shade alone. Furthermore, the results showed that increasing the effective shade mitigated the combined influence of high air temperature and low flow conditions and reduced the 7DADM for the entire length of the study section compared to the base case (Fig. 3-7).

The combined influence of modifying multiple parameters was also apparent on the stream's heat budget. I show four potential scenarios of the different effective shade conditions (base case, low, medium, and high) all under 4 °C warmer air and low stream flow (Fig. 3-8). With base case riparian vegetation or low effective shade, low flow conditions caused the stream to gain less heat in shortwave radiation during daytime, than the base case conditions (Fig. 3-8a). The stream also dissipated less heat in longwave radiation and convective heat because of warmer air. Under the same conditions of low flow and warmer air, the stream dissipated less heat during the nighttime (Fig. 3-8b) than the base case conditions. Over the course of a full day and with low effective shade, the influence of warmer air and low flow shifted the stream's net heat from heat dissipation state to heat gain state. With increasing effective shade along the study section, the stream's net heat decreased despite warm air and low flow conditions. Under high effective shade conditions, heat input from shortwave radiation declined during the daytime (Fig. 3-7a) leading to a lower net heat over the course of full day. As a result, high effective shade was able to offset the influence of warm air and low flow conditions (Fig. 3-8c).

The influence of stream flow on the 7DADM varied with changing effective shade (Fig. 3-9a). HQ decreased the 7DADM and LQ increased the 7DADM under conditions of low effective shade conditions, but differences in 7DADM caused by changing flow are small. As effective shade increased and reached about 45%, results showed that changing flow had no effect on 7DADM. However, LQ decreased the 7DADM and HQ increased the 7DADM under conditions of high effective shade.

The influence of changing air temperature on the 7DADM varied negligibly under different effective shade conditions (Fig. 3-9b). Heat input in longwave radiation and convective heat increased as air temperature increased regardless of the influence of effective shade on the stream's heat budget.

Discussion

This study defined the range of stream temperature sensitivity to the combined effect of changing riparian vegetation, air temperature, and stream flow. Stream temperature was greatly sensitive to changes in riparian vegetation and moderately sensitive to changes in air temperature, while it was the least sensitive to changes in streamflow. Riparian vegetation has a greater influence on MFJD stream temperature than air temperature or stream flow. Results shown in this study are similar to several studies suggesting that increasing the effective shade (e.g., replanting tall and dense riparian vegetation) causes stream temperature maxima to decline (Cristea and Janisch, 2007; Groom *et al.*, 2011; Johnson, 2004; Lee *et al.*, 2012; Zwieniecki and Newton, 1999). Increasing the effective shade along the 37 km of this study section decreased heat input from shortwave radiation to the stream and caused stream temperature maxima to decline by 9.6 °C in comparison with low effective shade conditions. Johnson (2004) found that shading a 200 m stream section decreased the maximum water temperature by 1 °C in comparison with the same section being unshaded. Zwieniecki and Newton (1999) also reported that average stream temperature increased by almost 1.1 °C due to harvest of the riparian vegetation along 180 m of the stream.

High effective shade offset the influence of warmer air on stream temperature. Simulation results showed that stream temperature increased with increasing air temperature. Where predictions estimate that air temperature will increase by 3-5 °C throughout the 21st century (Mantua *et al.*, 2010; Mote and Salathé, 2010), warmer air would increase stream temperatures by 1-2 °C (Mohseni *et al.*, 1999; Pilgrim *et al.*, 1998; Webb *et al.*, 2003). The addition of heat input to the stream via convective heat and the reduction of heat dissipation via evaporative heat were mitigated by the reduction of heat input from shortwave radiation leading to decreased 7DADM. Trees at age of 10-15, on average, reach the maturity level to provide the desired shading effect. Thus, restoring riparian vegetation needs to take place well in advance to mitigate the influence of future changes in air temperature.

Stream flow had a small influence on MFJD's stream temperature and depended on effective shade conditions. With low-to-medium effective shade, increasing streamflow slightly decreased the 7DADM in most scenarios, so heat input from either shortwave radiation or convection was diluted in a greater water volume. With high effective shade, increasing streamflow increased the 7DADM. HQ conditions increased flow velocity and reduced travel time in the channel. Reduced travel time allows less time for heat exchange with the environment. With low effective shade, this normally generates less heat gain and, therefore, lower increase in temperature than LQ. Conversely, HQ with high effective shade generates less heat dissipation and lower reduction in temperature than LQ.

We modified input parameters in a uniform pattern (spatially and temporally) to estimate the stream's temperature responsiveness to a changing environment. Uniform modifications are not the most accurate representation of a natural environment (Diabat *et al.*, 2012; Gooseff *et al.*, 2005). For example, recent studies reported non-uniform changes of air temperature over the diurnal cycle (Alexander *et al.*, 2006; Morak *et al.*, 2011). Warmer daytime and warmer nighttime conditions differ in their impact on stream temperature both from each other and from uniform warming (Diabat *et al.*, 2012; Gooseff *et al.*, 2005). Similarly, spatially homogenous riparian vegetation is possible, but unlikely. An expansive wildfire can remove most of the riparian vegetation of an entire basin. Replanting riparian vegetation, however, has not usually been accomplished over an entire basin.

Uncertainties in simulation results are constituted in three major components: boundary conditions of upstream input and tributaries, inflow from groundwater, and hyporheic flow. In this study, stream discharge was modified without modifying water temperature of the boundary conditions. Water temperature of the boundary conditions is also subject to increase because of air warming (Erickson and Stefan, 2000; Mohseni *et al.*, 1998, 1999). To test this uncertainty factor, I simulated stream temperature for the study section and modified water temperature of the boundary conditions using the air-water regression equation in Mohseni et al. (1999) and Erickson and Stefan (2000). Results of the test simulation indicated that temperature of the boundary conditions had minor effect on the 7DADM along the study section. However, I did not examine the influence of changing either groundwater inflow or temperature on stream temperature. Hyporheic flow could create local conditions of thermal refugia especially during the summer (Arrigoni *et al.*, 2008; Ebersole *et al.*, 2003). The percentage of heat exchange through the hyporheic zone increases as stream discharge decreases (Wondzell, 2012). Stream discharge along this study section during the summer ranged between 0.3 to 1 m^3s^{-1}. Using regression correlation presented in Wondzell (2012), the hyporheic flow in the existing channel is estimated to range between 1.3 and 0.47% per 100 m stream length, which lead to the conclusion that hyporheic flow remains a negligible factor to influence stream temperature even when stream discharge fluctuate between +30% and -30%.

Results of this study may be applicable to similar watersheds where restoration projects aim to mitigate the impacts of warming climate on small stream temperature. In comparing the effectiveness to mitigate the influence of increasing air temperature by restoring riparian vegetation or restoring in-stream flow, the benefits from restoring riparian vegetation far exceed those from restoring stream flow.

Conclusions

Stream temperature simulations for the study section of the MFJD showed that riparian vegetation had greater influence on stream temperature than air temperature or stream flow. Results also showed that change in stream flow was the least influential. The study suggests that restoring riparian vegetation where the stream is poorly shaded has the potential to offset the influence of increasing air temperature. Any change in riparian vegetation that increases the effective shade along the study section will probably lead to a decreased in the maxima of summer stream temperatures in the MFJD. Warmer air increased the stream's 7DADM in a ratio close to 2:1.5. The influence of warmer air remained constant regardless of effective shade. Lastly, stream flow had a minor influence on stream temperature and did not mitigate the effect of warmer air. However, the influence of stream flow depended on effective shade conditions: high flow decreased 7DADM under low effective shade and increased 7DADM under high effective shade. The analysis is one of few studies that tested the cumulative influence of changing multiple parameters on stream temperature. The range of temperature responses shown in the study provides useful guidance for watershed managers in improving forest management practices.

Acknowledgements

The authors are thankful for constructive collaboration with and funding from the following agencies and organizations. The US Geological Survey and the US Forest Service Pacific Northwest Research Station provided funding through joint venture agreement 10-JV-11261991-055 with Oregon State University. Julia Crown and Ryan Mechie from Oregon Department of Environmental Quality who provided the total maximum daily load reports and monitoring records. The Confederated Tribes of the Warm Springs provided support for fieldwork and access to the study area.

Table 3-1: Modifications applied to the input data.

a) Air Temperature	
Name	**Change in Air Temperature (Δ °C)**
Ta0	0
Ta2	+2
Ta4	+4

b) Stream Flow	
Name	**Change in Flow (Δ %)**
BCQ	0
HQ	-30
LQ	+30

c) Effective shade			
Name	**Tree Height (m)**	**Canopy Density (%)**	**Average Effective Shade (%)**
Base Case Effective Shade	various	various	19
Low Effective Shade	1	10	7
Medium Effective Shade	10	30	34
Maximum Effective Shade	30	50	79

Figure 3-1: Map of the state of Oregon, USA showing the John Day River basin (small map) and the basin of the study site (large map).

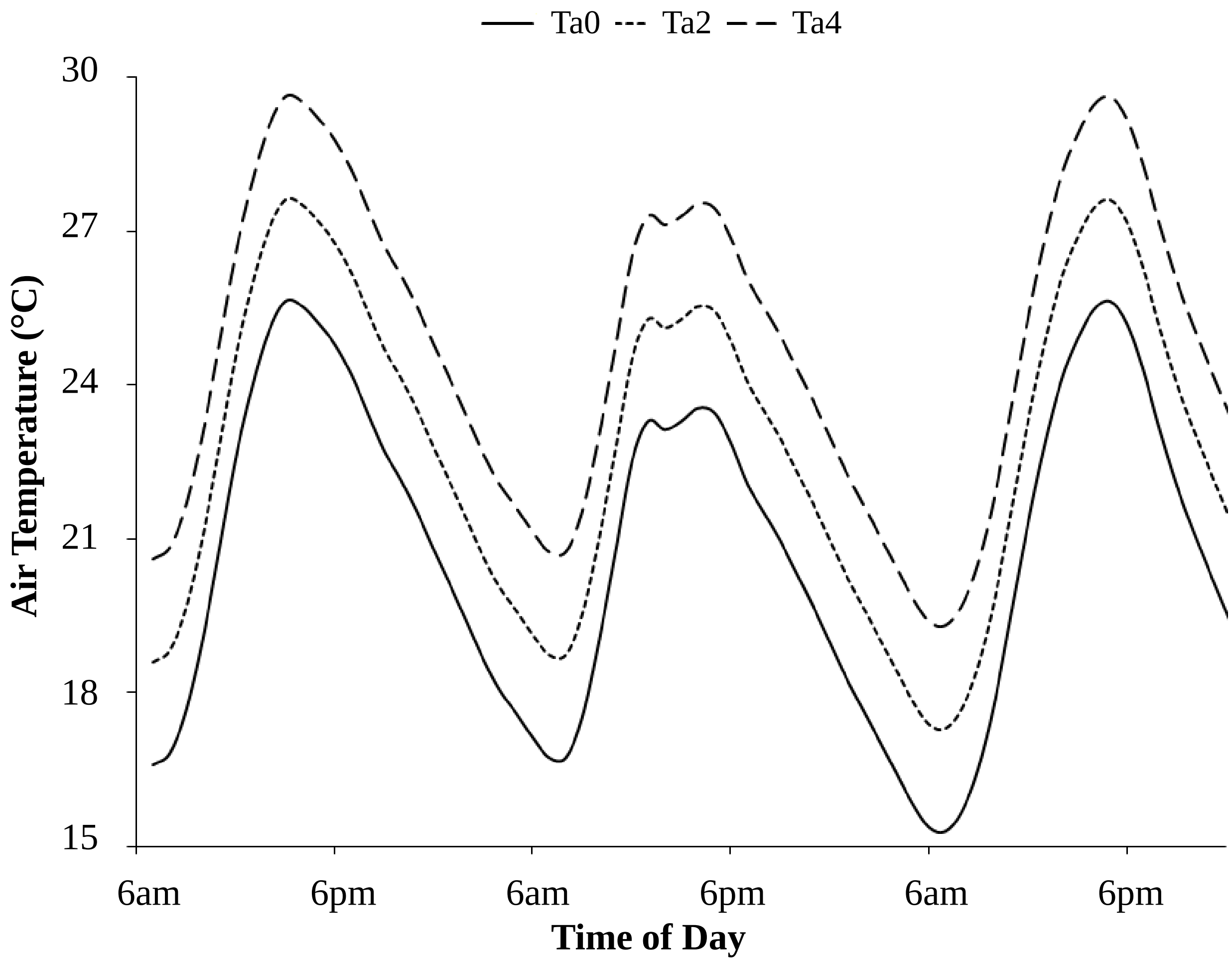

Figure 3-2: input values of air temperature over the diurnal cycle for three climate conditions base case (Ta0), 2 °C warmer air (Ta2), and 4° warmer air (Ta4). Warmer air data was produced using the delta method. Dates are July 13th – 15th.

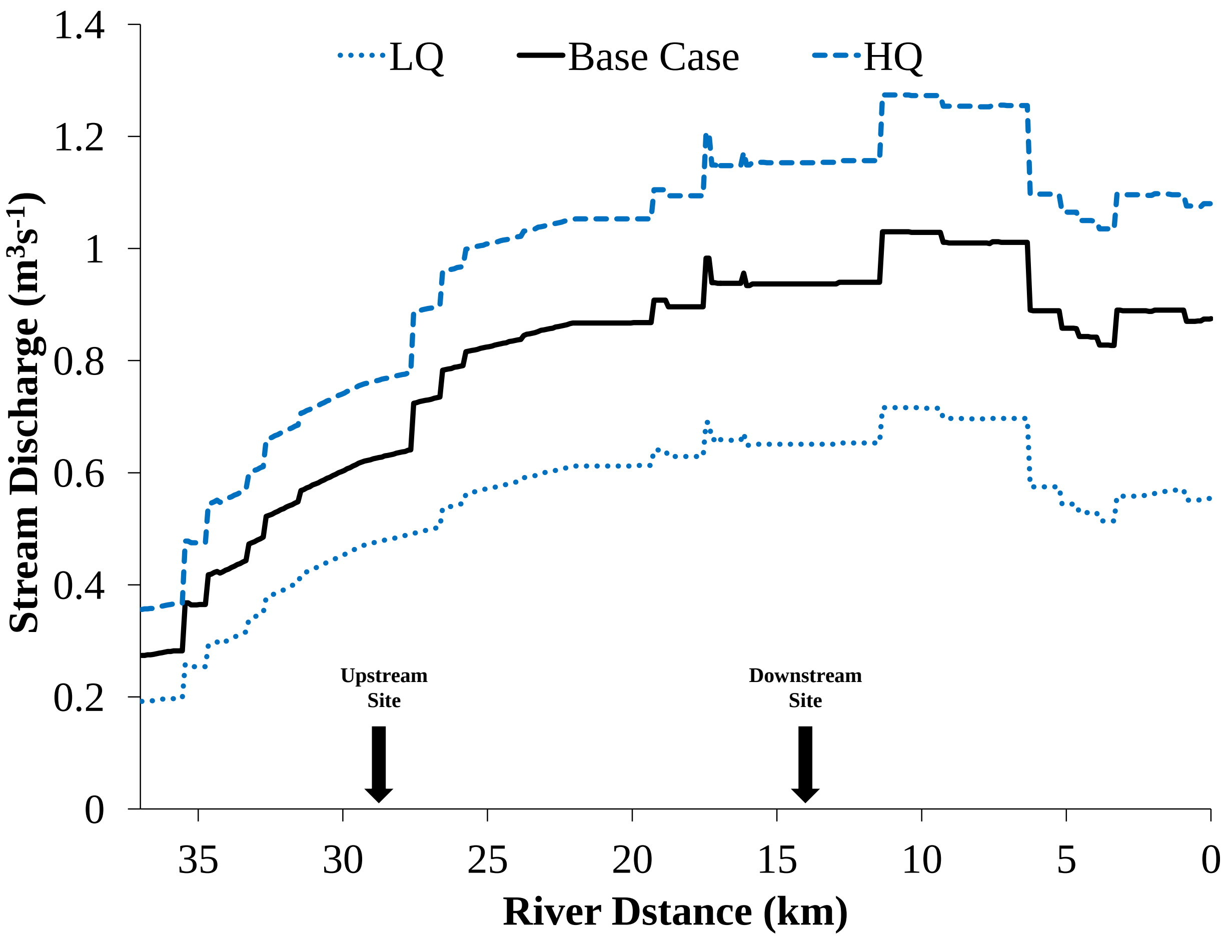

Figure 3-3: Simulated flow along the study section for base case flow (BCQ) and modified flow of boundary conditions (upper most point and tributaries). Modified boundary conditions represent 30% reduction in flow (LQ) and 30% increase of flow (HQ) relative to the base case values. Values are on July 14th.

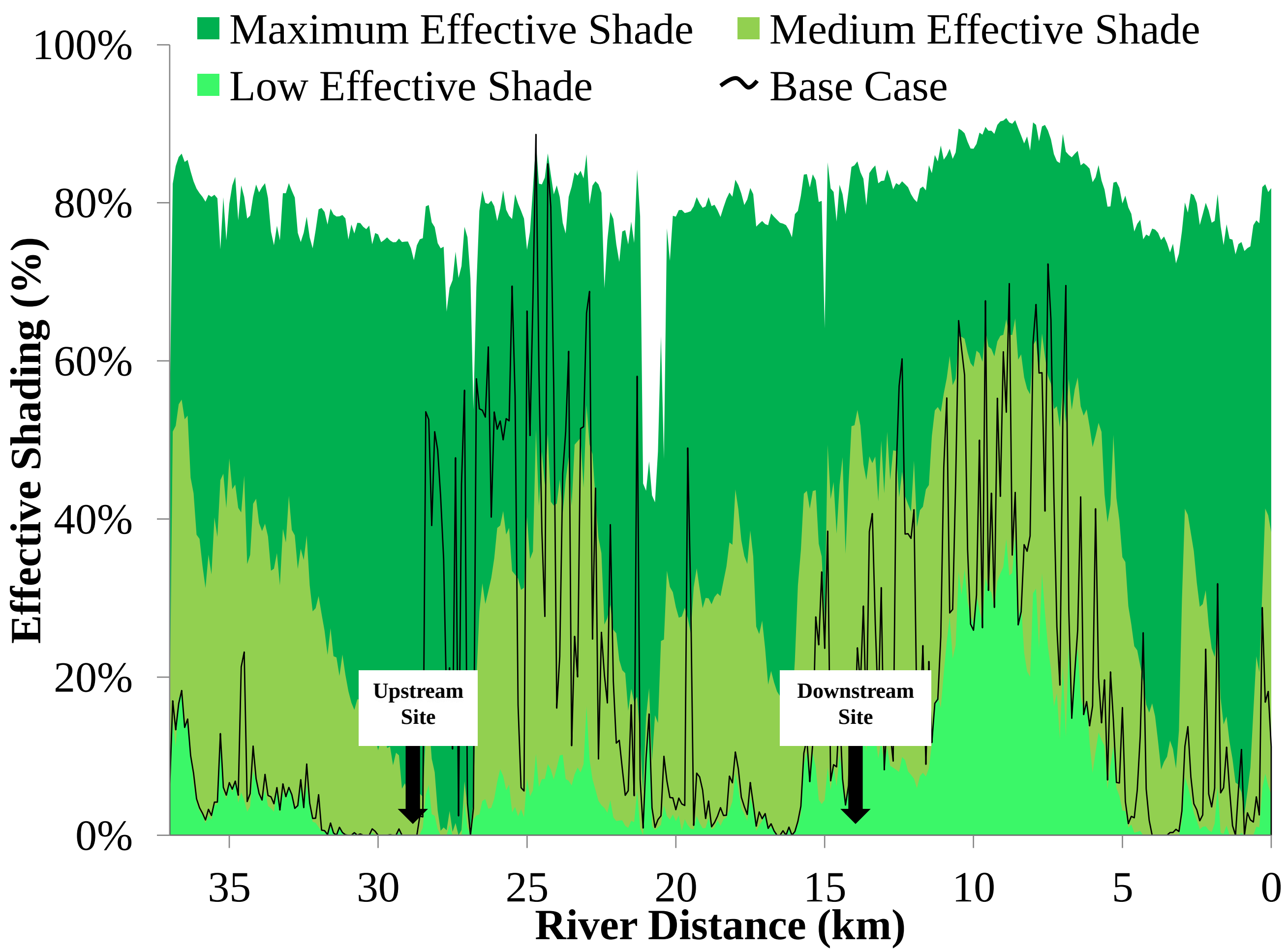

Figure 3-4: Calculated effective shade along the study section for current conditions, low effective shade, medium effective shade, and high effective shade. Values are on July 14th.

Figure 3-5: 7-day average daily maximum (7DADM) values along the study section under separate, different conditions of a) effective shade, b) air temperature, and c) stream flow. Modifying effective shade caused wider range of change in 7DADM than air temperature or stream flow.

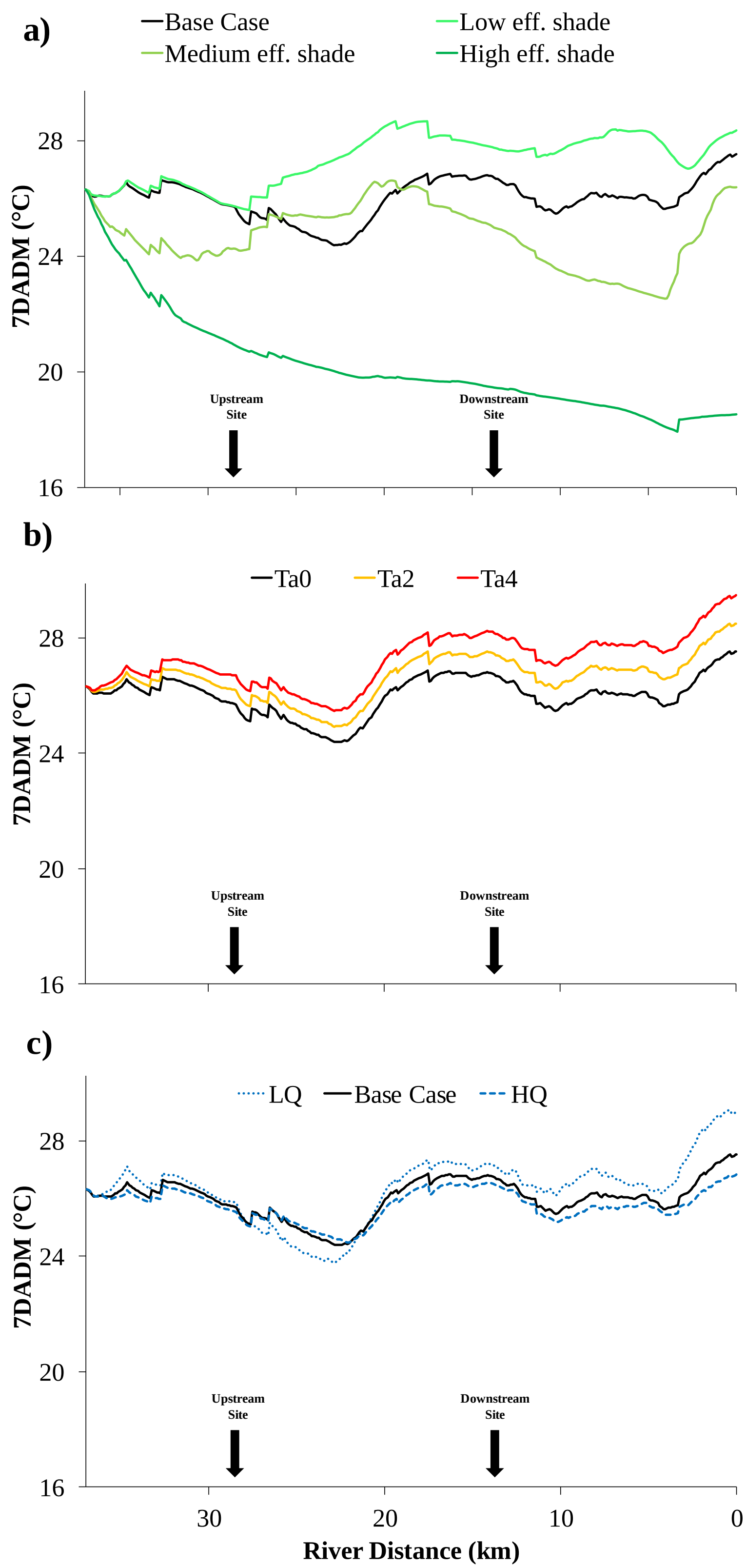

a)
Base Case
Low eff. shade
Medium eff. shade
High eff. shade
7DADM (°C)
28
24
20
16
Upstream Site
Downstream Site
b)
Ta0
Ta2
Ta4
7DADM (°C)
28
24
20
16
Upstream Site
Downstream Site
c)
LQ
Base Case
HQ
7DADM (°C)
28
24
20
16
Upstream Site
Downstream Site
30
20
10
0
River Distance (km)

Figure 3-5

Figure 3-6: Changes in heat fluxes under different conditions of effective shade, air temperature, and stream flow. Changes are summarized as the average over a) daytime, b) nighttime, and c) 24-hours duration. Modifying effective shade caused wider range of change in stream's heat budget than air temperature or stream flow any time of the day. Black vertical line marks the average heat flow of the base case conditions for the specific heat flux or net heat.

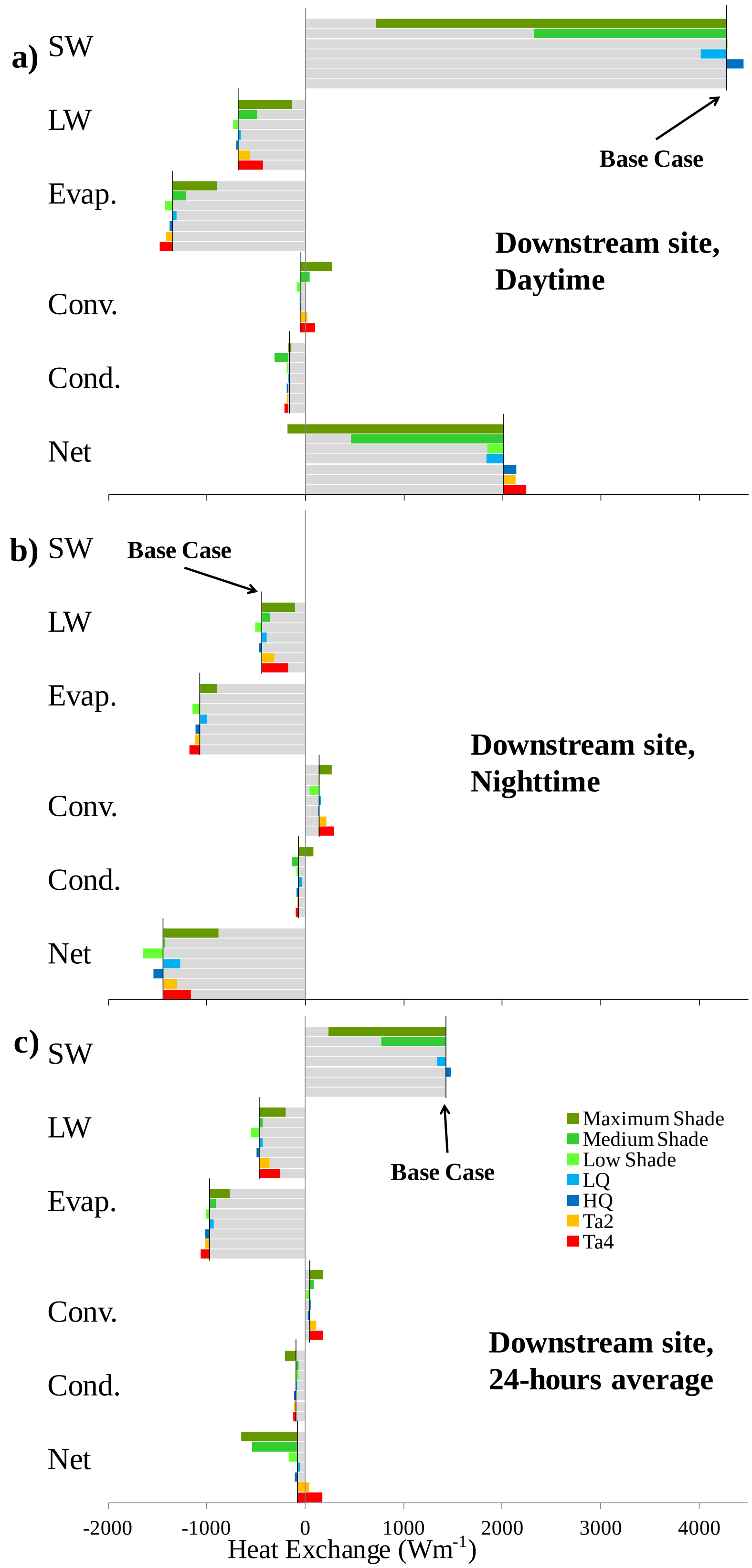

a)
SW
LW
Evap.
Conv.
Cond.
Net
Base Case
Downstream site, Daytime
b)
SW
LW
Evap.
Conv.
Cond.
Net
Base Case
Downstream site, Nighttime
c)
SW
LW
Evap.
Conv.
Cond.
Net
Base Case
Maximum Shade
Medium Shade
Low Shade
LQ
HQ
Ta2
Ta4
Downstream site, 24-hours average
-2000
-1000
0
1000
2000
3000
4000
Heat Exchange (Wm-1)

Figure 3-6

Figure 3-7: Ranges of 7DADM under the combined influence of all conditions: effective shade, air temperature, and stream flow. Results are color-grouped according to effective shade conditions. The upper border of each group is highlighted in a different color and labeled. The lower border if each group is the same and it is the base case 7DADM under that specific effective shade.

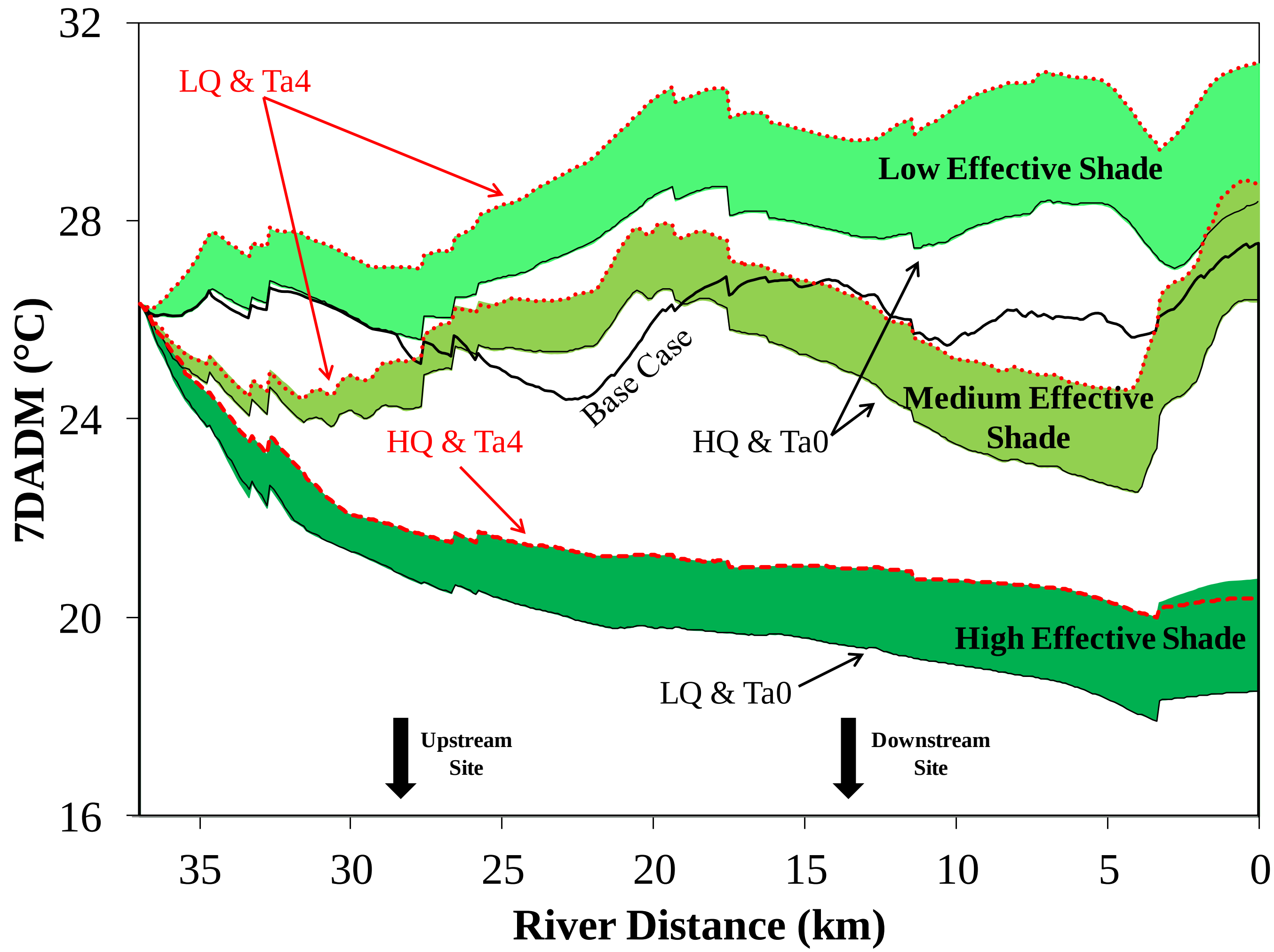
32
28
24
20
16
7DADM (°C)
35
30
25
20
15
10
5
0
River Distance (km)
LQ & Ta4
HQ & Ta4
Base Case
HQ & Ta0
LQ & Ta0
Low Effective Shade
Medium Effective Shade
High Effective Shade
Upstream Site
Downstream Site

Figure 3-7

Figure 3-8: in heat fluxes under combined conditions of effective shade, air temperature, and stream flow. Changes are summarized as the average over a) daytime, b) nighttime, and c) 24-hours duration. Modifying effective shade mitigated the influence of air warming: despite warmer air conditions, high effective shades reduce the net heat during the daytime and enhanced daily heat dissipation.

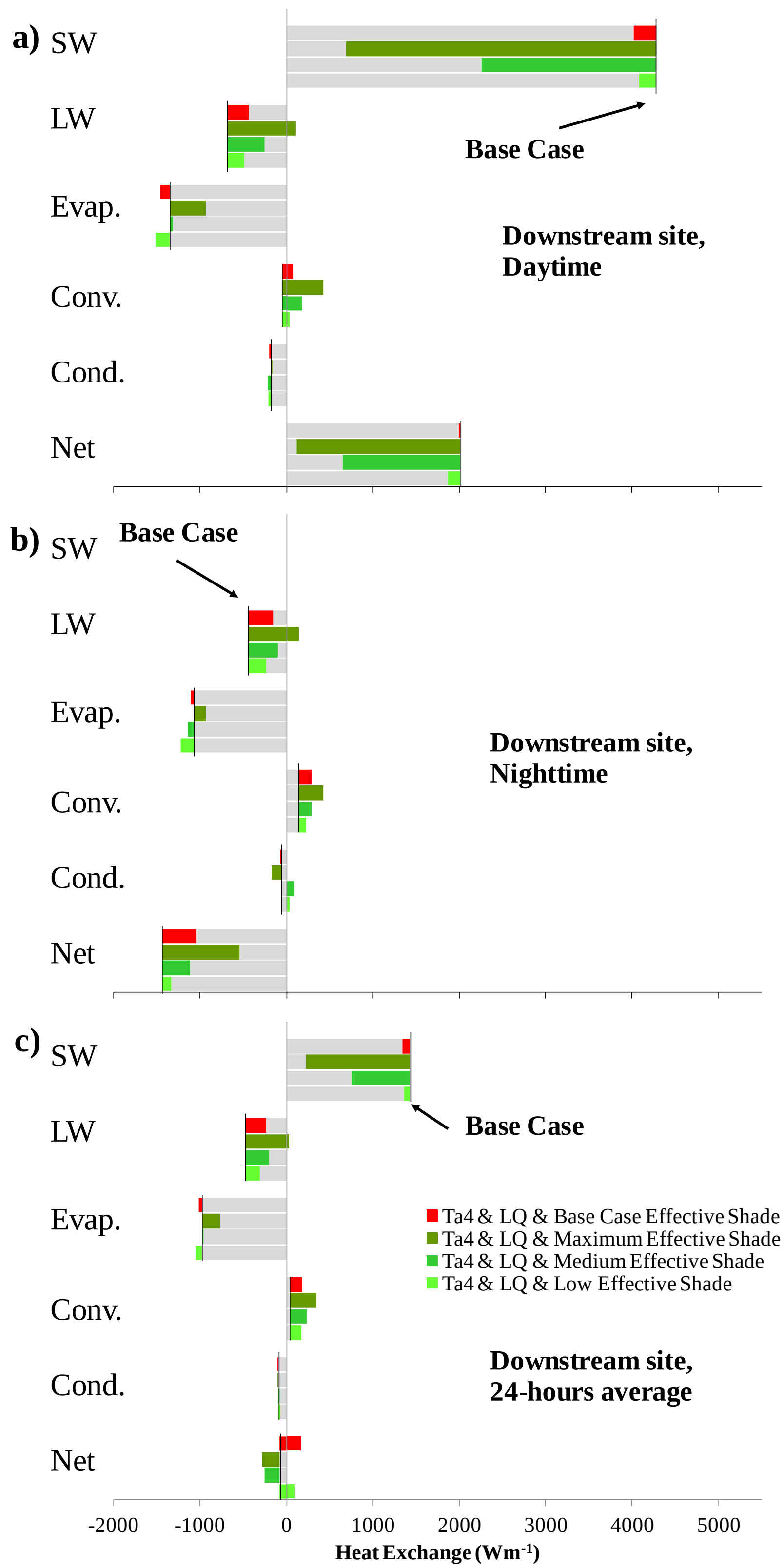
a) SW
LW
Evap.
Conv.
Cond.
Net
Base Case
Downstream site, Daytime
b) SW
LW
Evap.
Conv.
Cond.
Net
Base Case
Downstream site, Nighttime
c) SW
LW
Evap.
Conv.
Cond.
Net
Base Case
Ta4 & LQ & Base Case Effective Shade
Ta4 & LQ & Maximum Effective Shade
Ta4 & LQ & Medium Effective Shade
Ta4 & LQ & Low Effective Shade
Downstream site, 24-hours average
-2000
-1000
0
1000
2000
3000
4000
5000
Heat Exchange (Wm-1)

Figure 3-8

Figure 3-9: 7DADM under the combined influence of effective shade and a) stream flow and b) air temperature. While the influence of flow varied according to effective shade conditions, the influence of air temperature almost remained constant.

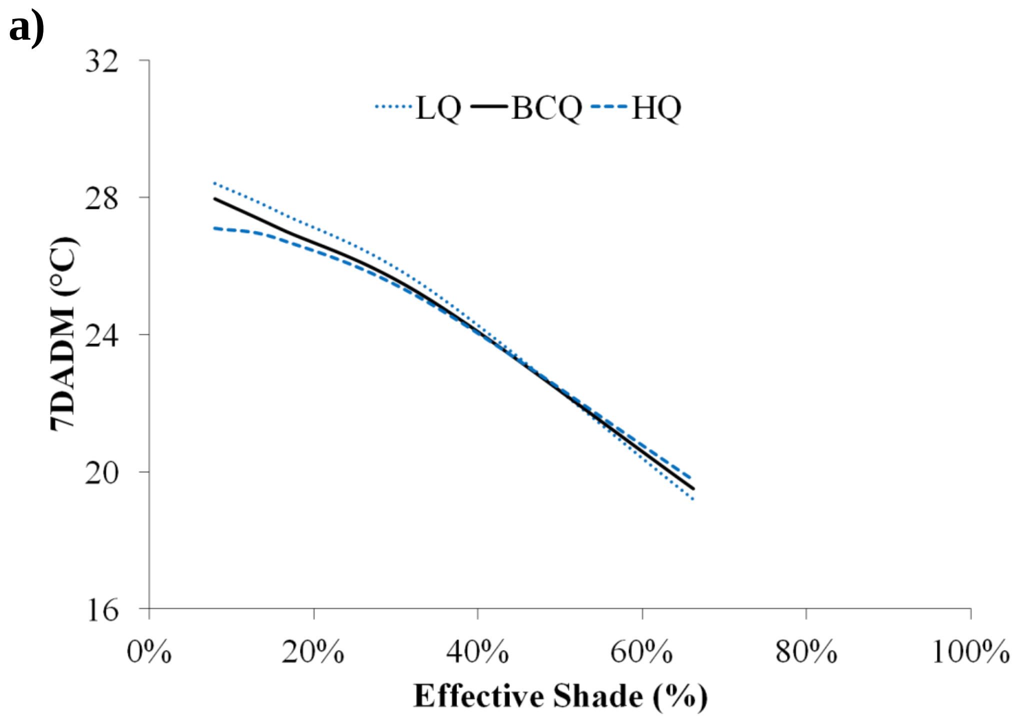
a)
32
28
24
20
16
LQ
BCQ
HQ
7DADM (°C)
0%
20%
40%
60%
80%
100%
Effective Shade (%)

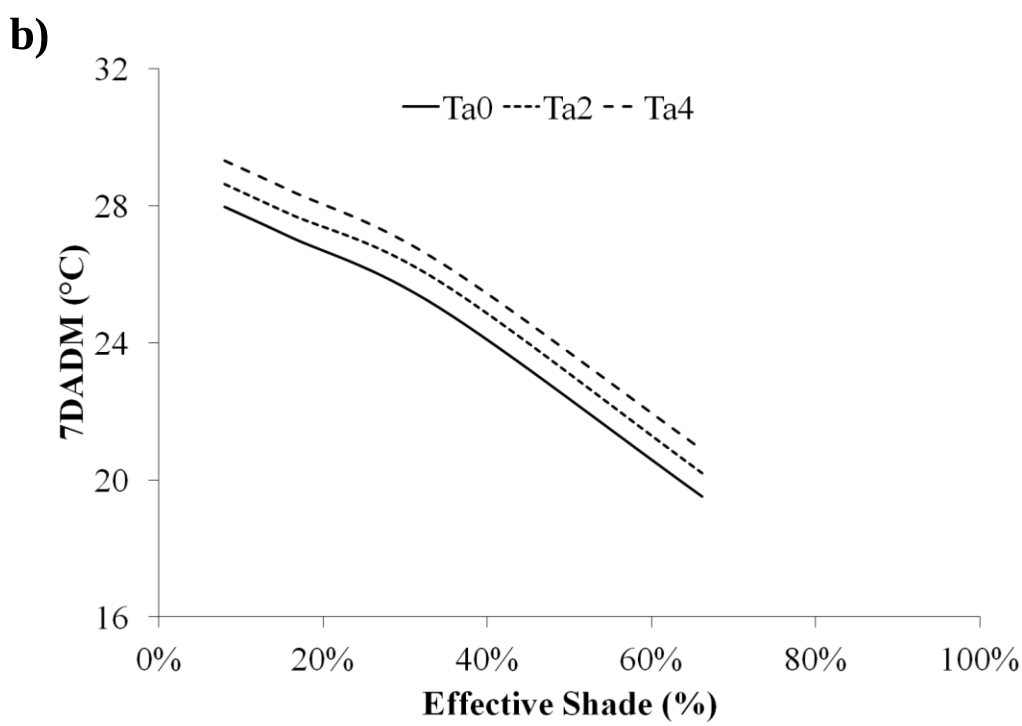
b)
32
28
24
20
16
Ta0
Ta2
Ta4
7DADM (°C)
0%
20%
40%
60%
80%
100%
Effective Shade (%)

Figure 3-9

4. Estimating Stream Temperature Response to Channel Reconstruction and Riparian Re-vegetation and the Potential to Mitigate Warmer Air Conditions

Mousa Diabat
Roy Haggerty
Steven M. Wondzell

Abstract

Stream temperature is an essential physical property of aquatic freshwater habitats all over the world. Restoration practices aim to improve the water quality of sites that were negatively impacted by human activities in the past and to mitigate the influence of future climate conditions. Common restoration practices influencing stream temperature include replanting riparian vegetation and reconstructing channel meanders. I examined stream temperature along a 1.5-km stream section along the upper part of the Middle Fork John Day River, Oregon, USA. The study section was dredged and straightened because of mining for gold. Also, large trees are currently absent across the floodplain. Restoration designs call for restoring both the channel structure and the riparian vegetation. I used the software Heat Source to simulate stream temperature in 12 scenarios that represent all potential scenarios that combine current climate or 4 °C warmer air with current riparian vegetation (low effective shade), medium effective shade, or high effective shade and with existing channel or reconstructed channel. Heat budget analysis showed that constructing a longer, narrower, and deeper channel led to increasing the heat accumulation during the daytime, which in turn increased stream daily maximum temperatures. Results indicated that restoring the channel without replanting the riparian vegetation would increase the stream's daily maximum temperature relative to the existing channel. Furthermore, the restored channel was warmer than the existing channel when the riparian vegetation for both was replanted to achieve high effective shade conditions. The restored channel was cooler than the existing channel only with replanted riparian vegetation that does not exceed a medium effective shade conditions for both channels. In addition, results indicated that restoring riparian vegetation was sufficient to mitigate the influence of warmer air on stream temperature, while restoring the channel alone did not. It is important to emphasize that stream temperature is one of many goals that restoration activities aim to improve and that the difference in stream temperature maxima between both channels did not exceed

0.4 °C, which might be negligible in such a short section but might be amplified for longer sections.

Introduction

Stream temperature regulates physical and biochemical processes of aquatic freshwater habitats by influencing oxygen solubility and nutrient cycling as well as metabolism, growth rate, and mortality of aquatic organisms (Feldhaus *et al.*, 2010; McCullough, 1999; Myrick and Cech, 2005; Richter and Kolmes, 2005). Small changes to a stream's thermal regime can lead to changes in physiological and behavioral characteristics of various aquatic organisms (Reeves *et al.*, 2009; Tinus and Reeves, 2001) with more extreme changes causing mortality (Feldhaus *et al.*, 2010). In addition, anthropogenic impacts are among the most important causes to stream temperature degradation. For example, the legacies of past mining activities for gold and of timber harvest are still influencing stream temperature in the Pacific Northwest (Beschta and Ripple, 2005; Grant, 1994; Lyon, 2010). Climate projections for the Pacific Northwest estimate that air temperature will increase during the current century (Mantua *et al.*, 2009, 2010). Therefore, there is an increasing interest to understand the influence of major factors on stream temperature guiding restoration strategies.

Understanding the mechanisms in which the major factors influence stream temperature is an essential step for this study. Stream temperature (T_w) is a function of heat concentration in water, which is the net heat content (H) that is distributed in a water volume in the channel (V):

$$T_w \propto \frac{H}{V} \qquad \text{EQ. 4-1}$$

where, T_w is stream temperature (°C), H is heat content (J), and V is water volume (m^3).

Both the heat content and water volume are subject to change as a result of changing climate, channel structure, or streamflow (Hawkins *et al.*, 1997; Mohseni and Stefan, 1999; Poole and Berman, 2001). Therefore, the change in stream temperature depends on the changes in heat concentration:

$$\Delta T_w \propto \Delta\left(\frac{H}{V}\right) \qquad \text{EQ. 4-2}$$

Five major heat fluxes influence the heat content: shortwave radiation, longwave radiation, evaporation, convection with the atmosphere, and conduction with the streambed. The stream gains most of the heat in shortwave radiation and dissipates most of the heat in evaporation and longwave radiation (Brown, 1969; Sinokrot and Stefan, 1994). Therefore, any alteration to the major heat fluxes greatly influences stream temperature.

Alterations may occur to the stream's shading, streamflow, or channel structure influencing stream temperature. Shading the stream limits incoming shortwave radiation leading to reducing the heat content and therefore stream temperature maxima decline (Johnson, 2004). Streamflow has a first order influence that inversely affects stream temperature. Sinokrot and Gulliver (2000) indicated that reduced streamflow caused high water temperatures and Webb et al. (2003) indicated that the air-water relationship tends to be stronger for lower-than median flows. Both streamflow and channel structure define water surface area, flow velocity, and water volume in the channel (Caissie *et al.*, 2007; Constantz, 1998; Mohseni and Stefan, 1999). Water surface area (A) determines the available interface for heat exchange. The wider and longer the stream is, the larger its surface area and thus heat exchange with the environment increases (Constantz, 1998; Mohseni and Stefan, 1999; Poole and Berman, 2001). Flow velocity dictates the duration of time that water in the channel is subject to heat exchange conditions, defined as travel time (t_t). Therefore, the net heat load (H) is the product of net heat flux (H_{net}) at the water surface (A) and the travel time (t_t) and net heat load can be quantified as follows:

$$\mathrm{H} = \mathrm{H_{net}} \cdot \mathrm{A} \cdot \mathrm{t_t} \qquad \text{EQ. 44-3}$$

Where H is heat content (J), H_{net} is heat exchange between the stream and its environment ($J \cdot s^{-1} \cdot m^{-2}$), A is water surface area of the stream (m^2), and t_t is travel time (s).

Increasing the water volume in the stream channel provides a buffering effect because more heat is required to change the stream temperature. Change in stream temperature therefore, is a function of the interactions between external and internal factors that influence heat concentration in the stream and this function is summarized by the following relationship:

$$\Delta T_W \propto \Delta\left(\frac{H_{net} \cdot A \cdot t_t}{V}\right) \qquad \text{EQ. 4-4}$$

The accumulated change to the heat budget is function of travel time that, in turn, is function of streamflow velocity and length of stream section. For example, augmenting streamflow increases flow velocity and, in turn, reduces travel time and decreases the total heat exchange between the stream and its environment. So, reducing the travel time decreases the accumulated heat gain of a heat-gaining section and decreases the accumulated heat dissipation along a heat-losing section relative to longer travel time (Moore *et al.*, 2005; Quinn and Wright-Stow, 2008). Reducing diversions or assigning a minimum streamflow was also suggested as a strategy for reducing temperature maxima, but reducing diversions cannot eliminate stream warming (Sinokrot and Gulliver, 2000). The presence of large water volume in the channel (for example, deep channel versus shallow channel or high flow versus low flow) provides a buffering effect that prevents rapid changes in temperature (Webb *et al.*, 2003).

The objectives of this study are: 1) to estimate stream temperature response to riparian re-vegetation and channel reconstruction, 2) to compare among stream temperature responses to both restoration practices, and 3) to identify the favorable combination of restoration practices that leads to reducing daily maximum stream temperature.

Methods

Study site

The study site is a 1.5-km stream section located between river kilometers 92 and 94 of the Middle Fork John Day River (MFJDR) in northeastern Oregon, USA (Fig. 4-1). The study section is entirely in the Oxbow Conservation Area, which is owned by the Confederated Tribes of the Warm Springs. The drainage area for the study section is approximately 500 km^2. Streambed elevations of the study section range from 1125.5 m to 1134.5 m. Channel flow at the upper most point of the study section drops from 1.4 $m^3 \cdot s^{-1}$ in early summer to 0.5 $m^3 \cdot s^{-1}$ in late summer. The bedrock in the study section is predominantly Columbia River Basalt Group (Hunt and Stepleton, 2004). A high degree of channel network complexity existed before anthropogenic activities disconnected the active channel from its flat-sloped floodplain during the early 1900’s.

Anthropogenic activities severely affected the active channel and its riparian floodplain during the late 1930’s through the late 1940’s, especially dredge-mining for gold. Several dredges worked the mainstem and tributaries of MFJDR in the study section starting in the fall of 1939. The dredge used was built on a boat that floated on a self-made pond, which was filled with tailings as the dredge advanced. Tailings from this period are still present across the floodplain. Mining activities channelized the stream, straightened its natural meanders, and forced the channel to the north side of the valley floor. Dredging and channelization disconnected the active channel from its floodplain and restricted its lateral migration. Similarly, timber harvest and grazing degraded land cover across the floodplain (Lyon, 2010). The lack of effective shade from riparian vegetation increased stream temperatures in the MFJDR (Beschta and Ripple, 2005; Grant, 1994).

Stream temperature is of specific concern because of the rearing and spawning habitats in the MFJDR for spring Chinook salmon (*Oncorhynchus tshawycha*), steelhead (*Oncorhynchus mykiss*), and bull trout (*Salvelinus confluentus*) (Lyon, 2010). The study reach is on the section of the MFJDR that is listed as an impaired water body on the Clean Water Act 303(d) list because it exceeds water temperature criteria. Both steelhead and bull trout in the MFJDR are on the U.S.A. Federal Endangered Species Act Threatened and Endangered list. Additionally, the study section is among a number of reaches along the MFJDR that the Oregon Department of Environmental Quality (ODEQ) designated for fish use, as it contains core cold-water habitats that support both salmon and steelhead rearing and bull trout migration. However, stream temperatures in the MFJDR are subject to increase due to changing climate, especially air warming conditions, during the current century (Diabat *et al.*, 2012).

Data of current channel of restoration design

The study focuses on a major restoration project that is currently underway in the Oxbow Conservation Area. The main goal of the project is to improve habitat conditions for bull trout, steelhead, and other salmonid species. Restoration plans call for filling parts of the existing channel, restoring channel meanders, and replanting the riparian vegetation. Channel reconstruction addresses the lack of channel meanders and pools along the existing channel so the reconstructed channel will contain more and deeper pools than currently found along the existing channel. In addition, increasing meanders will increase channel length by about 20%. Plans also call for replanting riparian vegetation after channel restoration is completed. All replanted vegetation will be native to the John Day River and include ponderosa pine (*Pinus ponderosa*) and cottonwood (*Populus balsamifera*), as well as alder (*Alnus incana*), dogwood (*Cornus sericea*), and willow (*Salix exigua*).

I used the software Heat Source version 8.04 to model stream temperature and hydraulic routing (Boyd and Kasper, 2003; Oregon Department for Environmental Quality, 2014). Heat Source simulates stream temperatures by calculating the change in the stream's heat budget along the channel. Heat Source requires extensive spatial and temporal input data, including channel structure and riparian floodplain characteristics (Crown and Butcher, 2010). Channel structure data are broken up into elevation and gradient of streambed, streambank angles, and roughness coefficient of the channel. Heat Source also requires temporal data for boundary conditions of both flow and temperature for the upstream end of the channel as well as for all entry points of surface or subsurface inflow (tributaries and groundwater). The model requires data both about locations of water diversions and diversion rates, if such diversions exist. Data for channel structure and flow at boundaries are used for hydraulic routing of stream flow.

Data for both atmospheric conditions and riparian floodplain characteristics (vegetation and topography) are essential to calculate the stream's heat budget. Temporal data for the atmospheric conditions include wind speed, air temperature, cloudiness, and relative humidity. Heat Source utilizes the data for atmospheric conditions in calculating evaporative heat flux and convective heat flux. Data for riparian floodplain characteristics consist of topographic elevations and vegetation parameters (tree height and canopy density). Heat Source utilizes the data for riparian vegetation and topography of the basin in calculating effective shade along the channel by using the algorithm 'Shade-a-lator'. The effective shade is the complement of the percentage of shortwave radiation that reaches the water surface from the theoretical shortwave above the riparian vegetation. Theoretical shortwave radiation is calculated from the sun's angle and time of day.

I obtained data for channel structure of the reconstructed channel (Michael Sixta, U.S. Bureau of Reclamation, Denver, CO). Information about the channel structure was extracted at 1 m spatial resolution using HEC-RAS, which is the platform used to design the channel (Appendix B). I utilized those data to regenerate the spatial data of the channel structure in Heat Source. Two tributaries enter the existing channel: Beaver Creek at distance 100 m and Ruby Creek at distance 1,100 m. However, my summer surveys for 2011-2013 showed that only Beaver Creek had running water.

Ruby Creek dried before reaching the mainstem channel. These observations agree with those from Crown and Butcher (2010). Therefore, I utilized flow and temperature data found in Crown and Butcher (2010), in which flow ranged between 0.5 $m \cdot s^{-1}$ and 1.5 $m \cdot s^{-1}$ and water temperature ranged between 9.5 °C and 27.8 °C in July and August. The model setup showed that Beaver Creek entered the existing channel at distance 100 m and the reconstructed channel at distance 124 m. There are no water diversions along the study section. I simulated stream hydraulics representing summer low flow (1 $m^3 \cdot s^{-1}$) both in Heat Source and in HEC-RAS for comparison (Appendix B)

Preparation of Scenarios

I prepared 12 models in Heat Source to simulate stream temperature under different scenarios of air temperature, channel structure, and riparian vegetation. For each of the two channel structures I simulated three riparian vegetation conditions and two air temperature conditions. Generating the riparian vegetation conditions constituted of: 1) current riparian vegetation that generated an average effective shade of 6%, and modified data of tree height and canopy cover to generate 2) medium effective shade (average of 21%) and 3) high effective shade (average of 66%). Generating the air temperature scenarios constituted of 1) current air temperature and modified air temperature data to generate 2) 4 °C warmer in air conditions.

Boundary conditions (water temperature and streamflow) for both the existing and reconstructed channels were identical. I imported data for the boundary conditions from the corresponding location and after simulating stream temperature Heat Source along an upper 37-km section of Middle Fork John Day River along, which was based on Crown and Butcher (2010). However, simulating stream temperature for the 37-km section included two major modifications to the original, parameterized model (Appendix C). The first modification was changing the confluence point of Granite Boulder Creek with the mainstem MFJDR to be about 500 m upstream of the study section, reflecting the results of 2012 restoration project above the study area. The second modification was simulating stream temperature in spatial resolution of 100 m instead of 300 m as used by ODEQ. I generated data (flow and water temperature) of the upper most end of the study section for current climate conditions and for 4 °C warmer air conditions (Appendix C).

Input data of current atmospheric conditions and existing riparian vegetation were based on the total maximum daily load (TMDL) model described in Crown and Butcher (2010) developed with data collected in 2002. In their TMDL report, Crown and Butcher (2010) interpolated atmospheric data from the metrological station in Prairie City in 2002 and generated hourly air temperatures at different elevation along the Middle Fork John Day River. Air temperature at the closest location to the study section ranged between 0.5 and 39.6 °C in the summer. I used the 'delta method' to modify air temperature data representing warmer air conditions (Diabat *et al.*, 2012; Mote and Salathé, 2010). The delta method is defined by adding a constant value to the air temperature data throughout the simulation period. Air temperature of the warmer scenario ranged between 4.5 and 43.6 °C.

For the existing channel, Heat Source calculated a longitudinal average effective shade of 6% for existing shade, 21% for medium, and 66% for high effective shade scenario all (Fig. 4-2). For the reconstructed channel, the longitudinal average effective shade was 9% for existing, 37% for medium, and 74% for high effective shade (Fig. 4-2). Fig. 4-3 shows the route of the existing and reconstructed channels with different riparian vegetation scenarios. Riparian vegetation varied along the existing channel (Fig. 4-3a), but was dominated by low shrubs and grass. I modified the data of riparian vegetation to represent medium and high effective shade conditions (Fig. 4-3b) that currently exist along some portions of the study section. Medium effective shade was the result of 5 m tree height with 70% canopy density representing riparian vegetation that consists of low, dense trees such as alder (*Alnus incana*) and willow (*Salix exigua*). High effective shade was the result of 30 m tree height with 50% canopy density representing conditions of large trees such as ponderosa pine (*Pinus ponderosa*) and cottonwood (*Populus balsamifera*). The reconstructed channel was routed across the floodplain and was influenced by the existing riparian vegetation (Fig. 4-3c) or the restored vegetation (Fig. 4-3d).

To analyze the results, I examined the stream's hydraulic characteristics, temperature, and heat budget. Results of hydraulic characteristics and channel structure assist in identifying the differences in water surface area, flow velocity, and water volume in the channel. I then examined the 7-day average daily maximum temperature (7DADM) along the full length the study channels for temperature comparison. The 7DADM is a common water quality standard representing the maximum values of the 7-day running average of the daily maximum stream temperature.

Change in heat concentration along the channel assists in explaining the change in temperature. I calculated the change in heat concentration in the water for each segment between the channel's inlet and outlet. A segment is an interval of channel defined in the simulation.

$$\Delta H_{c_i} = \Delta\left(\frac{H_{net_i} \cdot t_{t_i} \cdot A_i}{V_i}\right) \qquad \text{EQ. 4-5}$$

Where ΔH_{c_i} is heat concentration (J·m^{-3}) for segment i, H_{net_i} is the net heat exchange (J·s^{-1}·m^{-2}) between the stream and it environment for segment i, t_{t_i} is the travel time (s) for segment i, A_i is the water surface area (m^2) for segment i, and V_i is the water volume in the channel (m^3) for segment i.

Then, I calculated the average of accumulated change in heat concentration for a short period of time prior to when stream temperature reached its maxima on daily basis in order to directly relate the change in heat concentration to the 7DADM.

$$\overline{\Delta H_c} = \sum_{i=in}^{i=out} \Delta H_{c_i} \qquad \text{EQ. 4-6}$$

Where $\overline{\Delta H_c}$ is the average change in heat concentration between the inlet (*in*) and the outlet (*out*) for all segments (*i*).

I calculated the average accumulation for only 3 hours prior to the time of the daily maximum for two reasons. First, the water volume in which heat accumulates exits the channel in less than 3 hours, as the average travel time was 1.5 hours for the existing channel and 2 hours for the reconstructed channel during low flow. Second, daily maximum temperature is the result of accumulated heat during the afternoon of each day as this is the period of time during which the stream absorbs heat the most. I summarized the accumulated average heat concentration in a way similar to calculating the 7DADM.

The highest 7DADM in the study section occurred on July 14th for all scenarios. Therefore, the heat budget analysis was only for July rather the rest of the summer. I represented each day in July with a daily average heat concentration over a 3-hour window, which is 1 hour longer than the travel time of the reconstructed channel. The 3-hour window was just before the daily maximum temperature occurred. Then, I calculated the 7-day running average of daily heat concentration. Lastly, I extracted the maximum heat concentration for each segment along the study section and plotted it against the travel time for each channel.

Results

Channel Structure and Hydraulics

The reconstructed channel was longer, narrower, and deeper than the existing channel (Fig. 4-4a, 4-4b, and 4-4c). The reconstructed channel would be 1,858 m long, which is 20% longer than the existing 1,544 m channel. The top wetted width of the reconstructed channel was narrower than the existing channel. The variations in the reconstructed streambed's elevation indicated that it would be consistently deeper than the existing channel.

Given the differences in both channel structures, reconstructing the channel will decrease the water surface area by 8% and increase the water volume available in the channel by 27% relative to the existing channel. In addition, reconstructing the channel reduced the average flow velocity from 0.55 $m \cdot s^{-1}$ in the existing channel to 0.37 $m \cdot s^{-1}$. Because of reducing streamflow velocity and extending channel length, travel time increased from 1.6 hours in the existing channel to 2.0 hours in the reconstructed channel (Fig. 4-4d).

Temperature

Downstream warming was present in both channels with existing conditions of effective shade and climate (Fig. 4-5) but also varied over the diurnal cycle among the different conditions of channel construction, effective shade, and climate (Fig. 4-5a and Fig. 4-5b). The reconstructed channel increased stream temperature maxima relative to the existing channel with existing effective shade (Fig. 4-5a). Increasing the effective shade reduced stream temperature maxima along both channels and at their outlet (Fig. 4-5c-5f). However, daily temperature maxima for the reconstructed channel were lower than existing channel only with medium effective shade conditions.

At either existing or high effective shade, the reconstructed channel was always warmer than the existing channel. With existing effective shade, the reconstructed channel increased the 7DADM (Fig. 4-6) by 0.2 °C along the length of the channel and by an average of 0.3 °C at outlet (Figures 6a). Increasing the effective shade decreased the 7DADM substantially. The reconstructed channel decreased the 7DADM better than the existing channel only with medium effective shade conditions. With medium effective shade, the 7DADM decreased by approximately 0.2 °C throughout both channels and by 0.4 °C at the outlet of the channel. Although the reconstructed channel reduced the 7DADM with increasing effective shade, with high effective shade conditions, 7DADM along the existing channel remained lower than the reconstructed channel. High effective shade caused the 7DADM to decline throughout the existing channel by close to 0.4 °C and throughout the reconstructed channel by 0.3 °C.

Results were similar for warmer air conditions (Fig. 4-6b). The 7DADM throughout the reconstructed channel was higher than the existing channel. Although increasing the effective shade led to declining temperatures, the 7DADM at their outlets remained higher than the existing channel under current climate conditions.

Heat budget

The daily average net heat exchange was positive for current effective shade conditions for both the existing and reconstructed channels and caused downstream warming. However, the reconstructed channel had lower net heat exchange (Fig. 4-7a), mainly because it had lower heat input from shortwave radiation (Fig. 4-7b) relative to the existing channel. The reconstructed channel also dissipated less heat by evaporation and in long wave radiation (Fig. 4-7c and Fig. 4-7d).

The stream's heat budget showed a counterintuitive correlation with 7DADM. Reconstructing the channel decreased the net heat exchange but also increased the 7DADM in comparison to the existing channel. Both long channel and slow flow velocity increased heat accumulation in the constructed channel (Fig. 4-8). For current effective shade and current air temperature, the accumulated change in heat concentration almost doubled in the reconstructed channel in comparison with the existing channel (Fig. 4-8a). Increasing the effective shade changed the stream's heat budget and reduced the positive accumulation of net heat gradually converting it to heat-dissipation by reaching the channel's outlet. With medium effective shade, the accumulated change in heat concentration remained positive for the existing channel but became negative for the reconstructed channel (Fig. 4-8a). Finally, for high effective shade, the accumulated change in heat concentration was negative for both channels, indicating that the stream dissipated heat in both channels, but the existing channel dissipated more energy than the reconstructed (Fig. 4-8a). A similar response was repeated under warmer air conditions with minor differences (Fig. 4-8b). The most apparent difference was that both the restored and existing channel reached the same accumulated heat concentration at the outlet of the study section for high effective shade conditions.

Discussion

Riparian vegetation had a greater influence than restoring the channel on stream temperature, increasing the effective shade alone better mitigated the influence of warmer air on stream temperature than restoring the meanders. Increasing effective shade reduced the 7DADM regardless of channel structure. Other than conditions of medium effective shade, the 7DADM remained higher in the reconstructed channel than the existing channel. However, the differences in 7DADM between the existing and the restored channel were small and could be neglected as long as both the channel and riparian vegetation were restored.

Stream temperature was sensitive to changes in three hydraulic parameters that were modified with reconstructing the channel: 1) water surface area decreased by 8%, 2) water volume in the channel increased by 27%, and 3) stream velocity represented by travel time that increased by 25%. In turn, heat exchange between the stream and its environment was affected so both heat gain and dissipation modified along the channel.

Heat exchange between the stream and its environment depends on water surface area and the duration allowing for this interaction. Heat exchange increases with larger water surface area and longer travel time. Therefore, the relative influence between both factors determines the net heat exchange. In this study, the influence of longer travel time on the stream heat budget was stronger than smaller water surface area leading increasing the heat concentration and stream temperature. Mohseni and Stefan (1999) showed that longer travel time also increased heat exchange between the stream and atmospheric conditions causing stronger heat exchange with its environment leading to stronger relationship with the atmosphere. In addition, the reconstructed channel was narrower and the overall water surface area was smaller than the existing channel. Due to reduced water surface area, the stream gained less heat from shortwave radiation but also dissipated less heat in evaporation and longwave radiation (Fig. 4-8). As a result, the accumulated change in net heat for the reconstructed channel was greater than for the existing channel.

The 7DADM increased because lengthening the channel and slowing the streamflow led to increased travel time. In turn, the stream's net heat budget remained under the influence local conditions for a longer time it would have been with the existing channel. Hence, the stream's net heat budget with existing effective shade was positive and the longer travel time caused the stream to gain more heat leading to increasing the 7DADM.

Both the effective shade and channel structure are important factors to control stream temperature. Results of this study were in agreement with existing literature showing that the net heat decreased with medium and high effective shade for both channels (Cole and Newton, 2013; Johnson, 2004; Pollock *et al.*, 2009), where greater reduction in stream temperatures occurred with longer travel time along shaded sections (Groom *et al.*, 2011). With medium effective shade, the accumulated change in heat concentration remained positive in the existing channel and became negative in the reconstructed channel. In turn, the 7DADM was higher in the existing channel than the reconstructed channel.

With high effective shade, 7DADM results were counterintuitive with lower 7DADM in the existing channel than the reconstructed channel. Although, the accumulated change in heat concentration became negative in both channels, heat dissipation in the reconstructed channel remained lower than in the existing channel. The stream's heat budget along the reconstructed channel showed both lower heat input from shortwave radiation and reduction in heat dissipation in evaporation and longwave radiation than the existing channel corresponding with the difference in water surface area. This outcome agrees with existing studies regarding the importance of water surface area for cooling effect (Sinokrot and Stefan, 1993). In turn, reconstructing the channel led to hydraulic changes that decreased the effectiveness of higher shade.

During the afternoon, reducing the water surface area caused the positive net heat to decline along the reconstructed channel but the 7DADM remained higher than the existing channel that is attributed to higher travel time and greater water volume. The additional channel length increased the duration to accumulate more heat between the inlet and the outlet during the daytime. In addition, the reconstructed channel held more water than the existing channel dictating that more heat must to be dissipated to reduce temperature maxima. Although the reconstructed channel had less water surface area and lower net heat gain, it was not sufficient to decrease the stream's maximum temperature over the length of the reconstructed channel relative to the existing channel.

Reconstructing the channel would also influence the hyporheic flow along the streambed (Wondzell, 2006). Hyporheic flow could create local conditions of thermal refugia especially when stream temperature is high during the summer (Arrigoni *et al.*, 2008; Ebersole *et al.*, 2003). The percentage of heat exchange through the hyporheic zone increases as stream discharge decreases (Wondzell, 2012). Stream discharge along this study section during the summer did not exceed 1 m^3s^{-1}. Using regression correlation generated in Wondzell (2012), the hyporheic flow in the existing channel is estimated to be 0.47% in 100 m stream length. Even with lengthening the stream channel by 20% (due to restoration), hyporheic flow remains a negligible factor to influence stream temperature.

I recognize that stream temperature is only one of many physical and bio-chemical parameters that restoration projects might aim to improve. Reconstructing the channel meanders and adding deeper and more pools would provide heterogeneous hydraulic characteristics in the channel that support a wide variety of aquatic organisms. Reconstructing the channel will affect stream temperature, which can be crucial for the cold- and cool-water organisms in the MFJDR.

Conclusions

Increasing the effective shade with riparian re-vegetation reduced daily maximum stream temperature and mitigated the influence of warmer air temperature in both the existing and the reconstructed channels. Furthermore, the higher the effective shade, the greater reduction in 7DADM. Reconstructing the channel without riparian re-vegetation increased daily maximum stream temperature. However, the reconstructed channel was favorable relative to the existing channel in reducing stream temperature maxima only with medium effective shade.

Channel reconstruction generated a longer, deeper, and slower flowing stream relative to the existing channel. The presence of a larger volume of water for a longer period generated a buffering effect and prevented the desired cooling effect. Channel reconstruction provided heterogeneous hydraulic characteristics that may benefit the ecosystem as a whole, while the difference in 7DADM between the existing and the reconstructed channels under the same effective shade and air temperature conditions was small, and not always of the same sign.

Acknowledgements

The authors are thankful for constructive collaboration with and funding from the following agencies and organizations. This study is the result of a generous funding from a joint venture between the US Geological Survey, the US Forest Service Pacific Northwest Research Station, and Oregon State University (10-JV-11261991-055). Ryan Mechie from Oregon Department of Environmental Quality who provided the total maximum daily load reports and monitoring records. Staff of the North Fork John Day River Watershed Council and the Confederated Tribes of the Warm Springs provided support for fieldwork and access to the study area.

Figure 4-1: Map indicating the study site along the Middle Fork John Day River.

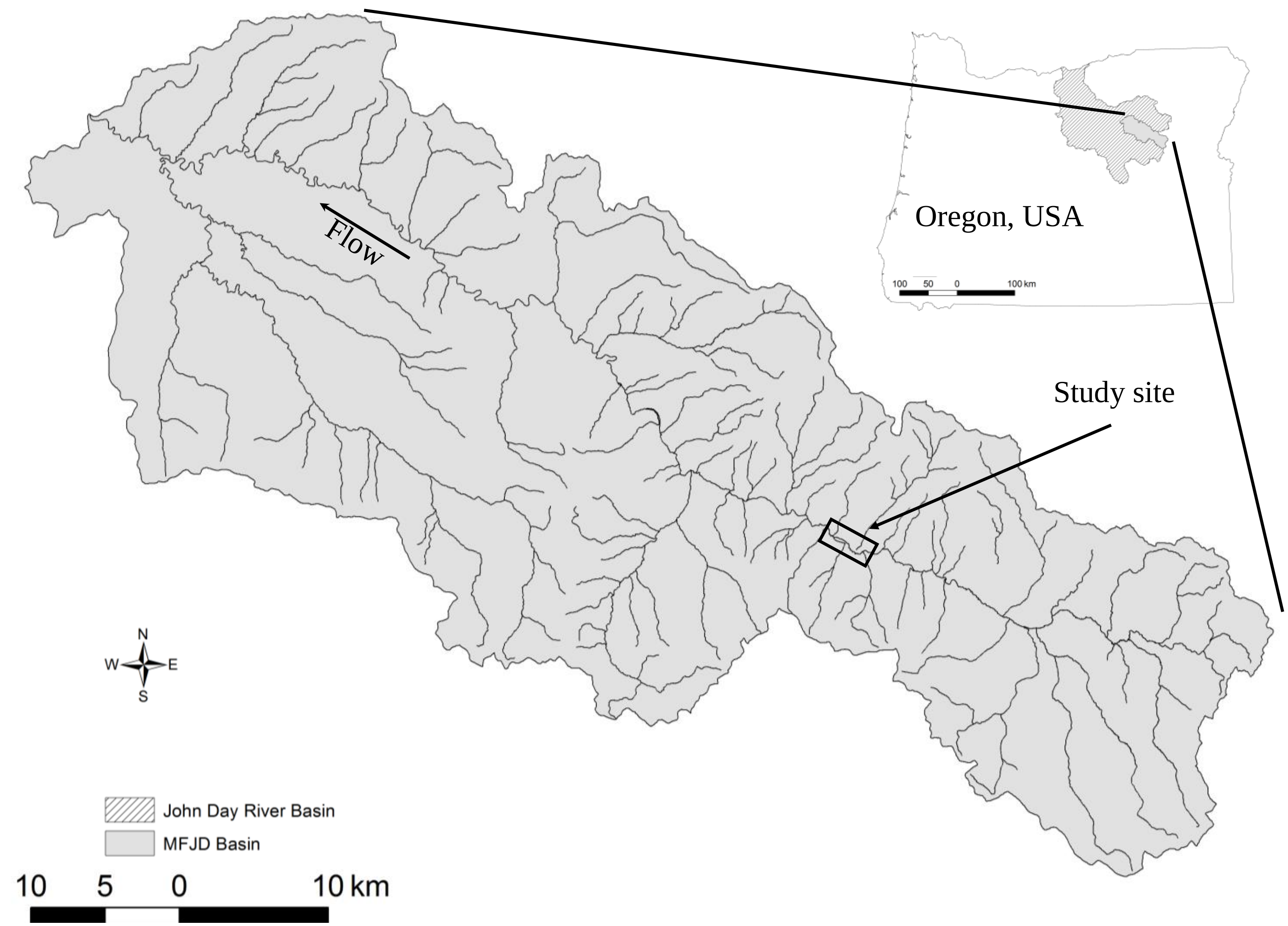
Oregon, USA
100 50 0 100 km
Flow
Study site
N
W
E
S
John Day River Basin
MFJD Basin
10 5 0 10 km

Figure 4-1

Figure 4-2: Effective shade for both the existing and the reconstructed channel. Figure shows solid filling color for the existing channel and dashed lines for the reconstructed channel.

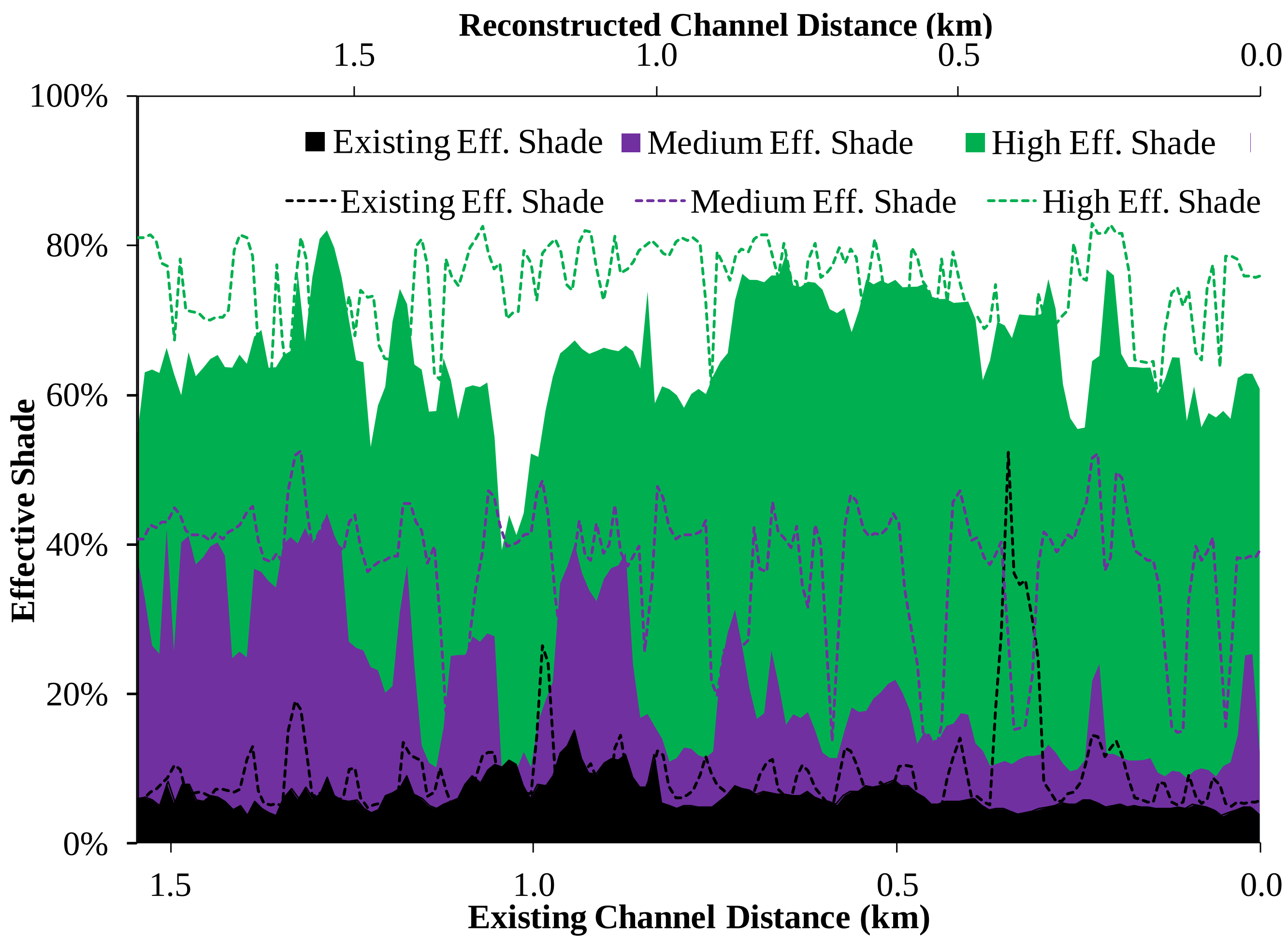
Reconstructed Channel Distance (km)
1.5
1.0
0.5
0.0
100%
80%
60%
40%
20%
0%
Existing Eff. Shade
Medium Eff. Shade
High Eff. Shade
Existing Eff. Shade
Medium Eff. Shade
High Eff. Shade
Effective Shade
1.5
1.0
0.5
0.0
Existing Channel Distance (km)

Figure 4-2

Figure 4-3: Study area showing scenarios of channel (existing in a and b and reconstructed in c and d) and vegetation.

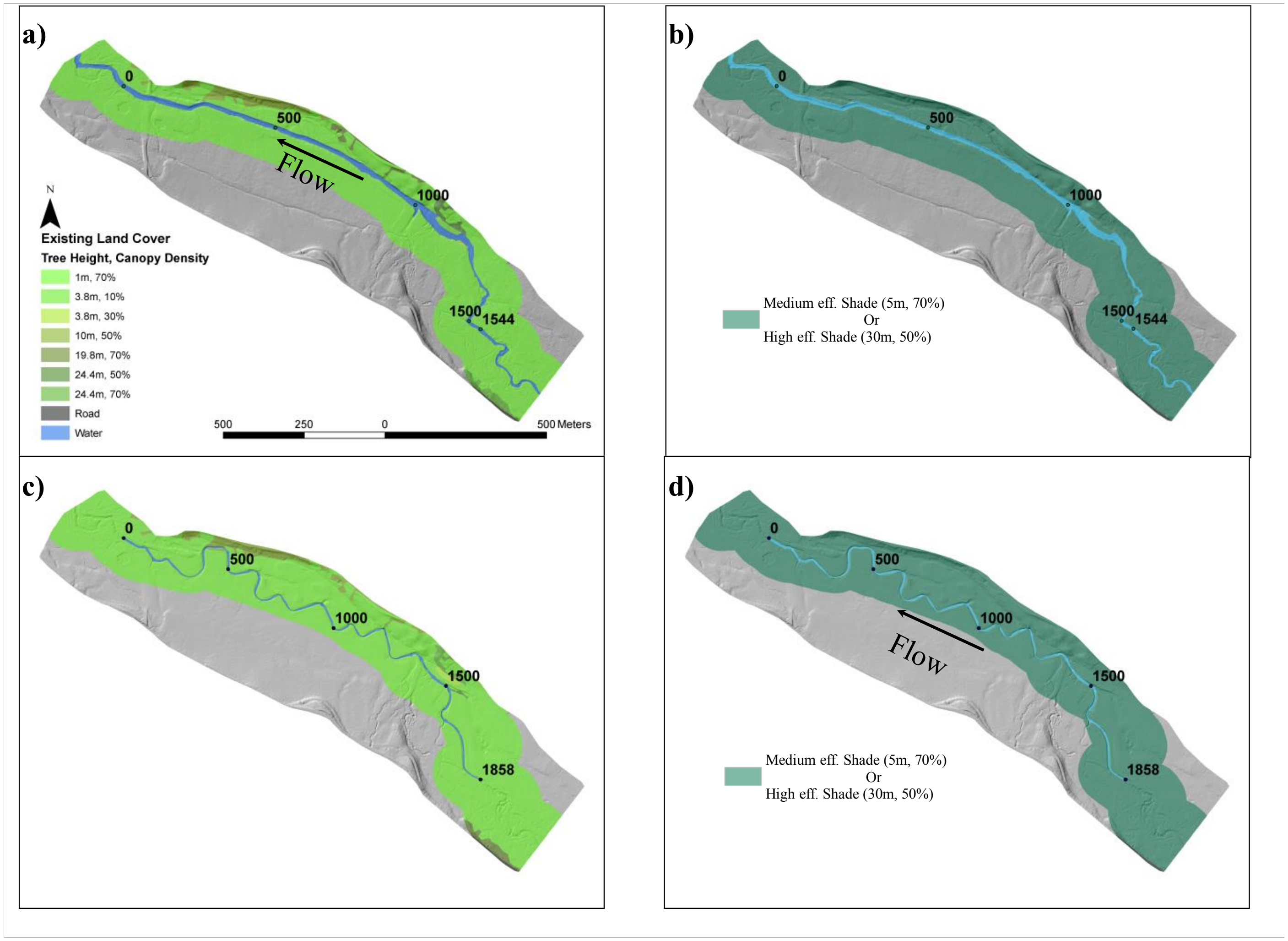
a)
0
500
Flow
1000
1500
1544
N
Existing Land Cover
Tree Height, Canopy Density
1m, 70%
3.8m, 10%
3.8m, 30%
10m, 50%
19.8m, 70%
24.4m, 50%
24.4m, 70%
Road
Water
500
250
0
500 Meters
b)
0
500
1000
1500
1544
Medium eff. Shade (5m, 70%)
Or
High eff. Shade (30m, 50%)
c)
0
500
1000
1500
1858
d)
0
500
1000
Flow
1500
1858
Medium eff. Shade (5m, 70%)
Or
High eff. Shade (30m, 50%)

Figure 4-3

Figure 4-4: Hydraulic characteristics both of the existing and reconstructed channel: a) streambed elevation, b) hydraulic depth, c) top width of wetted channel, and d) cumulative travel time.

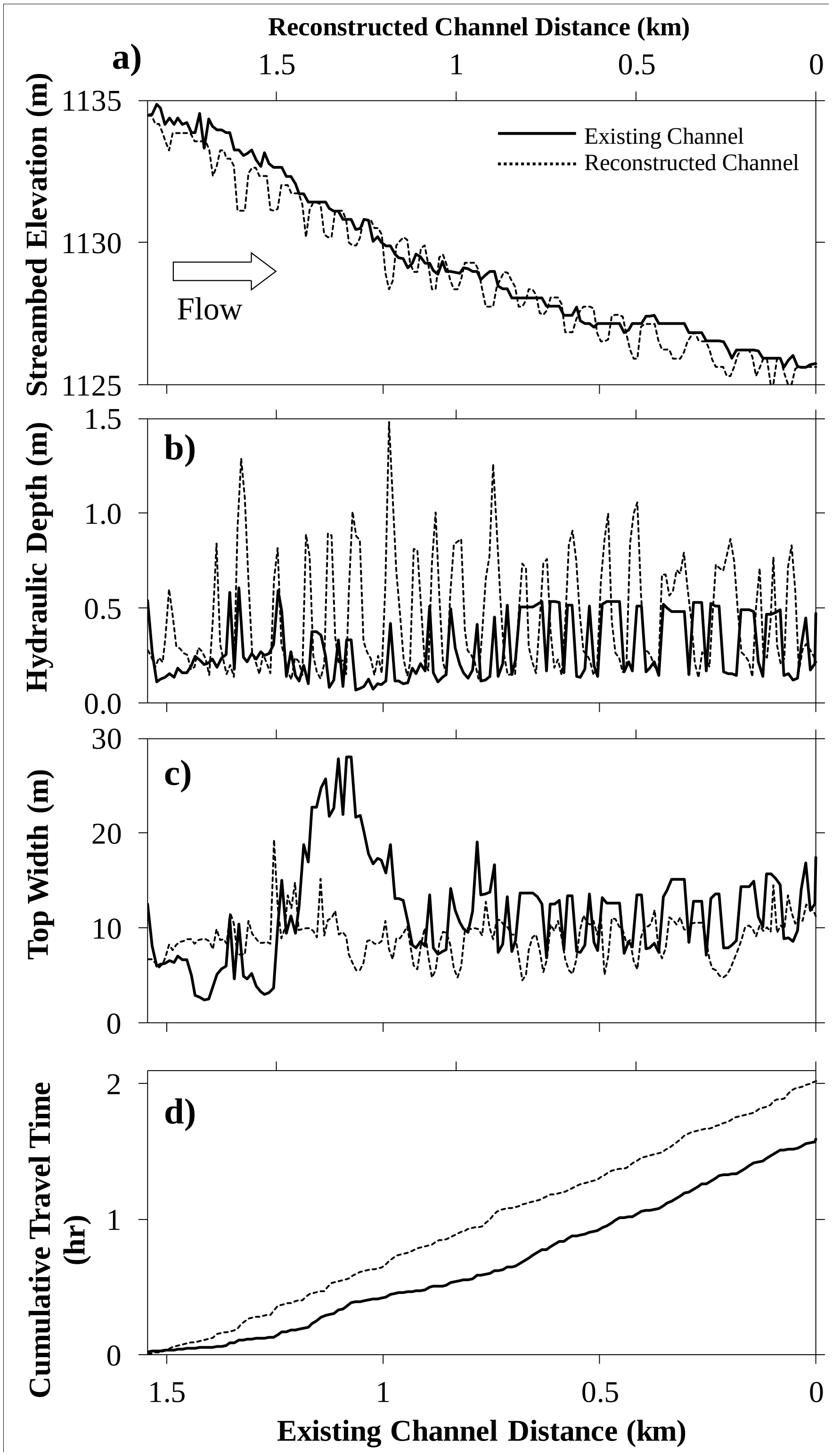

Reconstructed Channel Distance (km)
a)
1.5
1
0.5
0
1135
1130
1125
Streambed Elevation (m)
Existing Channel
Reconstructed Channel
Flow
b)
1.5
1.0
0.5
0.0
Hydraulic Depth (m)
c)
30
20
10
0
Top Width (m)
d)
2
1
0
Cumulative Travel Time (hr)
1.5
1
0.5
0
Existing Channel Distance (km)

Figure 4-4

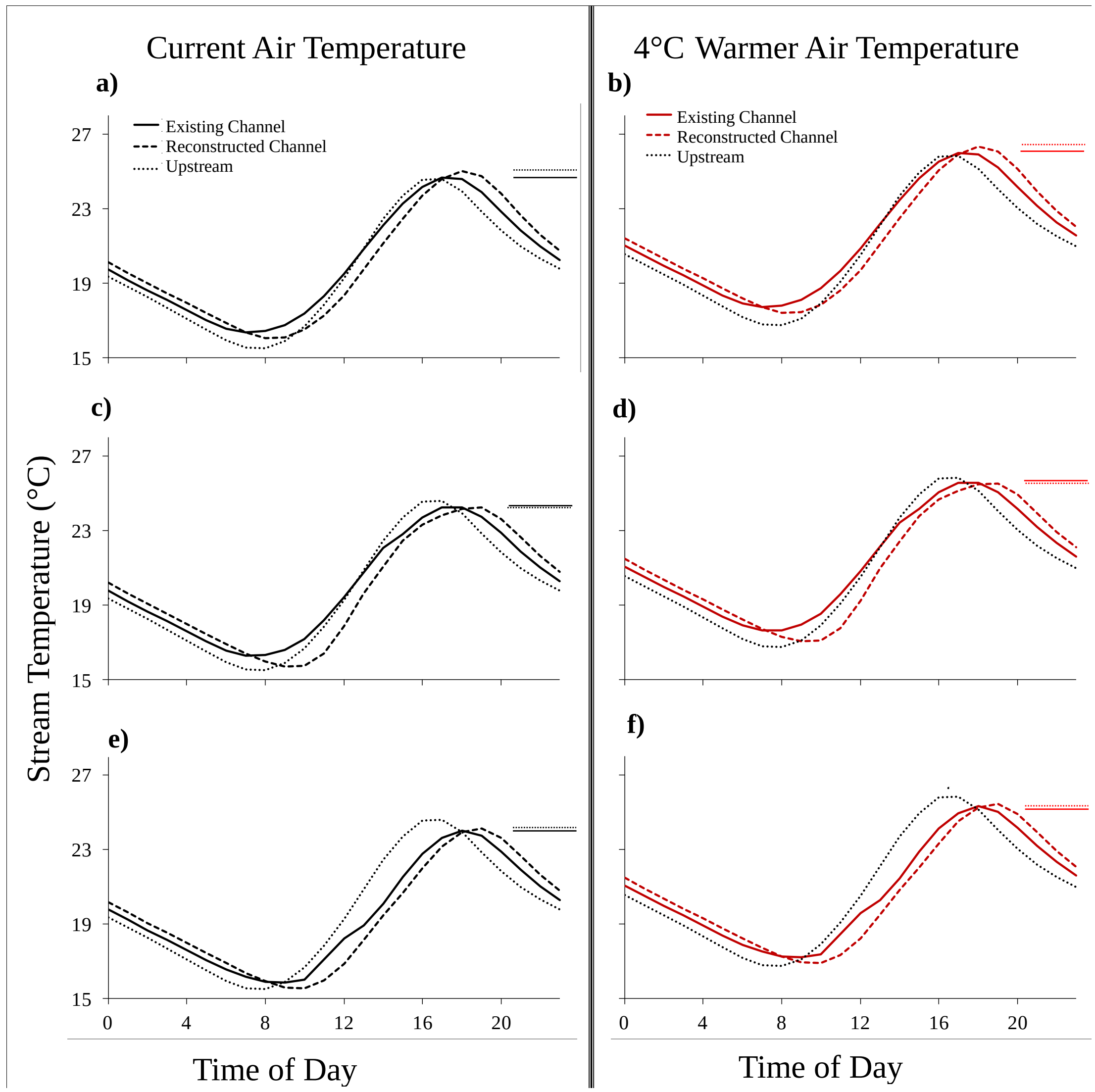

Figure 4-5: Average stream temperature at the inlet as dotted line (same boundary conditions for both channels) and at the outlet of each channel as solid for existing channel and dashed for reconstructed channel. Figures in the left side column are for current air temperature and figures in the right side column are for 4 °C warmer air temperature.

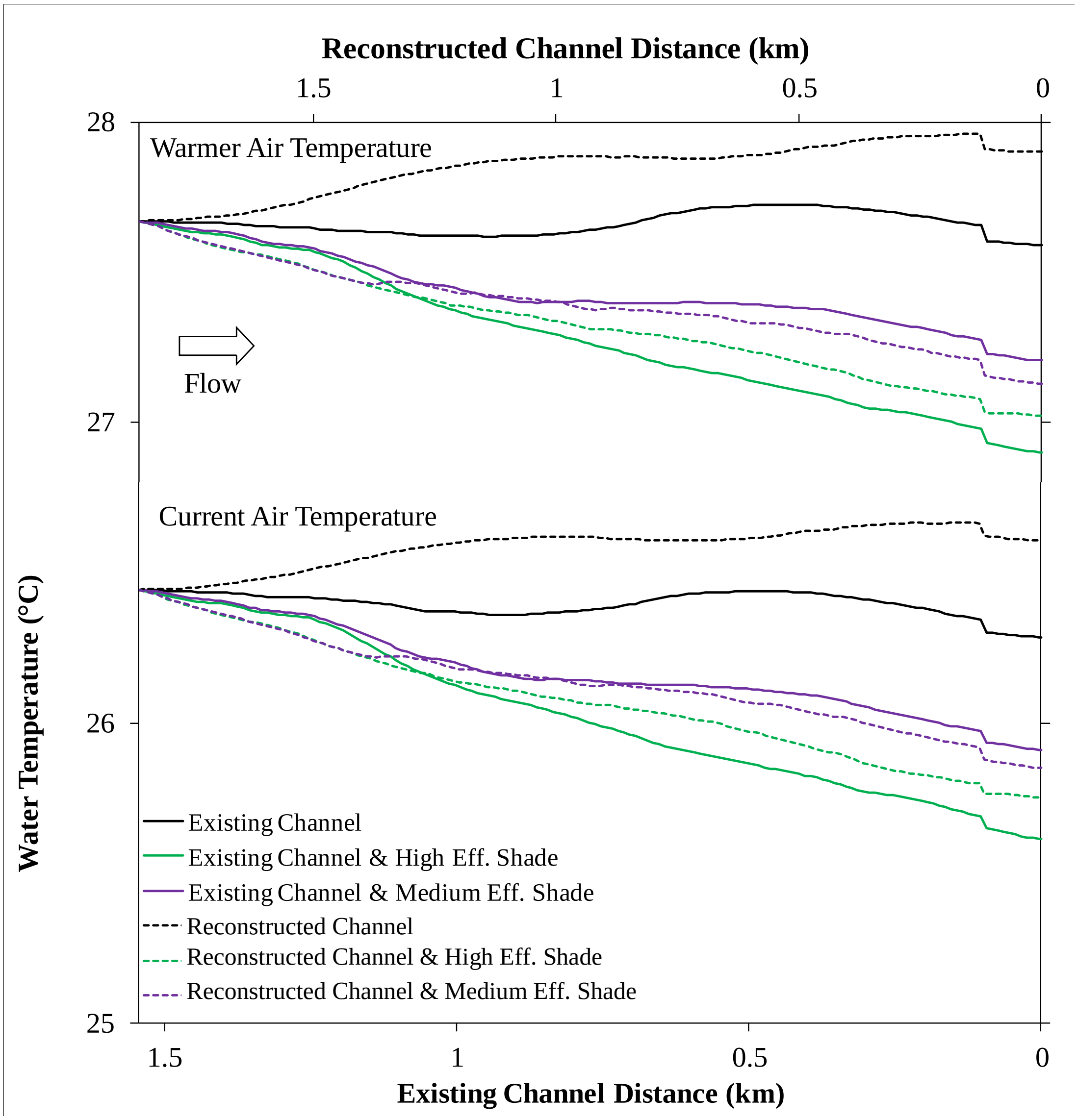

Figure 4-6: 7-day average daily maximum (7DADM) along the channel for all scenarios. The lower part of the figure shows current air temperature 7DADM and the upper part of the figure shows warmer air temperature 7DADM. For warmer air conditions, the 7DADM at the inlet of both channels is higher because I used results from a simulation of upstream temperature to establish the boundary conditions.

Figure 4-7: Heat flow along both channels. The lower horizontal axis is the distance along the existing channel and the upper axis is the distance along the reconstructed channel. Figures are a) net heat flow, b) shortwave radiation, c) evaporation heat, and d) longwave radiation.

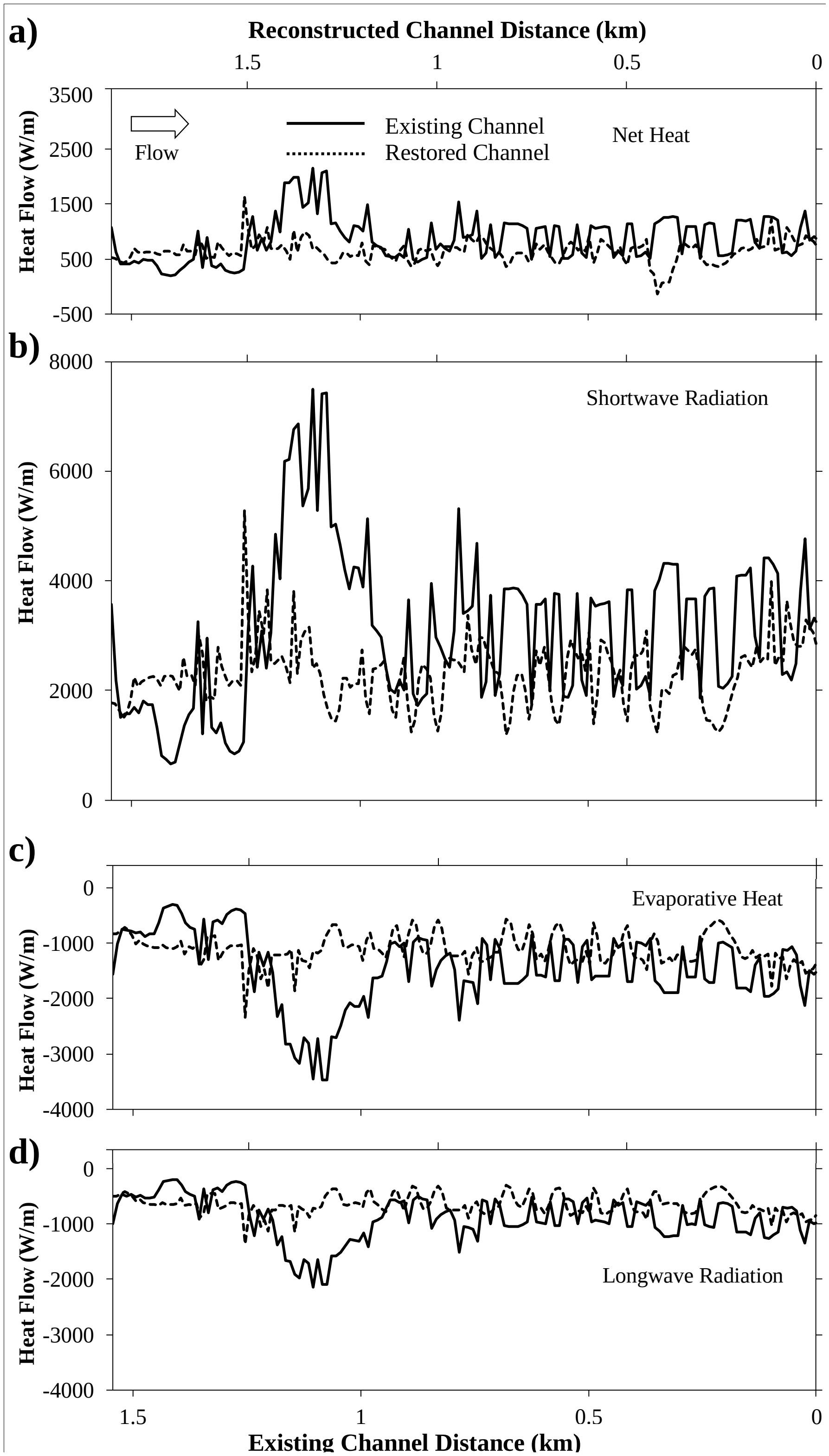
a)
Reconstructed Channel Distance (km)
1.5
1
0.5
0
3500
2500
1500
500
-500
Heat Flow (W/m)
Flow
Existing Channel
Restored Channel
Net Heat
b)
8000
6000
4000
2000
0
Shortwave Radiation
c)
0
-1000
-2000
-3000
-4000
Evaporative Heat
d)
Longwave Radiation
Existing Channel Distance (km)

Figure 4-7

Figure 4-8: Cumulative of average heat as a function of travel time for a) existing air temperature and b) warmer air conditions. Horizontal axes are accumulated travel time along the channel where 0 is at the inlet. For each figure, the lower axis is for the existing channel and the upper axis is for the reconstructed channel.

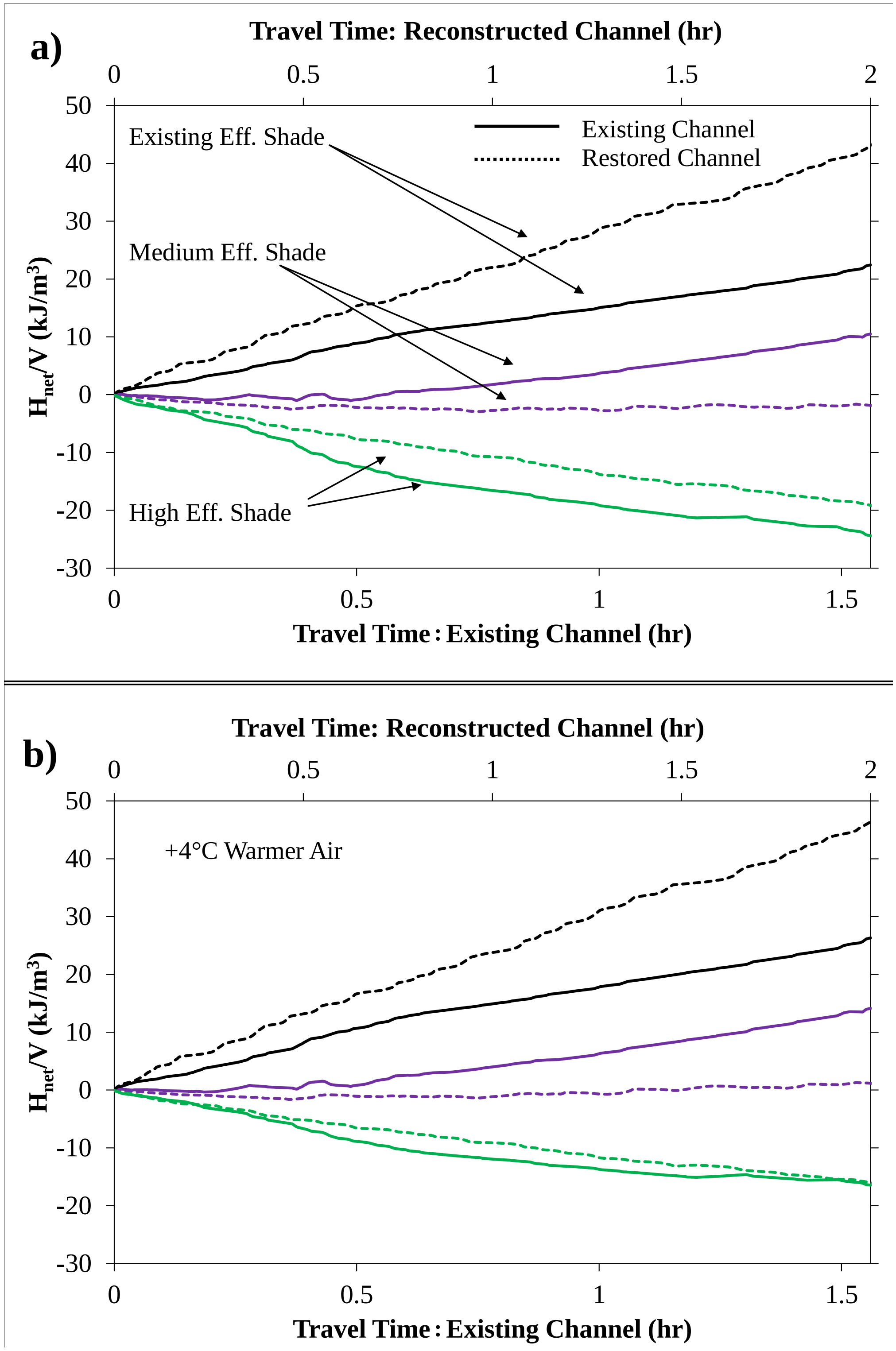

a)
Travel Time: Reconstructed Channel (hr)
0
0.5
1
1.5
2
50
40
30
20
10
0
-10
-20
-30
H_{net}/V (kJ/m^3)
Existing Eff. Shade
Medium Eff. Shade
High Eff. Shade
Existing Channel
Restored Channel
0
0.5
1
1.5
Travel Time : Existing Channel (hr)
b)
Travel Time: Reconstructed Channel (hr)
+4°C Warmer Air
H_{net}/V (kJ/m^3)
Travel Time : Existing Channel (hr)

Figure 4-8

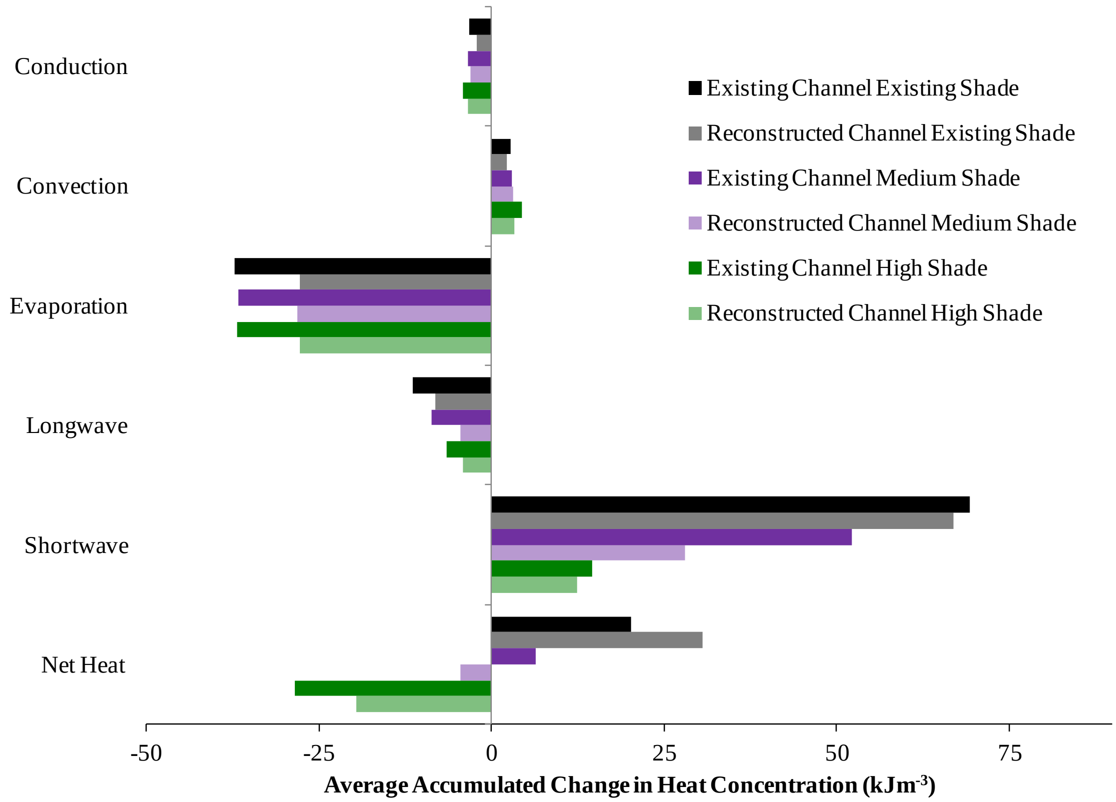

Figure 4-9: Average accumulated change in heat along both channels with different effective shade conditions for current air temperature. Figure shows that the reconstructed channel does not dissipate heat as much as the existing channel because of low surface area. Similar pattern also resulted under 4 °C warmer air.

5. General Conclusions

Throughout my research (chapter 2, 3 and 4), I examined the influence of different parameters on stream temperature and was able to list these parameters according to their magnitude of influence. In addition, I was able to indentify correlations among those parameters. The effective shade was the dominant parameter affecting the stream's heat budget and had a greater influence on stream temperature than air temperature or streamflow. The effective shade also influenced the efficacy of reconstructing channel meanders. Results of this study agree with existing literature that already identified increasing effective shade as a feasible strategy to cope with warming of small stream (Beschta and Taylor, 1988; Brown and Krygier, 1970). Increasing the effective shade along the 37-km study section of the Middle Fork John Day River (MFJDR) both reduced the 7-day average daily maximum (7DADM) and mitigated the influence of air warming on stream temperature. High effective shade conditions reduced the 7DADM by approximately 7 °C relative to current conditions, while low effective shade conditions increased the 7DADM by approximately 3 °C. Increasing air temperature by 4 °C from current conditions increased the 7DADM by ≤2 °C and modifying stream flow between ±30% changed the 7DADM in a range of ≤1 °C. Although increasing effective shade, as a proxy to riparian re-vegetating, reduced stream temperatures substantially, no scenario resulted in a 7DADM ≤18 °C to meet the regulatory standards for the State of Oregon. Riparian re-vegetating using characteristics of forest canopy native to the MFJDR reduced daily maximum stream temperature and potentially would restore historic temperatures and mitigate additional warming due to warmer air (Rutherford *et al.*, 1997). Both experimental studies (Johnson, 2004) and scenario-based simulations (Cristea and Burges, 2010; Kristensen *et al.*, 2013; Roth *et al.*, 2010) proved that limiting heat input from shortwave radiation was important to reduce heat gain and to prevent stream warming.

Changing the effective shade may influence the role of streamflow on stream temperature. The increased flow with low effective shade and the increased streamflow with high effective shade influenced stream heat budget differently. The results agreed with existing literature that the increased streamflow reduced stream temperatures (van Vliet *et al.*, 2011; Webb *et al.*, 2003) but was limited to specific conditions of effective shade and channel structure. The increased streamflow and fast flowing stream decreased the travel time passing through unshaded sections of the stream leading to reduction in the overall heat gain from shortwave radiation and reduction of 7DADM. However, shaded sections have lower 7DADM because of reduction in heat gain or increase in heat dissipation so the increased streamflow decreased the travel time allowing those conditions to influence the stream. As a result, decreasing the travel time of water along unshaded section reduced the 7DADM, while decreasing the travel time of water along shaded section increased the 7DADM.

Streamflow was not the only method to change travel time and influence the stream heat budget. Reconstructing a deeper, narrower, and longer channel led to higher 7DADM relative to the existing, straightened channel. Reconstructing the channel decreased water surface area and led the stream to gain less heat from shortwave radiation but also increased the travel time and caused water to remain for a longer time in the unshaded section. The result of reconstructing the channel alone was increasing the overall heat gain increasing the 7DADM.

Increasing the effective shade reduced heat input from shortwave radiation so that the slow flowing stream remained longer time in the shaded section than the fast flowing stream. The reconstructed channel was favorable over the existing channel producing lower 7DADM only with medium effective shade conditions. Heat budget analysis showed that with medium effective shade, the net heat budget of the existing channel remained positive (net heat gain), while the net heat of the reconstructed channel became negative (net heat dissipation). Therefore, increasing the travel time of a net heat dissipation stream had lower 7DADM than increasing the travel time of a net heat gain stream.

High effective shade generated counterintuitive results with changing channel structure. The existing channel was favorable over the reconstructed channel. However, reconstructing the channel might lessen the effectiveness of increasing shade. Although the stream's net heat budget was no longer positive and became negative as shading increased for both channels, the reconstructed channel had lower surface area than the existing channel. As a result, the net heat dissipation of the existing channel was larger than the restored channel.

Additional counterintuitive results shown in this study revealed that higher daily maximum stream temperature would be an outcome of warmer air during the nighttime and not during the daytime or with uniform warming. The 7DADM increased by approximately the same magnitude in response to all three diurnally-varied-distributions of air warming. However, daily maxima and averages varied in response to different diurnal distributions of air warming. In addition, the duration of the response varied according to the timing of the warming. Stream temperature changes tended to be more extreme and of longer duration when driven by air temperatures concentrated in either daytime or nighttime instead of uniformly distributed across the diurnal cycle. Stream temperature changes were out of phase with air temperature changes, and therefore in many places, the greatest daytime increase in stream temperature was caused by nighttime warming of air temperatures.

Results of this study may be applicable for small to medium streams where the riparian vegetation can shade most or the entire channel width over a good portion of the daytime. Riparian vegetation consisting of dense and short tree stands was shown to shade the stream and to reduce its temperature. Furthermore, channel reconstruction described in this study is often applied for short sections (1-3 km) of small streams.

The model Heat Source requires extensive input data to run. In addition, running Heat Source at fine spatial and temporal resolution is computationally time consuming. Simulation results may differ slightly when run on relatively similar spatial resolution (100 m compared to 200 m). However, simulation results would not be comparable if run at very different spatial resolutions. For the purpose of this study, the simulation was run with the shortest spatial step that could be achieved in reasonable time.

Future work on the Middle Fork John Day River should include production of a new stream temperature model calibrated with updated monitoring parameters. Restoration activities changed riparian vegetation and channel structure at several portions of the river and should be incorporated in the new model setup. In addition, better boundary conditions should be collected in order to replace the existing ones, which were extrapolated from the North Fork John Day River.

Future work for this type of study might include additional sensitivity analysis for detailed riparian vegetation characteristics and channel structure. Since this study revealed that trees stands of different height and canopy density vary in their influence on stream temperature, additional studies may investigate the influence of re-vegetation activities on temporal scales over a number of years to a decade or more. The results would guide the planning activities of timber harvest and fire control to minimize the impacts on stream temperature.

The most important conclusion to reemphasize is that riparian re-vegetating of unshaded sections has the greatest influence on stream temperature. Reconstructing the channel without riparian re-vegetating may create warmer water than anticipated. It is also important to note that improving the effective shade could mitigate the cumulative influence of projected warmer air and low summer flow.

6. - Bibliography

Alexander, L. V., X. Zhang, T.C. Peterson, J. Caesar, B. Gleason, a. M.G. Klein Tank, M. Haylock, D. Collins, B. Trewin, F. Rahimzadeh, A. Tagipour, K. Rupa Kumar, J. Revadekar, G. Griffiths, L. Vincent, D.B. Stephenson, J. Burn, E. Aguilar, M. Brunet, M. Taylor, M. New, P. Zhai, M. Rusticucci, and J.L. Vazquez-Aguirre, 2006. Global Observed Changes in Daily Climate Extremes of Temperature and Precipitation. Journal of Geophysical Research 111:1–22.

Arismendi, I., S.L. Johnson, J.B. Dunham, R. Haggerty, and D. Hockman-Wert, 2012. The Paradox of Cooling Streams in a Warming World: Regional Climate Trends Do Not Parallel Variable Local Trends in Stream Temperature in the Pacific Continental United States. Geophysical Research Letters 39:1–7.

Arrigoni, A.S., G.C. Poole, L.A.K. Mertes, S.J. O'Daniel, W.W. Woessner, and S.A. Thomas, 2008. Buffered, Lagged, or Cooled? Disentangling Hyporheic Influences on Temperature Cycles in Stream Channels. Water Resources Research 44:W09418.

Bates, B., Z. Kundzewicz, S. Wu, and J. Paluch, 2008. Climate Change and Water. Technical Paper of the Intergovernmental Panel on Climate Change, IPCC Secretariat. Geneva, 210 pp.

Beschta, R.L. and W.J. Ripple, 2005. Rapid Assessment of Riparian Cottonwood Recruitment: Middle Fork John Day River, Northeastern Oregon. Ecological Restoration 23:150–156.

Beschta, R.L. and R.L. Taylor, 1988. Stream Temperature Increases And Land-Use In A Forested Oregon Watershed. Water Resources Bulletin 24:19–25.

Boyd, M.S., 1996. Heat Source: Stream, River, and Open Channel Temperature Prediction (Master's Thesis). Oregon State University, Corvallis.

Boyd, M. and B. Kasper, 2003. Analytical Methods for Dynamic Open Channel Heat and Mass Transfer: Methodology for Heat Source Model Version 7.0. Watershed Sciences Inc.,. Portland, OR, USA.

Brazier, J. and G. Brown, 1973. Buffer Strips for Stream Temperature Control. Corvallis, OR, USA. 9 pp.

Brown, G.W., 1969. Predicting Temperatures of Small Streams. Water Resources Research 5:68–75.

Brown, G.W. and J.T. Krygier, 1970. EFFECTS OF CLEAR-CUTTING ON STREAM TEMPERATURE. Water Resources Research 6:1133–1139.

Caissie, D., N. El-Jabi, and M.G. Satish, 2001. Modelling of Maximum Daily Water Temperatures in a Small Stream Using Air Temperatures. Journal of Hydrology 251:14–28.

Caissie, D., M.G. Satish, and N. El-Jabi, 2007. Predicting Water Temperatures Using a Deterministic Model: Application on Miramichi River Catchments (New Brunswick, Canada). Journal of Hydrology 336:303–315.

Clair, E. and J. Fields, 2004. Aquatic and Riparian Restoration Plan for the Dunstan Homestead Preserve. The Nature Conservancy. Portland, OR, USA.

Cole, E. and M. Newton, 2013. Influence of Streamside Buffers on Stream Temperature Response Following Clear-Cut Harvesting in Western Oregon. Canadian Journal of Forest Research 43:993–1005.

Constantz, J., 1998. Interaction between Stream Temperature, Streamflow, and Groundwater Exchanges in Alpine Streams. Water Resources Research 34:1609–1615.

Crisp, D.T. and G. Howson, 1982. Effect Of Air-Temperature Upon Mean Water Temperature In Streams In The North Pennines And English Lake District. Freshwater Biology 12:359–367.

Cristea, N.C. and S.J. Burges, 2010. An Assessment of the Current and Future Thermal Regimes of Three Streams Located in the Wenatchee River Basin, Washington State: Some Implications for Regional River Basin Systems. Climatic Change 102:493–520.

Cristea, N. and J. Janisch, 2007. Modeling the Effects of Riparian Buffer Width on Effective Shade and Stream Temperature. Washington State Department of Ecology. Olympia,Washington, USA. 64 pp.

Crown, J. and D. Butcher, 2010. John Day River Basin Total Maximum Daily Load (TMDL) and Water Quality Management Plan (WQMP). Oregon Department of Environment, Portland, OR, USA. 166 pp.

Davidson, B. and R. Bradshaw, 1967. Thermal Pollution of Water Systems. Environmental Science & Technology 1:618–630.

Diabat, M., R. Haggerty, and S.M. Wondzell, 2012. Diurnal Timing of Warmer Air under Climate Change Affects Magnitude, Timing and Duration of Stream Temperature Change. Hydrological Processes 27:2367–2378.

Ebersole, J.L., W.J. Liss, and C.A. Frissell, 2003. Thermal Heterogeneity , Stream Channel Morphology , and Salmonid Abundance in Northeastern Oregon Streams. Canadian Journal of Fisheries and Aquatic Science 60:1266–1280.

Elsner, M.M., L. Cuo, N. Voisin, J.S. Deems, A.F. Hamlet, J.A. Vano, K.E.B. Mickelson, S.-Y. Lee, and D.P. Lettenmaier, 2010. Implications of 21st Century Climate Change for the Hydrology of Washington State. Climatic Change 102:225–260.

Erickson, T.R. and H.G. Stefan, 2000. Linear Air/Water Temperature Correlations For Streams During Open Water Periods. Journal of Hydrologic Engineering 5:317–321.

Feldhaus, J.W., S.A. Heppell, H. Li, and M.G. Mesa, 2010. A Physiological Approach to Quantifying Thermal Habitat Quality for Redband Rainbow Trout (Oncorhynchus Mykiss Gairdneri) in the South Fork John Day River, Oregon. Environmental Biology of Fishes 87:277–290.

Gooseff, M.N., K. Strzepek, and S.C. Chapra, 2005. Modeling the Potential Effects of Climate Change on Water Temperature Downstream of a Shallow Reservoir, Lower Madison River, MT. Climatic Change 68:331–353.

Grant, K., 1994. Oregon River Restoration: A Sensitive Management Strategy Boosts Natural Healing. Restoration and Management Notes 12:152–159.

Groom, J.D., L. Dent, L.J. Madsen, and J. Fleuret, 2011. Response of Western Oregon (USA) Stream Temperatures to Contemporary Forest Management. Forest Ecology and Management 262:1618–1629.

Gu, R., S. Montgomery, and T. Al Austin, 1998. Quantifying the Effects of Stream Discharge on Summer River Temperature. Hydrological Sciences Journal 43:885–904.

Hamlet, A.F.F., P. Carrasco, J. Deems, M.M.M. Elsner, T. Kamstra, C. Lee, S.-Y. Lee, G. Mauger, E.P. Salathe, I. Tohver, L.W. Binder, and S.-Y.L. C. Lee, 2010. Final Project Report for the Columbia Basin Climate Change Scenarios Project, [www.hydro.washington.edu/2860/]. Seattle, WA, USA. http://warm.atmos.washington.edu/2860/report/.

Hamlet, A.F., M.M. Elsner, G. Mauger, S.-Y. Lee, I. Tohver, and R.A. Norheim, 2013. An Overview of the Columbia Basin Climate Change Scenarios Project : Approach , Methods , and Summary of Key Results. Atmosphere-Ocean 51:392–415.

Hawkins, C.P., J.N. Hogue, L.M. Decker, and J.W. Feminella, 1997. Channel Morphology, Water Temperature, and Assemblage Structure of Stream Insects. Journal of the North American Benthological Society 16:728–749.

Hunt, R.M.J. and E. Stepleton, 2004. Geology and Paleontology of the Upper John Day Beds, John Day River Valley, Oregon: Lithostratigraphic and

Biochronologic Revision in the Haystack Valley and Kimberly Areas (Kimberly and Mt. Misery Quadrangles). Bulletin of the American Museum of Natural History 282:1–90.

Imholt, C., C. Soulsby, I.A. Malcolm, and C.N. Gibbins, 2013. Influence of Contrasting Riparian Forest Cover on Stream Temperature Dynamics in Salmonid Spawning and Nursery Streams. Ecohydrology 6:380–392.

IPCC, 2007. Climate Change 2007: The Physical Science Basis. Contribution of Working Group I to the Fourth Assessment Report of the Intergovernmental Panel on Climate Change. Solomon, S., D. Qin, M. Manning, Z. Chen, M. Marquis, K.B. Averyt, M.Tignor and H.L. Miller. Cambridge University Press, Cambridge, United Kingdom and New York, NY, USA.

Johnson, S.L., 2004. Factors Influencing Stream Temperatures in Small Streams: Substrate Effects and a Shading Experiment. Canadian Journal of Fisheries and Aquatic Sciences 61:913–923.

Johnson, S.L. and J.A. Jones, 2000. Stream Temperature Responses to Forest Harvest and Debris Flows in Western Cascades, Oregon. Canadian Journal of Fisheries and Aquatic Sciences 57:30–39.

Kibler, K.M., A. Skaugset, L.M. Ganio, and M.M. Huso, 2013. Effect of Contemporary Forest Harvesting Practices on Headwater Stream Temperatures: Initial Response of the Hinkle Creek Catchment, Pacific Northwest, USA. Forest Ecology and Management 310:680–691.

Kristensen, P.B., E.A. Kristensen, T. Riis, A.J. Baisner, S.E. Larsen, P.F.M. Verdonschot, and A. Baattrup-Pedersen, 2013. Riparian Forest as a Management Tool for Moderating Future Thermal Conditions of Lowland Temperate Streams. Hydrology and Earth System Sciences Discussions 10:6081–6106.

Lawrence, D.J., J.D. Olden, and C.E. Torgersen, 2012. Spatiotemporal Patterns and Habitat Associations of Smallmouth Bass (Micropterus Dolomieu) Invading Salmon-Rearing Habitat. Freshwater Biology 57:1929–1946.

LeBlanc, R.T., R.D. Brown, and J.E. FitzGibbon, 1997. Modeling the Effects of Land Use Change on the Water Temperature in Unregulated Urban Streams. Journal of Environmental Management 49:445–469.

Lee, T.Y., J.C. Huang, S.J. Kao, L.Y. Liao, C.S. Tzeng, C.H. Yang, P.K. Kalita, and C.P. Tung, 2012. Modeling the Effects of Riparian Planting Strategies on Stream Temperature: Increasing Suitable Habitat for Endangered Formosan Landlocked Salmon in Shei-Pa National Park, Taiwan. Hydrological Processes 26:3635–3644.

Lyon, E.W.J., 2010. Oxbow Conservation Area Reach Assessment, Middle Fork John Day River. U.S. Department of Interior, Bureau of Reclamation, Pacific Northwest Region, Boise, Idaho.

Mantua, N., I. Tohver, and A.F. Hamlet, 2009. Impacts of Climate Change on Key Aspects of Freshwa-Water Salmon Habitat in Washington State. Washington Climate Change Impacts Assessment: Evaluating Washington's Future in a Changing Climate. University of Washington, Seattle, WA, Seattle, WA, p. 37.

Mantua, N., I. Tohver, and A. Hamlet, 2010. Climate Change Impacts on Streamflow Extremes and Summertime Stream Temperature and Their Possible Consequences for Freshwater Salmon Habitat in Washington State. Climatic Change 102:187–223.

McCullough, D.A., 1999. A Review and Synthesis of Effects of Alterations to the Water Temperature Regime on Freshwater Life Stages of Salmonids, with Special Reference to Chinook Salmon U. S. E. P. Agency (Editor). U.S. Environmental Protection Agency, Boise, ID, USA.

Mellina, E., R.D. Moore, S.G. Hinch, J.S. Macdonald, and G. Pearson, 2002. Stream Temperature Responses to Clearcut Logging in British Columbia: The Moderating Influences of Groundwater and Headwater Lakes. Canadian Journal of Fisheries and Aquatic Sciences 59:1886–1900.

Mitchell, S., 1999. A Simple Model for Estimating Mean Monthly Stream Temperatures after Riparian Canopy Removal. Environmental Management 24:77–83.

Mohseni, O., T.R. Erickson, and H.G. Stefan, 1999. Sensitivity of Stream Temperatures in the United States to Air Temperatures Projected under a Global Warming Scenario. Water Resources Research 35:3723–3733.

Mohseni, O. and H.G. Stefan, 1999. Stream Temperature/air Temperature Relationship: A Physical Interpretation. Journal of Hydrology 218:128–141.

Mohseni, O., H.G. Stefan, and T.R. Erickson, 1998. A Nonlinear Regression Model for Weekly Stream Temperatures. Water Resources Research 34:2685–2692.

Moore, R.D., D.L. Spittlehouse, and A. Story, 2005. Riparian Microclimate and Stream Temperature Response to Forest Harvesting: A Review. Journal of the American Water Resources Association 41:813–834.

Morak, S., G.C. Hegerl, and J. Kenyon, 2011. Detectable Regional Changes in the Number of Warm Nights. Geophysical Research Letters 38:L17703.

Mote, P.W. and E.P. Salathé, 2010. Future Climate in the Pacific Northwest. Climatic Change 102:29–50.

Myrick, C.A. and J.J. Cech, 2005. Effects of Temperature on the Growth, Food Consumption, and Thermal Tolerance of Age-0 Nimbus-Strain Steelhead. North American Journal of Aquaculture 67:324–330.

Neumann, D.W., B. Rajagopalan, and E.A. Zagona, 2003. Regression Model for Daily Maximum Stream Temperature. :667–674.

Oregon Department for Environmental Quality, 2014. Water Quality- Total Maximum Daily Loads (TMDLs) Program. http://www.deq.state.or.us/wq/tmdls/tools.htm. Accessed 10 Feb 2014.

Pilgrim, J.M., X. Fang, and H.G. Stefan, 1998. Stream Temperature Correlations with Air Temperatures in Minnesota: Implications for Climate Warming. Journal of the American Water Resources Association 34:1109–1121.

Pollock, M.M., T.J. Beechie, M. Liermann, and R.E. Bigley, 2009. Stream Temperature Relationships to Forest Harvest in Western Washington1. JAWRA Journal of the American Water Resources Association 45:141–156.

Poole, G.C. and C.H. Berman, 2001. An Ecological Perspective on In-Stream Temperature: Natural Heat Dynamics and Mechanisms of Human-Caused Thermal Degradation. Environmental Management 27:787–802.

Quinn, J.M. and A.E. Wright-Stow, 2008. Stream Size Influences Stream Temperature Impacts and Recovery Rates after Clearfell Logging. Forest Ecology and Management 256:2101–2109.

Reeves, G.H., J.B. Grunbaum, and D.W. Lang, 2009. Seasonal Variation in Diel Behaviour and Habitat Use by Age 1+ Steelhead (Oncorhynchus Mykiss) in Coast and Cascade Range Streams in Oregon, U.S.A. Environmental Biology of Fishes 87:101–111.

Richter, A. and S.A. Kolmes, 2005. Maximum Temperature Limits for Chinook, Coho, and Chum Salmon, and Steelhead Trout in the Pacific Northwest. Reviews in Fisheries Science 13:23–49.

Roth, T.R., M.C. Westhoff, H. Huwald, J.A. Huff, J.F. Rubin, G. Barrenetxea, M. Vetterli, A. Parriaux, J.S. Selker, and M.B. Parlange, 2010. Stream Temperature Response to Three Riparian Vegetation Scenarios by Use of a Distributed Temperature Validated Model. Environmental Science & Technology 44:2072–2078.

Rutherford, J.C., S. Blackett, C. Blackett, L. Saito, and R.J. Davies-Colley, 1997. Predicting the Effects of Shade on Water Temperature in Small Streams. New Zealand Journal of Marine and Freshwater Research 31:707–721.

Sinokrot, B.A. and J.S. Gulliver, 2000. In-Stream Flow Impact on River Water Temperatures. Journal of Hydraulic Research 38:339–349.

Sinokrot, B.A. and H.G. Stefan, 1993. Stream Temperature Dynamics: Measurements and Modeling. Water Resources Research 29:2299–2312.

Sinokrot, B.A. and H.G. Stefan, 1994. Stream Water-Temperature Sensitivity to Weather and Bed Parameters. Journal of Hydraulic Engineering 120:722–736.

Stefan, H.G. and E.B. Preud'homme, 1993. Stream Temperature Estimation from Air Temperature. Water Resources Bulletin 29:27–45.

Stefan, H.G. and B.A. Sinokrot, 1993. Projected Global Climate Change Impact on Water Temperatures in Five North Central U.S. Streams. Climatic Change 24:353–381.

St-Hilaire, A., G. Morin, N. El-Jabi, and D. Caissie, 2000. Water Temperature Modelling in a Small Forested Stream: Implication of Forest Canopy and Soil Temperature. Canadian Journal of Civil Engineering 27:1095–1108.

Sugimoto, S., F. Nakamura, and A. Ito, 1997. Heat Budget and Statistical Analysis of the Relationship between Stream Temperature and Riparian Forest in the Toikanbetsu River Basin , Northern Japan. Journal of Forest Research 7:103–107.

Tinus, C.A. and G.H. Reeves, 2001. Redside Shiner (Richardsonius Balteatus) Shoals Provide a Behavioral Competitive Refuge for Subordinate Juvenile Steelhead Trout (Oncorhynchus Mykiss). Canadian Journal of Fisheries and Aquatic Sciences 58:319–324.

U.S. Environmental Protection Agency, 2003. EPA Region 10 Guidance For Pacific Northwest State and Tribal Temperature Water Quality Standards. Region 10 Office of Water, Seattle, Seattle, WA.

Van Vliet, M.T.H., F. Ludwig, J.J.G. Zwolsman, G.P. Weedon, and P. Kabat, 2011. Global River Temperatures and Sensitivity to Atmospheric Warming and Changes in River Flow. Water Resour. Res. 47:W02544.

Webb, B.W., P.D. Clack, and D.E. Walling, 2003. Water-Air Temperature Relationships in a Devon River System and the Role of Flow. Hydrological Processes 17:3069–3084.

Wells, A.F., 2006. Deep Canyon and Subalpine Riparian and Wetland Plant Associations of the Malheur, Umatilla, and Wallowa-Whitman National Forests. Gen. Tech. Rep. PNW-GTR-682. Portland, OR, USA. U.S. Department of Agriculture, Forest Service, Pacific Northwest Research Station. 277 p.

Wilkerson, E., J.M. Hagan, D. Siegel, and A.A. Whitman, 2006. The Effectiveness of Different Buffer Widths for Protecting Headwater Stream Temperature in Maine. 52:221–231.

Wissmar, R.C., E. Jeanetle, B.A. Mclntosh, H.W. Li, G.H. Reeves, and J.R. Sedell, 1994. A History of Resource Use and Disturbance in Riverine Basins of Eastern Oregon and Washington. Northwest Science 68:35 p.

Wondzell, S.M., 2006. Effect of Morphology and Discharge on Hyporheic Exchange Flows in Two Small Streams in the Cascade Mountains of Oregon, USA. Hydrological Processes 20:267–287.

Wondzell, S.M., 2012. Hyporheic Zones in Mountain Streams : Physical Processes and Ecosystem Functions. Stream Notes January-Ap:11.

Wu, H., J.S. Kimball, M.M. Elsner, N. Mantua, R.F. Adler, and J. Stanford, 2012. Projected Climate Change Impacts on the Hydrology and Temperature of Pacific Northwest Rivers. Water Resources Research 48:W11530.

Zwieniecki, M. and M. Newton, 1999. Influence of Streamside Cover and Stream Features on Temperature Trends in Forested Streams of Western Oregon. West. J. Appl. For. 14:106–112.

7. Appendices

Appendix A- Assigning projections of air temperature and streamflow in Heat Source

The purpose of this appendix is to describe the procedure for assigning forecasts of air temperature and streamflow for the Middle Fork John Day River (MFJDR) in Heat Source. Heat Source required hourly input values of air temperature for seven nodes spatially distributed along the study section of the MFJDR. Modeling of stream temperature under a warmer climate was the product of combining two data sources:

1. The existing Heat Source model prepared by Oregon Department of Environmental Quality (ODEQ) for the total maximum daily load (TMDL) report (Crown and Butcher, 2010).
2. Air temperature and streamflow forecasts prepared by the Climate Impact Group (CIG) at the University of Washington (Elsner *et al.*, 2010; Mantua *et al.*, 2010; Mote and Salathé, 2010)[1].

Air Temperature forecasts

To prepare the original model for the MFJDR, Crown and Butcher (2010) adjusted air temperature values (and the rest of required climatic data) using data from the Agrimet site in Prairie City, Oregon, located 22.0 km away from upstream end of the study section at elevation of 1079 m (44°27’42”N, 118°42’50”W). The accuracy/error of the model was confirmed for key days at the location of nodes report (Crown and Butcher, 2010).

The Climate Impact Group at the University of Washington prepared air temperature forecasts and reported results for 297 streamflow locations in the Columbia River Basin. CIG evaluated the future changes in air temperature under greenhouse emission scenarios A1B and B1 for the time horizons: 2020s, 2040, and 2080s. Both the A1B and B1 emission scenarios assume the same growth rate in the world’s

---

[1] The database is available at http://warm.atmos.washington.edu/2860.

population, but the B1 scenario uses lower emissions and cleaner energy technologies. CIG researchers evaluated air temperature changes using historic surface air temperature from the A1B and the B1 emission scenarios based on downscaled results from different General Circulation Models (GCMs) from the Fourth Assessment Report of the Intergovernmental Panel on Climate Change (Bates *et al.*, 2008). CIG spatially downscaled the results from the GCM models to correspond with streamflow locations within different watersheds in British Columbia, Montana, Washington, Oregon, and Idaho. CIG also downscaled the temporal resolution of the results from annual to monthly scales for air temperature and to monthly and daily for stream flow. However, the Middle Fork John Day River was not explicitly included among the reported stream flow locations and Heat Source requires hourly data of air temperature values.

To assign air temperature forecasts for all seven nodes along the MFJD, I examined air temperature forecasts for 10 of the stations reported by CIG near the MFJDR (Table 1; Map 1) and calculated the change in air temperature relative to historic values through the year (Fig. A1, Fig. A2 and Table 2). For calculating the average change in air temperature, I used results of the downscaling that CIG performed for 10 GCMs under A1B emission scenario and 9 GCMs under B1 emission scenario. GCM models used for A1B were CCM3, CGM3.1_T47, CNRM_CM3, ECHAM5, ECHO_G, HADCM, HADGEM1, IPSL_CM4, MICRO_3.2, and PCM1. GCM models used for B1 were the same as A1B excluding HADGEM1. Estimating the change in air temperature expected for the MFJDR was made in two steps. First, I calculated monthly averages and standard deviation of air temperature change across all GCM models for each watershed. Then, I calculated the monthly average and standard deviation across all watersheds (Table 2). Calculation of the monthly average showed that +4 °C warmer air would be reasonable increase in air temperature for simulation in Heat Source. Therefore, I downscaled the change in monthly average change in air temperature to the hourly time steps for Heat Source using equations 3, 4, and 5 in chapter 2.

Stream discharge forecasts

Original data sets for streamflow were generated by a combination of in-stream measurements and a generic temperature profile (Crown and Butcher, 2010). Crown and Butcher (2010) collected instantaneous measurements of streamflow on a monthly basis at a number of sites along the MFJDR including the boundary conditions (upper-most point of the study section and tributaries). The hourly time series was prepared by multiplying the daily average flow at a downstream United States Geological Survey gage station (14046000) at river distance 24.6 km by a modifier that was determined based on the ratio of flow measured at the uppermost point to that recorded at the gage station. The hourly time series of tributaries was prepared by interpolating the data of monitored tributaries in the North Fork John Day River based on drainage area, slope, and percentage of forested land cover.

To assign streamflow forecasts for boundary conditions in Heat Source, I examined the stations in Table 1. For each station and for all GCM models, I summarized results of CIG's modeling by calculating the percentage of change in monthly average streamflow of forecasts relative to historic. Then, I calculated the average change for three categories: minimum change, maximum change, and average of all forecasts for both emissions scenarios through the three time horizons (Fig. A3). Calculations showed the change in streamflow was similar during the summer (Table A3); most models project lower streamflow during the 21st century relative to historic values but there were minor increases (Table A3). Therefore, I assigned 30% increase and 30% decrease to cover the range of streamflow forecasts. To simulate the different flow conditions in Heat Source, I adjusted flow data of the study section's inlet and inflows by subtracting or adding the percentage of change.

Table A-1: Stations selected to calculate change in air temperature for watersheds around the Middle Fork John Day River.

Station Number (CIG)	Station (and location)
4003	North Fork Malheur River
4007	Powder River at Baker City
4011	Imnaha River at Imnaha
4012	Grande Ronde River at La Grande
4015	Umatilla River at Pendleton
4017	John Day River at Picture Gorge
4018	North Fork John Day River at Monument
4020	John Day River at McDonald ferry
6072	Asotin Creek at Asotin
6075	Tucannon River Near Starbuck

Table A-2: Changes in monthly average air temperature between forecasts and historic values.

Month	Forecast time horizon	A1B (Δ °C)	B1 (Δ °C)
July	2020s	+1.84±0.05	+1.62±0.22
	2040s	+3.15±0.04	+2.14±0.19
	2080s	+5.20±0.03	+3.30±0.04
August	2020s	+1.99±0.06	+1.77±0.28
	2040s	+3.29±0.08	+2.47±0.26
	2080s	+5.60±0.04	+3.83±0.06

Table A-3: Table summarizing change in summer streamflow for 2020s, 2040s, and 2080s, both for A1B and B1 GCM emission scenarios.

Forecast time horizon	A1B			B1		
	Min	Mean	Max	Min	Mean	Max
2020s	-56%	-27%	5%	-48%	-15%	5%
2040s	-53%	-30%	4%	-64%	-22%	5%
2080s	-74%	-42%	3%	-68%	-34%	-7%

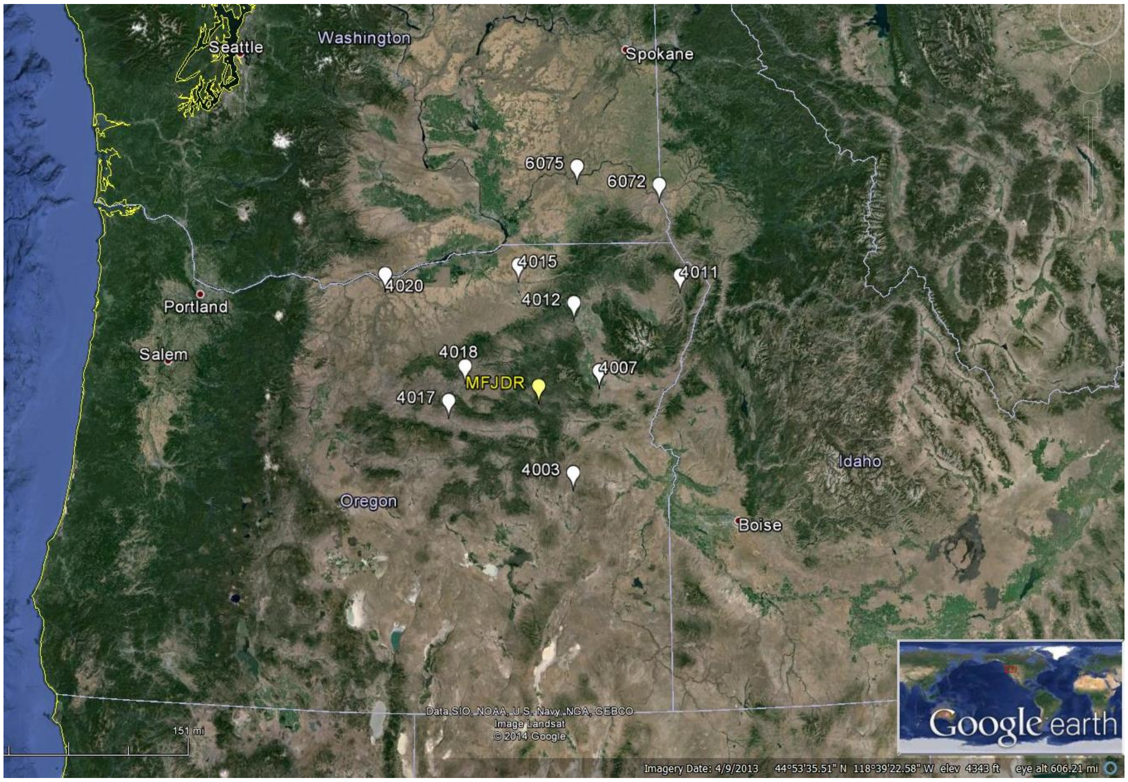

Figure A-1: Map showing locations of stations near the MFJDR used for estimating change in air temperature and flow (modified and updated from original by the Climate Impact Group database).

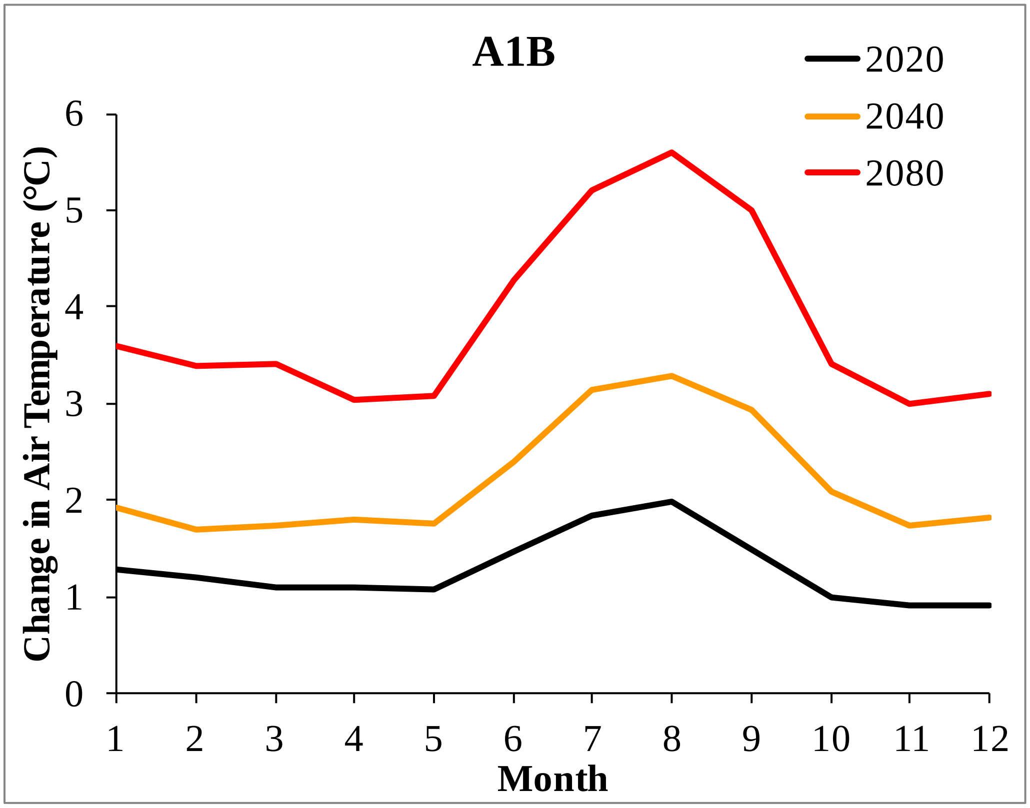

Figure A-2: Average change in monthly average air temperature under A1B emissions scenario, calculated for all stations in Table 1 and for all downscaled GCMs between forecasts and historic values.

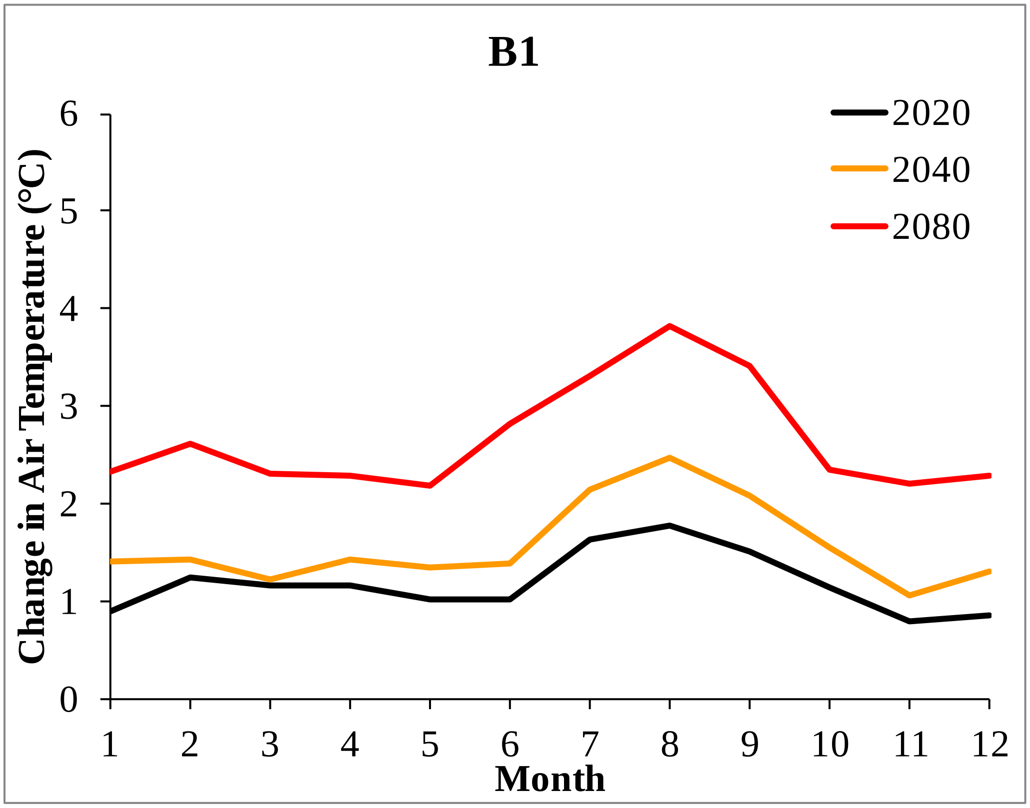

Figure A-3: Average change in monthly average air temperature under B1 emissions scenario, calculated for all stations in table 1 and for all downscaled GCMs between forecasts and historic values.

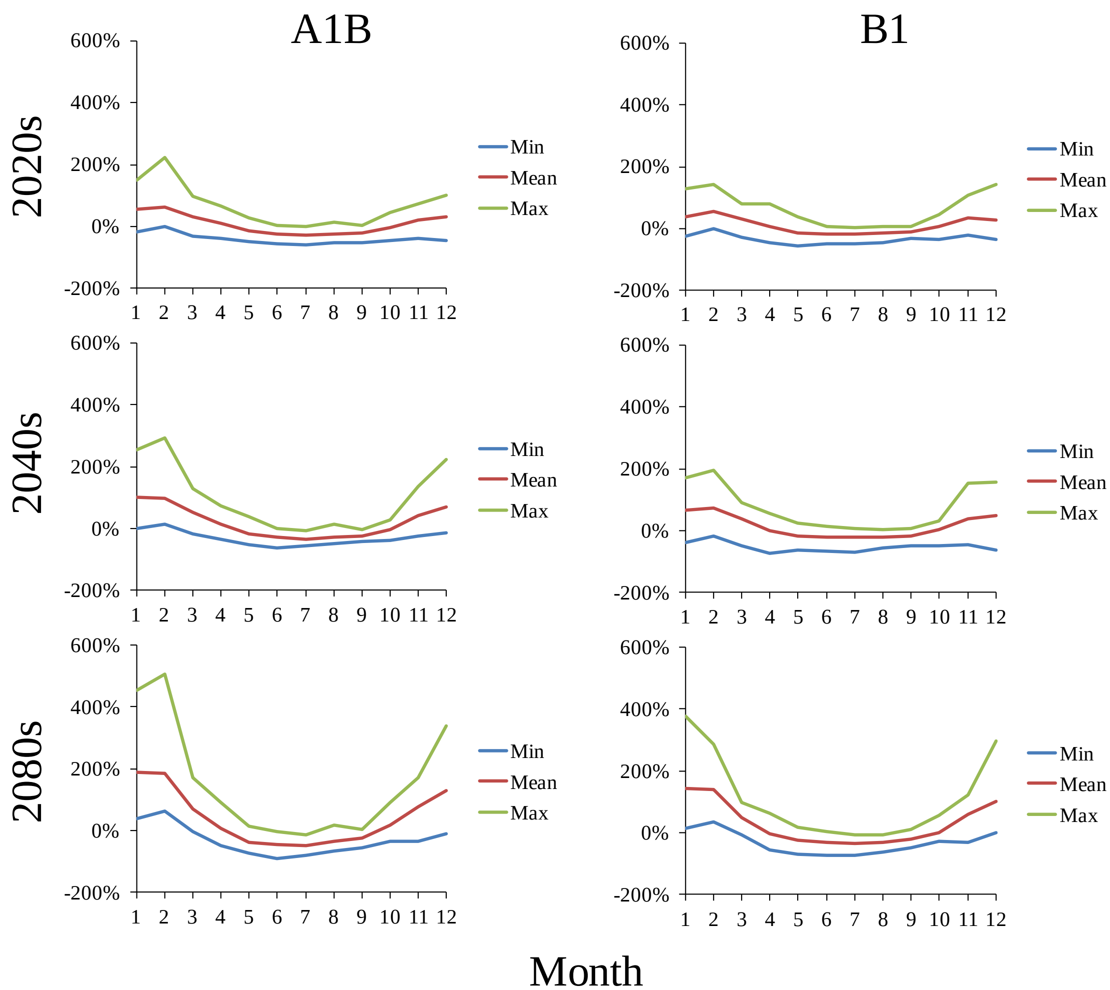

Figure A-4: Change in average monthly streamflow for 2020s, 2040s, and 2080s, for both A1B and B1 GCM emission scenarios (Prepared from original data reported by CIG).

Appendix B- Importing channel structure from HEC-RAS to Heat Source

The purpose of this appendix is to describe the procedure in which structure of the existing and the reconstructed channels were extracted using the Hydrologic Engineering Centers River Analysis System (HEC-RAS software).

Heat Source calculates hydraulic characteristics that are required for stream temperature simulations from boundary conditions (inlet and inflow) and parameters of channel structure. According to the user's definitions of spatial and temporal resolution, Heat Source calculates: average and maximum water depths, top width of the witted channel, flow velocity, discharge, and dispersion coefficient. Data for channel structure include streambed elevation, streambed width, gradient, stream bank angle, and roughness coefficient. The U.S. Bureau of Reclamation (USBR) at the Denver office, Colorado, prepared the designs of existing and to-be reconstructed channel using the software HEC-RAS[2].

In collaboration with the Michael Sixta from U.S. Bureau of Reclamation, I extracted channel structure information at 1 m spatial resolution. Data included longitude and latitude coordinates, streambed elevation relative to sea level, streambed width, and channel top width at the water surface. I calculated streambank angles from the hydraulic simulation results. Streambank angles are the ratio of transverse (z) to vertical length of sloping portion (d) of the trapezoidal channel. A value of z=0 indicates a rectangular channel form (Fig. B-1):

$$z = \frac{1}{2} * (top\ width - streambed\ width)$$

[2] Available for free at http://www.hec.usace.army.mil/software/hec-ras/

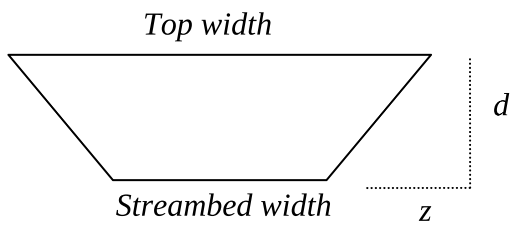

Figure B-1: Diagram depicting stream parameters to calculate streambank angles. Diagram is adapted from the MFJD Heat Source mode file.

I performed two modifications to the reconstruction design adapting the HEC-RAS model to summer flow conditions. USBR provided a channel design that was prepared to simulate high flow scenarios of 11.6 $m^3 \cdot s^{-1}$. At this streamflow, the stream will overflow outside of the active channel to the floodplain or to fill a side channel that is in place (Fig. B-2). Therefore, I modified the boundary conditions of the model to simulate a hydraulic steady state 1.0 $m^3 \cdot s^{-1}$, which is typical streamflow in early summer for the study section. Simulation results yielded channel with a top width that exceeded the expectation at a number of segments. Further investigations showed that the channel design also included side channels at the wide segments. Therefore, I manually modified the channel design to include barriers (levies) to prevent overflowing to the side channels.

I imported required data from HEC-RAS to Heat Source including streambed elevation, bottom width, and channel gradient. In addition, I modified the channel's roughness coefficient from 0.1 as Crown and Butcher (2010) assigned in Heat Source to 0.045 as suggested by USBR in HEC-RAS.

There was a poor fitting when comparing among hydraulic parameters of HEC-RAS and Heat Source results because of the difference in simulating flow between both models (Figures B-3a, B-3b, and B-3c). While flow simulation in HEC-RAS was in a steady state of 1.0 $m^3 \cdot s^{-1}$, flow simulation in Heat Source was in a variable flow that ranged between 0.9 and 1.0 $m^3 \cdot s^{-1}$ and the result of Heat Source were given as a daily average. The channel's top width, flow velocity, and average depth varied with changing flow depending on channel shape and structure. In addition, HEC-RAS simulated flow in much higher resolution than Heat Source, which increases the potential for difference between results.

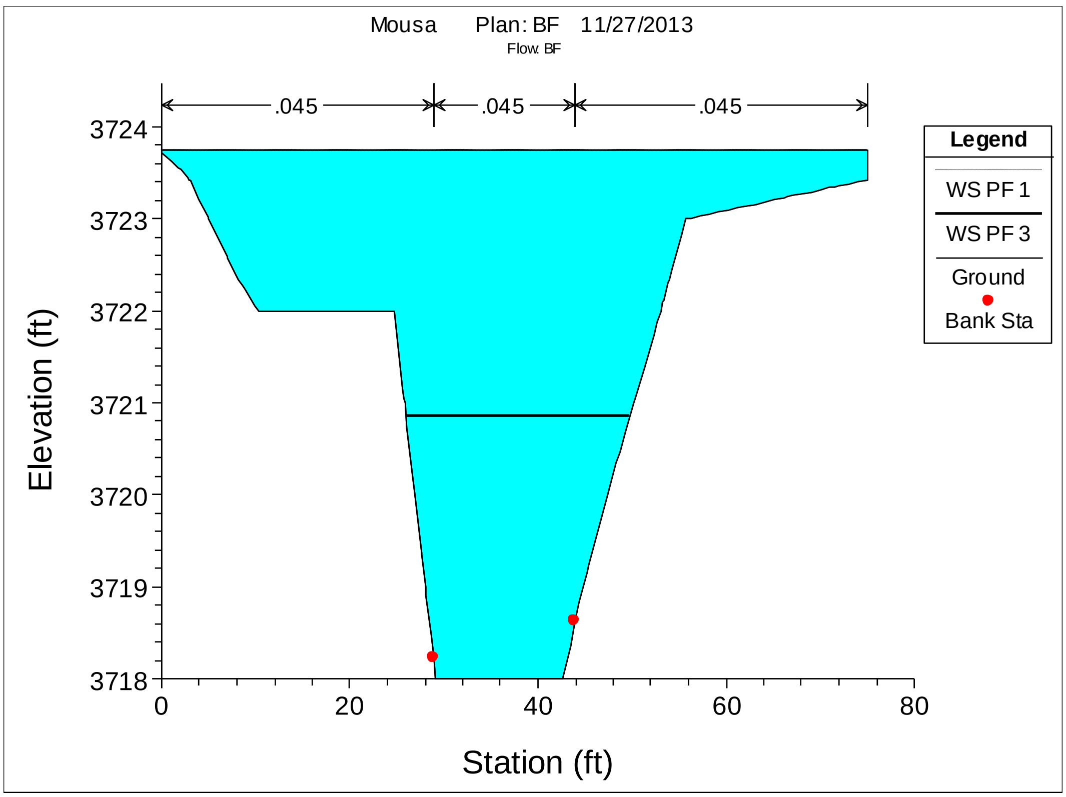

Figure B-2: Cross-section profile of water in the channel at one of the nodes (referred to as a 'station' in HEC-RAS) showing simulation result for 11 m3s-1 as water surface profile 1 (WS PF1) and the horizontal line in the middle of the cross-section for 1 m3s-1 as water surface profile 3 (WS PF3). Both red points were automatically assigned calculating streambed width.

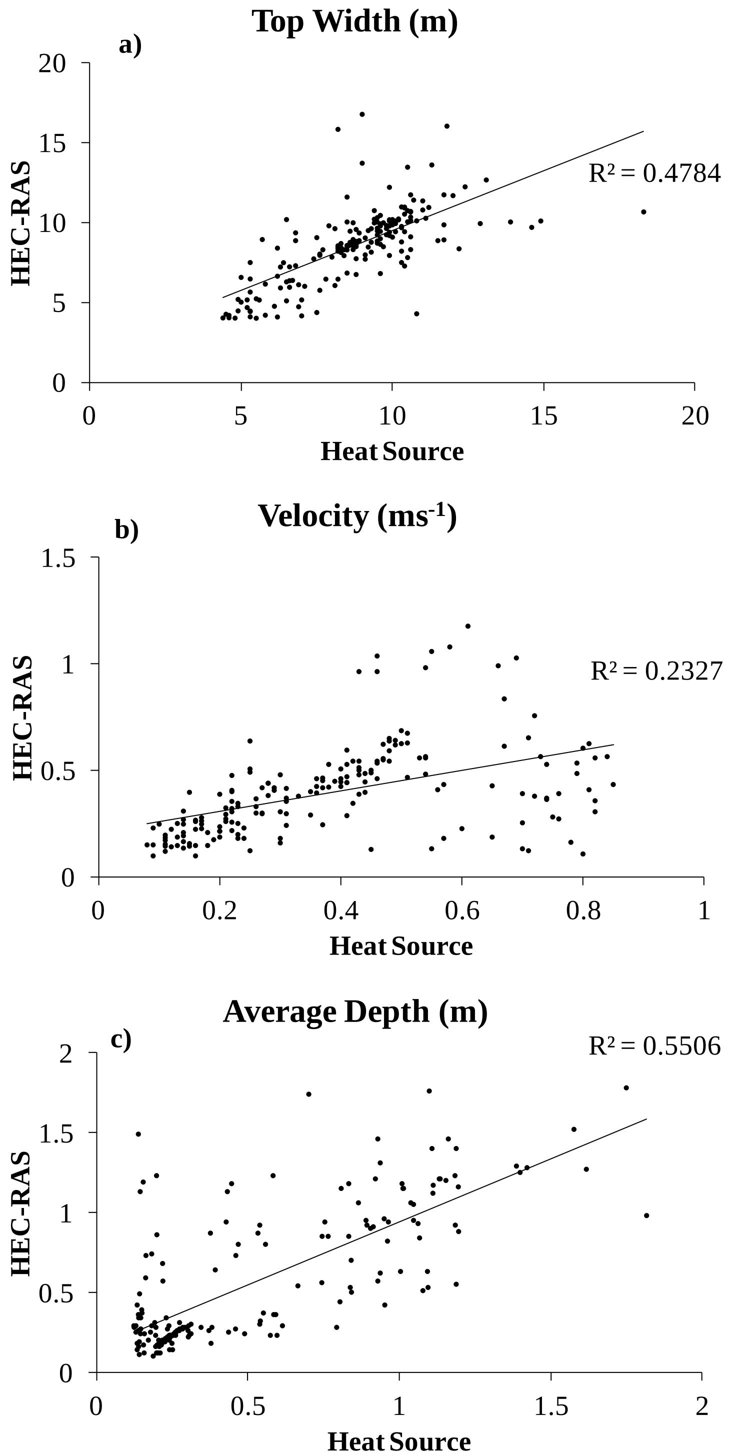

Figure B-3: Comparing between streamflow simulations in both HEC-RAS and Heat Source for top width (a), velocity (b), and average depth (c). Each point in figures above represents the result of same segment along the channel simulated by both models.

Appendix C- Preparing Boundary Conditions for the Study Section

The purpose of this appendix is to explain the procedure for producing updated data of boundary conditions (streamflow and temperature) at the uppermost point (inlet) of the study section. Boundary conditions for the study section cannot be directly extracted from the original Heat Source model (Crown and Butcher, 2010) because of a restoration project that was conducted in 2012 and modified channel structure upstream of the study section.

To generate the data of the boundary conditions at the inlet to the study section in chapter 4, I simulated stream temperature along the section upstream in Heat Source (Fig. C1). The study section designated for restoration is located between river kilometers 16.5 and 18.5 from the study section of chapter 2 (Diabat *et al.*, 2012), approximately between river kilometers 92 and 94 of the Middle Fork John Day River (MFJDR) in northeastern Oregon, USA (Fig. C1), and 20 km downstream of the upper most point in the total maximum daily load (TMDL) that Oregon Department of Environmental Quality (ODEQ) prepared (Crown and Butcher, 2010). I simulated stream temperature under two climate conditions: current climate conditions (2002 data) and projected +4 °C warmer air.

I simulated stream temperature with two major modifications to the original model. The first modification was changing the confluence point of Granite Boulder Creek with the mainstem MFJDR to be about 500 m upstream of the study section, reflecting the results of 2012 restoration project (phase II of the overall restoration plan) above the study area (Fig. C2). The Confederated Tribes of the Warm Springs restored the channel along 2-km section upstream of the study section. The mainstem of the MFJDR partially consisted of two channels flowing through the Oxbow Conservation Area (Fig. C3): a constructed channel along the middle of the valley floor (because of dredging) and a natural channel along the south edge of the valley floor. Phase II of the restoration filled the north channel and routed the water to flow in the south channel. The TMDL model originally routed all the water in the south channel only so there was no need to change model characteristics. However, restoration activities relocated the confluence of Granite Boulder Creek to meet the mainstem of the Middle Fork. Therefore, the adjusted location of the confluences was approximately 500 m upstream of the old location in the original Heat Source model.

The second modification was simulating stream temperature in spatial resolutions of 100 m instead of 300 m as used by ODEQ. This modification generated a finer spatial resolution of stream flow and temperature relative to the original TMDL model, which also allowed extracting streamflow and temperature results from a node of a simulation segment, to be used as input for the model in chapter 4.

Preparing the air temperature data for stream temperature simulation of warmer climate followed the delta method and was based on analysis from Appendix A. The delta method dictates adding a single defined value representing the change in air temperature to the hourly data. Simulation results of both current and warmer climate generated a 7-day average daily maximum of stream temperature (Fig. C-4). Fig. C-5 shows a sample of hourly stream temperature at the inlet to the study section of Chapter 4.

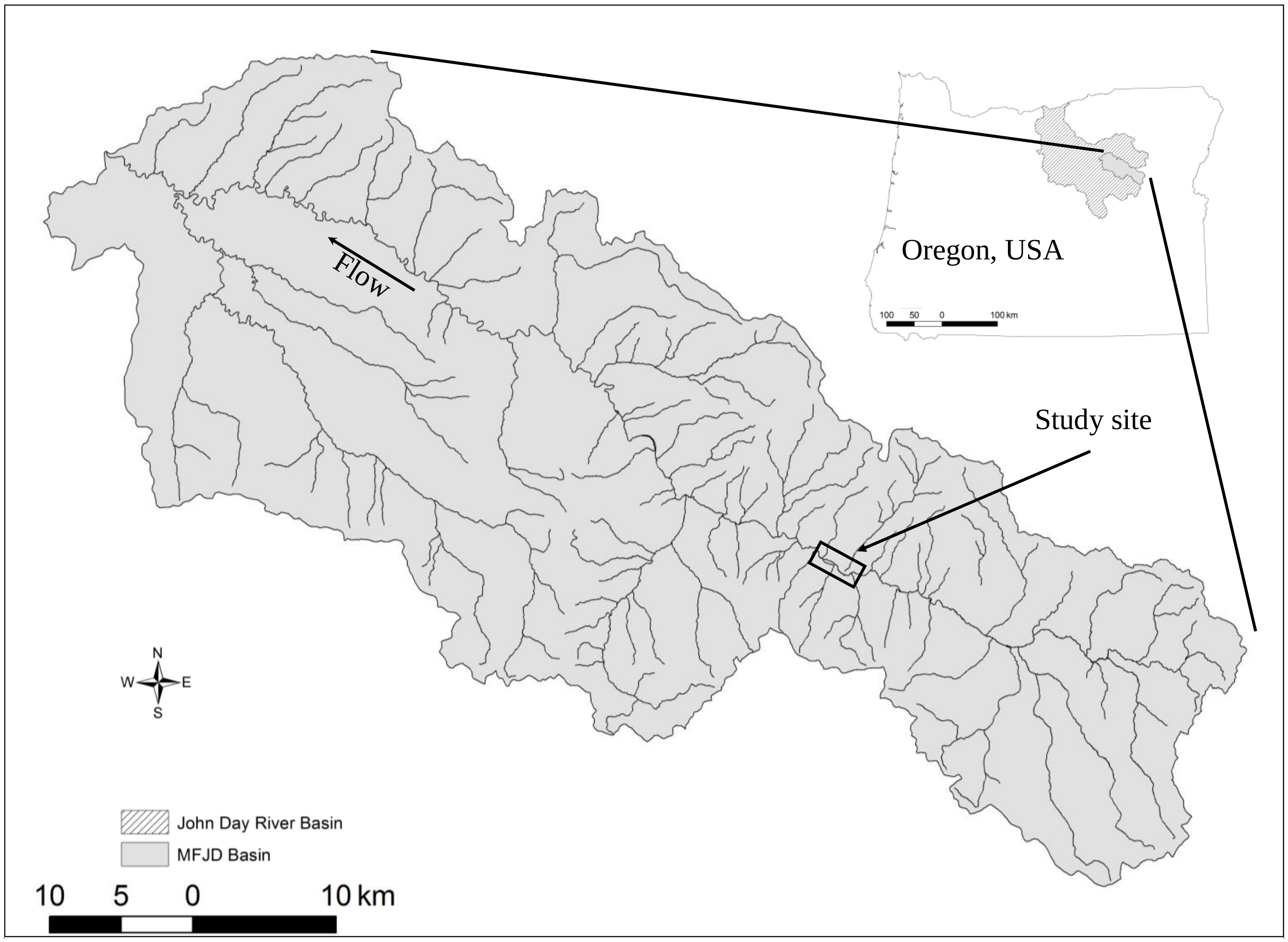

Figure C-1: Map indicating the study site along the Middle Fork John Day River.

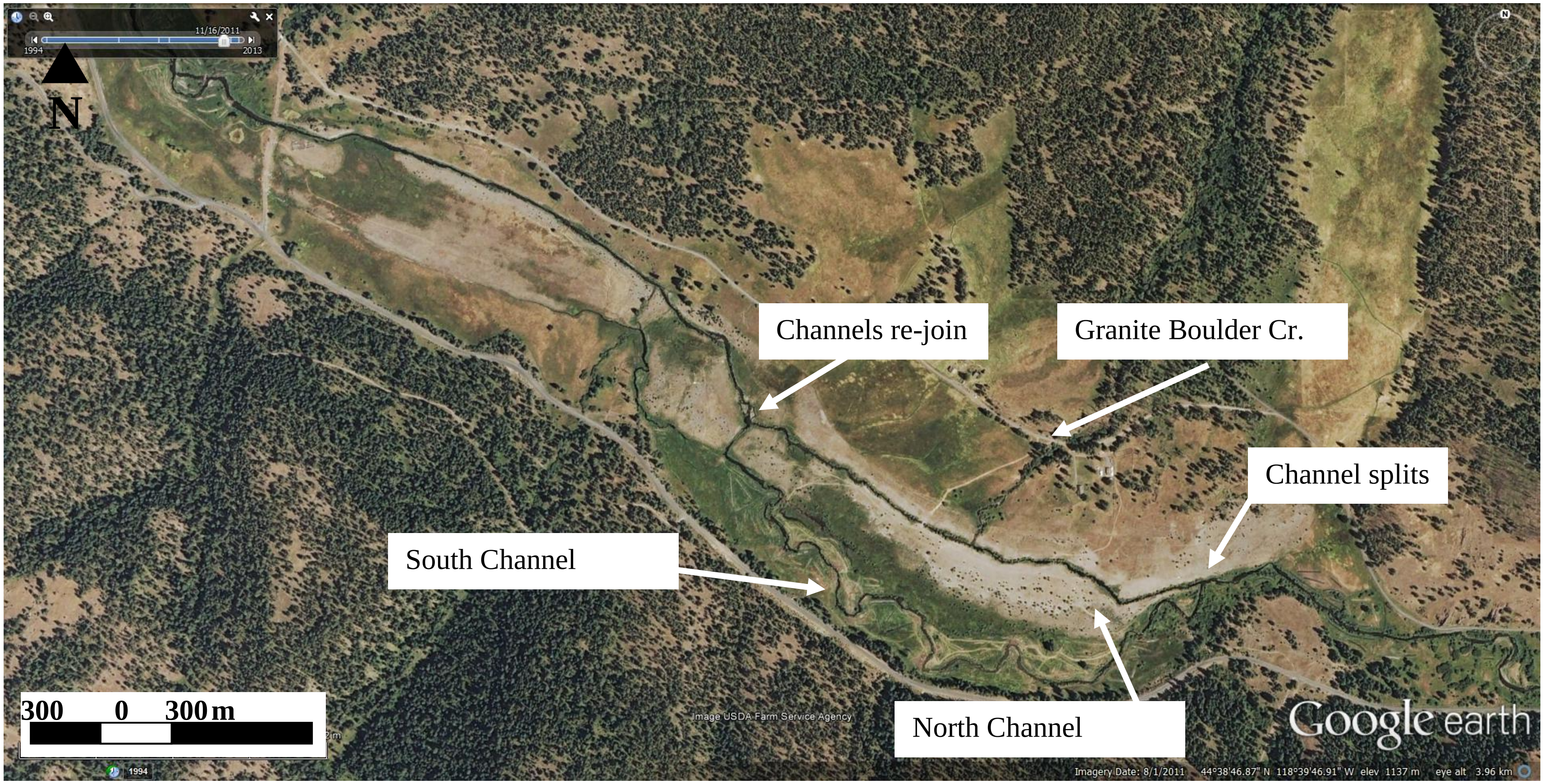

Figure C-2: Partial map of the Oxbow Conservation Area showing the north and south channels before the phase II of the restoration (Map is dated for November 16, 2011).

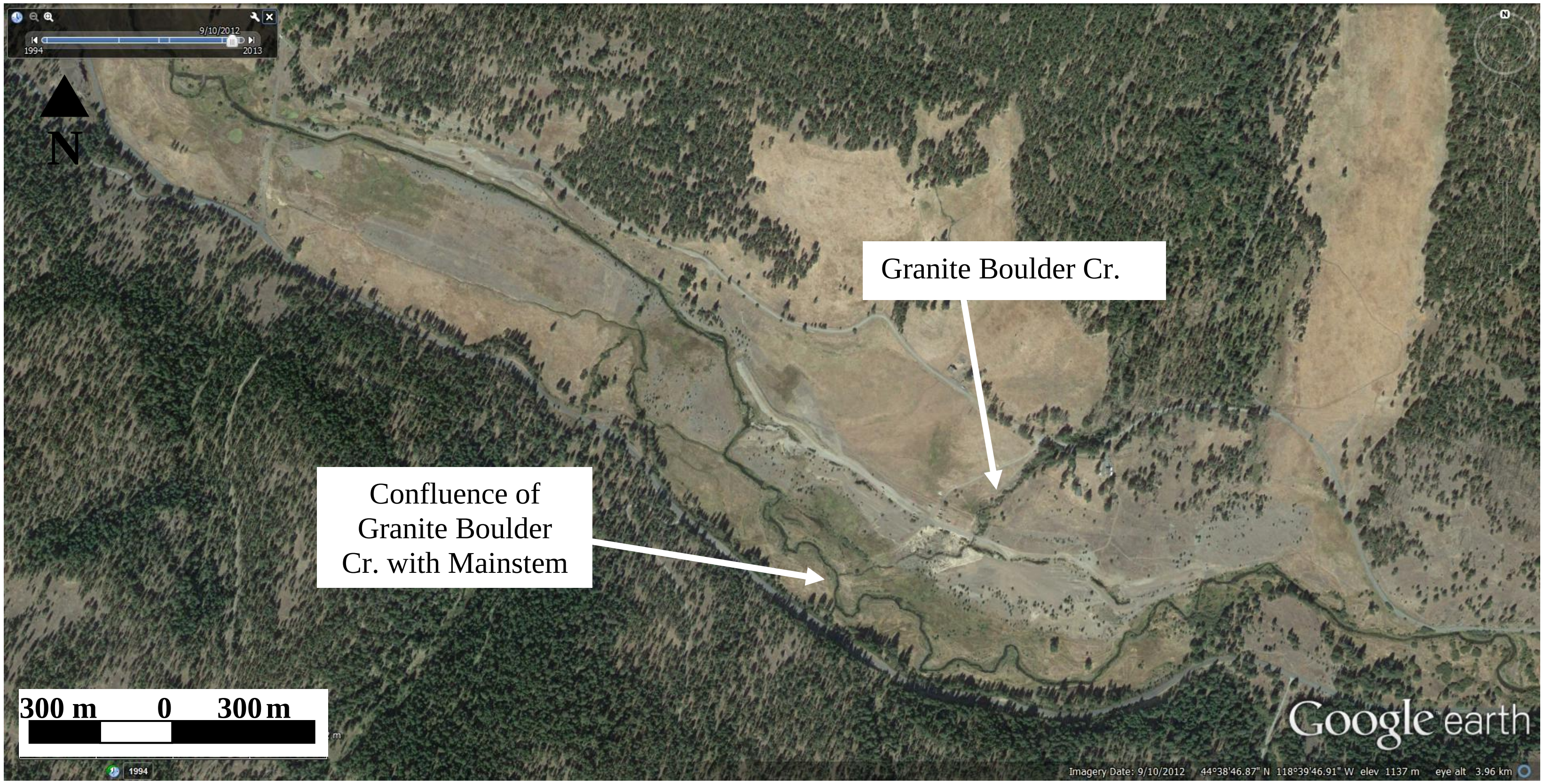

Figure C-3: Partial map of the Oxbow Conservation Area showing the confluence of Granite Boulder Creek with the mainstem channel after the phase II of the restoration (Map is dated for September 10, 2012).

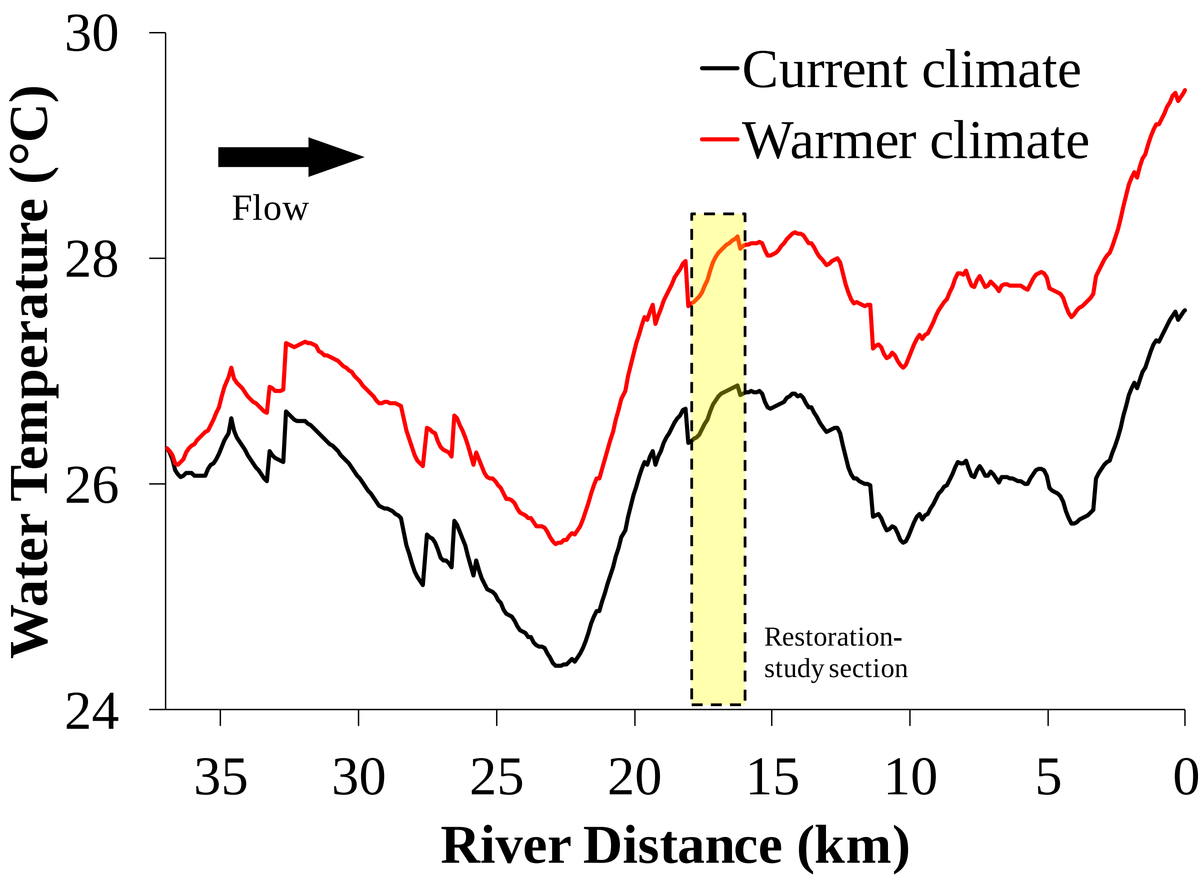

Figure C-4: 7-day average daily maximum along the upper 37 km of the Middle Fork John Day River both for current and for 4 °C warmer air temperature.

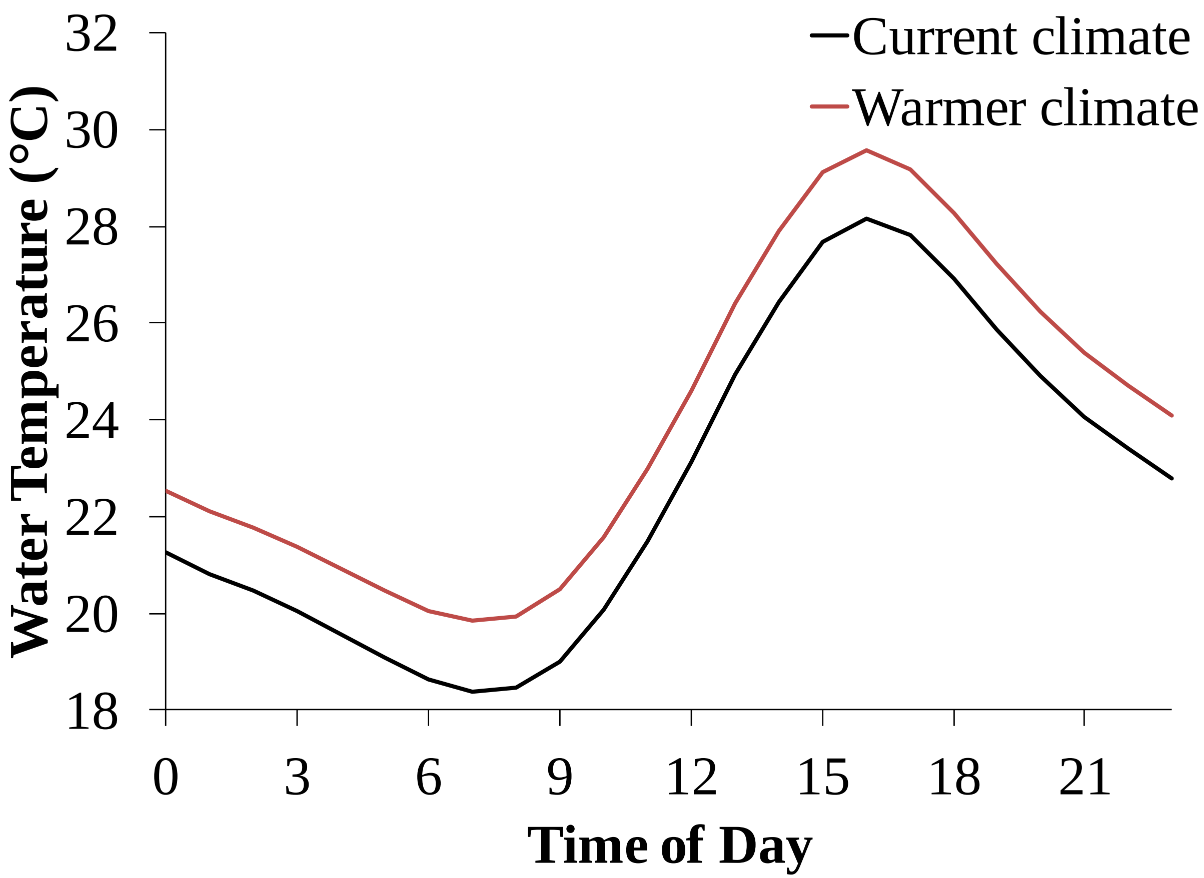

Figure C-5: Sample of stream temperature at the inlet to study section of chapter 4 on July 14th for current and 4 °C warmer climate.